NEW STUDIES ON HIGH ENERGY COSMIC RAY EXTENSIVE AIR SHOWERS DETECTED AT SEA LEVEL WITH EMPHASIS ON THE OBSERVATION OF CELESTIAL ULTRA HIGH ENERGY GAMMA -RAY SOURCES

Thesis submitted
for the degree of Doctor of Philosophy (Science)
of the University of North Bengal
by

Arunava Bhadra

High Energy and Cosmic Ray Research Centre
University of North Bengal
Darjeeling 734 430
INDIA

(February 1996)

****

To --

my parents and my elder brother

****

ACKNOWLEDGEMENTS

At the outset, I wish to express my gratitude to *Prof. N.Chaudhuri* for the guidence and valuable suggestions throughout the present investigation.

I acknowledge the support from the *University of North Bengal* and of the *University GrantsCommission* for research fellowship.

I am indebted to *Dr. Biswanath Ghosh, Dr. Samir Kumar Sarkar, Dr. Subrata Sanyal , Mr. Arindam Mukherjee* and *Mr. Gopal Saha* , my collaborators in the present investigation, for their co-operation. Thanks are due to *Mr. Ambarish Chetri* for his assistance in operation and day-to-day maintenance of the experimental system. I am also thankful to my junior colleagues , *Mr. Chadibrata Chakraborty* and *Mr. Dipesh Chanda* for their co-operation.

Dr. Swapan Kr. SenGupta , Head , University Science and Instrumentation Centre (USIC) has upgraded our old PC XT computer system to a 486 DX-2 system without which the present analysis could not be finished within this time. I am grateful to him.I like to thank *Mr. P. Tamang* for his suggestions in different technical aspects at various stages of the experiment. The USIC provides us technical support in different technical aspects . I am thankful to *all the members of the USIC.* I express my thankfulness to *all the members of the Department of Physics* for their co-operation.

Members of my family - my parents and *my elder brother* always encourage me and give moral support . I also like to mention the constant encouragement and affection of my freind *Mr. Gobinda Majumder* throughout the work.

Preface

Most of the energetic Cosmic Ray particles appear to be atomic nuclei. Cosmic Ray air shower observations so far have reported a number of events (eight to ten) in which the primaries had an energy greater than 10^{20} eV . Understanding the origin of charged Cosmic Ray particles has been difficult owing to the presence of a magnetic field in the Galaxy. Consequently , the Cosmic Ray origin problem has remained unsolved even though the study of Cosmic Rays began about a century ago. Recently , a great need has been recognised to observe emission of neutral particles (for example photons) from a number of discrete point sources which have been identified as candidate sources of Cosmic Rays , in addition to observing isotropic Cosmic Ray particles. This is also the thrust of the North Bengal University (NBU) extensive air shower (EAS) project which was started in 1980. The EAS detector array at a site on the NBU campus measures EAS arrival direction , size , muon distribution with a view to identifying the nature of the primary particles from various directions and also from the directions of the some specified discrete sources.

The author of the thesis joined the NBU project in 1992 holding a UGC junior research fellowship and has contributed to the expansion , development and operation of the EAS array in the following respects

1) Rearrangement of the detector array and resetting the individual detectors
2) Modernising the data-handling system
3) The calibrations of the detectors
4) Operation and day-to-day maintenance of the set-up
5) Data taking
6) Development of computer programs and analysis.

The analysis includes the following :

1) Reconstruction of the shower parameters from the observed shower data (Chapter 2)
2) Determination of arrival direction of individual showers (Chapter 2)
3) Study on shower front curvature and the time spread of the particles in the shower front.(Chapter 2)
4) Estimation of errors (Chapter 2)

5) Determination of the angular resolution of the array (Chapter 2)

6) Study on general characteristics of the observed showers (Chapter 3)

7) Study on shower parameters (Chapter 3)

8) Determination of the 'effective area' of the Aray (Chapter 3)

9) Search for excess air showers from the direction of four potential discrete point sources (Cygnus X-3 , Hercules X-1 , Crab Nebula and Geminga) (Chapter 3)

10) Phase analysis of the event times of the showers from two discrete point sources (Cygnus X-3 and Hercules X-1) (Chapter 3)

The previous work of other workers on emission of gamma-ray photons from discrete sources has been re-examined together with the present analysis and, the following features have been found in the present work:

1) The high muon content and high shower 'age' value of the excess showers from the direction of discrete point sources , as observed in a number of observations , may not be independent characteristics of the directional showers.

2) The high 'age' value of the directional showers can not be explained in terms of zenith angle.

3) No statistically significant excess of EAS from any of the observed sources has been found.

4) The phase analysis of the event time of EAS from the direction of Cygnus X-3 shows an excess of 2.11 σ in one phase bin.

As an additional support to the candidature , the author submits the following published papers to which the author has contributed.

1) An analysis of Cosmic Ray Air Showers for the Determination of Shower Age , Sanyal S. , Ghosh B. , Sarkar S.K. , Bhadra A. , Mukherjee A. and Chaudhuri N. , Aust. J. Phys. , 46 (1993) 589

2) A New lateral Distribution Function for Electrons in Extensive Air Showers (EAS) Detected near Sea Level. , Bhattacharyya B. , Bhadra A. , Mukherjee A. , Saha G. , Sanyal S. , Sarkar S. , Ghosh B. , and Chaudhuri N. , IL Nuovo Cimento , 18C (1995) 325

3) Measurement of the Charge Ratio of High Energy Muons in Cosmic Ray Extensive Air Shower (EAS) , Sarkar S.K. , Ghosh B. , Mukherjee N. , Sanyal S. , Bhadra A. , Mukherjee A. and Chaudhuri N. , in Proc. 23 rd International Cosmic ray Conference , Calgary, 4 (1993) 335

4) A study on the Cosmic Ray Age parameter , Sanyal S. , Ghosh B. , Sarkar S.K. , Mukherjee A. , Bhadra A. , and Chaudhuri N. , in Proc. 23 rd International Cosmic ray Conference , Calgary, 4 (1993) 339

5) Studies on the lateral Distribution of the Soft Component in the EAS , Bhattacharyya B. , Ghosh B. , Sarkar S.K. , Sanyal S. , Bhadra A. , Mukherjee A. and Chaudhuri N. , in Proc. 23 rd International Cosmic ray Conference , Calgary, 4 (1993) 331

6) Study of Electrons Simultaneously with Muons in Extensive Air Showers (EAS) initiated by Primary Cosmic Rays of Energy 10^{14} - 10^{16} eV., Chakrabarty C. , Chanda D. , Saha G. , Mukherjee A. , Bhadra A. , Sanyal S. , Sarkar S.K. , Ghosh B. and Chaudhuri N.,in Proc. 24 th International Cosmic ray Conference , Rome, 1995 , HE 3.2.5 .

7) A Search for Anistropy in the Arrival Direction of EAS by Cosmic Rays from Discrete Sources. , Chakrabarty C. , Chanda D. , Saha G. , Mukherjee A. , Bhadra A. , Sanyal S. , Chettri R. , Sarkar S.K. , Ghosh B. and Chaudhuri N., in Proc. 24 th International Cosmic ray Conference , Rome, 1995 , HE 3.3.14 .

8) Low and High Energy Muons in Extensive Air Showers of Size 10^4 to 10^6 Particles. , in Proc. 24 th International Cosmic ray Conference , Chakrabarty C. , Chanda D. , Saha G. , Mukherjee A. , Bhadra A. , Sanyal S. , Chettri R.K. , Sarkar S.K. , Ghosh B. and Chaudhuri N.,Rome, 1995 , HE 4.1.17 .

(Arunava Bhadra)
High Energy and Cosmic Ray
Research Centre , North Bengal University
Darjeeling 734-430 , INDIA

Contents : ~

*** Chapter 1 ***

1.1 Introduction

The mysteries and grandeur of the Universe fascinated mankind from long before the advent of the modern cosmology.From the time of earliest civilisations man has studied the movements of the heavenly bodies and from his observations has gradually built up ideas of the structure of the Universe.By ingenuity and perseverance through the centuries the nature of the Universe has gradually been unfolded.Man has acquired knowledge about the Universe entirely by interpretation of incoming radiation.Most astronomical information relies on measuring the electromagnetic radiation from space arriving at the earth.But there is another tool, which over the last few decades has become increasingly important - ***Cosmic Rays***.

The Cosmic radiation is a very specific sample of matter , a highly isotropic flux of relativistic particles,originates in the Cosmos. The study of cosmic rays originated approximately in the year 1900,as a result of observation of the ionisation in gases in closed vessels by *C.T.R. Wilson, Geitel and Elster*.In the year 1912 , Austrian scientist *Victor Hess* from his balloon flight experiment convincingly demonstrated that in closed vessel the air ionisation rate increases with height when moving away from the earth surface and he concluded that a very penetrating radiation is entering the atmosphere from outer space.However there was still another possibility that the observed radiation was gamma radiation from the radioactive substances present in the upper atmosphere. Hess results were confirmed in the subsequent observation by *Kohlhörster*. All doubts about the existence of a penetrating radiation from outside disappeared about 1927-28. *Millikan* gave the name *'Cosmic Rays'* to these penetrating radiations . *Hess* was later awarded the *'Noble prize'* in physics for his discovery of cosmic rays in 1936.

Cosmic rays are found in interstellar space of our own galaxy as well as in other galaxies. Thus cosmic rays are an important constituent of the Universe. The energy density of cosmic rays in our galaxy $\omega_{CT} \sim 10^6$ eV/m^3 , is of the same order as the energy density of the interstellar magnetic fields and as the energy density of the interstellar gas.The total estimated energy of the cosmic rays in the galaxy is about 10^{68} eV.

Cosmic rays are essentially extraterrestrial radiation having relativistic particles. The energy range of the cosmic ray particles are from 10^6 eV (super thermal energy) to about 10^{21}

deflection in the interstellar magnetic fields making it impossible to know the source direction. Stable electrically neutral particles are free from this problem.The commonly occurring neutral particles are neutrons , neutrinos and gamma ray photons. But neutrons are unstable and neutrinos , being weakly interacting, are not easy to detect.On the other hand gamma rays are ideal in view of both their production and interaction cross section being rather high and their being stable.

The starting point for gamma ray astronomy came from a paper by *Morrison* (5) in which he pointed out the prospects for gamma ray astronomy .Initially gamma ray detectors were carried by balloons.However high energy gamma ray astronomy was not to become established until satellites reduced the background problem and permitted long exposure. The successful flights of the *SAS-2* and *COSB* gamma ray experiments in the seventies established high energy gamma ray astronomy as a viable branch of astrophysics.

But the major problem at the UHE range is that the flux of UHE cosmic ray particles,in particular gamma rays, is so small that it can not be studied by balloons or satellites. As a result in the highest energy region cosmic ray observation are in general rather indirect. The only source of information about the highest energies is the '*Extensive Air Showers*' (EAS) .

The Extensive Air Shower :

Extensive Air shower is a phenomenon that results from the interaction of the high energy ($E > 10^{14}$ eV) primary cosmic ray particles with air nuclei in the earth's atmosphere.*Auger* and his colleagues first observed the phenomenon in the year 1938 (6).

When a high energy charged cosmic ray particle is incident on the top of the earth's atmosphere it interacts with the atmospheric nuclei.The products of this interaction are mainly charged and neutral pions with some kaons,nucleon , anti-nucleon pairs and other baryons.The secondary hadrons practically continue in the same direction of the primary and undergo further nucleon-nucleon collisions.Some of the charged pions and kaons interact while others decay to muons and neutrinos.Most of the muons survive to observation level.The neutral pions decay to gamma rays which initiate electromagnetic shower.In the electromagnetic cascade at each stage each gamma photon produces a pair of electrons which share its energy and each electron radiates

nearly half of its energy as a breinsstralhung gamma ray.As a result the number of particles grow until the energy of the individual electrons drops to the point that other interaction (e.g. absorption) processes compete with particle production.The total number of secondaries created in this phenomena can be as high as many millions.Because of the large energy involved , the secondary particles are strongly beamed in the forward direction , and on the average retain the directionality of the primary.At each interaction level , the particles spread out laterally mainly because of multiple coulomb scattering of the charged secondary leptons in the influence of air nuclei so that by the time the shower reaches the detector level , it has a lateral spread of hundred of meters.If a high energy cosmic gamma ray is incident on the top of the atmosphere it produces an electromagnetic cascade.

Charged cosmic rays are highly isotropic whereas cosmic gamma rays are supposed to directional.Hence, emission of gamma rays from a celestial source will be reflected in an excess number of showers from that direction of the celestial sphere.Since the convincing discovery of UHE gamma radiation from Cygnus X-3 by the Kiel group air shower arrays are extensively used in the search for point sources of cosmic rays.Several institutes have built new detector arrays or upgrade the existing ones to gather further information on gamma ray sources.In the last twelve years many observations of UHE gamma rays from various sources have been reported.However the present observational situation in UHE gamma ray astronomy is quite controversial.A brief review of the present status of observation of UHE gamma ray sources is described in next section.

1.2 Current status of observation of UHE gamma-ray sources :

In the year 1983 the Kiel group in Germany reported (1) detection of an excess flux of air showers of energies greater than 10^{15} eV from the direction binary x-ray source *Cygnus X-3*. That was the first positive observation of PeV radiation from a discrete source and with this observation a new era in gamma ray astronomy began.Since then many attempts have been made by different EAS groups to confirm the results of the Kiel group and to identify other discrete potential UHE gamma ray sources. Positive evidences of detection of UHE radiation were reported during last twelve years from several other sources e,g, *Crab nebula* , *Hercules X-1*, *Vela X-1* .

Search for UHE gamma rays from discrete sources started in the early sixties.For identification of gamma initiated showers against the large background of charged cosmic ray initiated showers it is essential to know the characteristics which distinguish gamma ray cascades from the charged cosmic ray initiated showers. Detailed calculation (2) have shown that air showers initiated by primary gamma rays should be deficient in muons by more than an order of magnitude compared to showers due to cosmic ray protons or heavier nuclei.The initial attempts to detect UHE gamma ray sources are based on looking for anisotropies in the cosmic ray flux using muon poor showers (3). But the initial attempts were unsuccessful.It was observed that cosmic rays in the PeV energy region are highly isotropic. Interest in UHE gamma ray astronomy was revitalized after the announcement of positive observation by the Kiel group. After many years of frustrating searches now a few sources in the UHE range , mostly of galactic origin , are established.

The summary of the status of observations can be represented by '*source catalog*'.Those sources which satisfy the criteria of at least three statistically significant independent observations are included in the source catalog which is presented in table 1.2.1 . The most numerous class of UHE gamma ray sources consist of x-ray binaries.The galactic x-ray sky is dominated by closed binaries in which one of the pair of stars is a compact object (white dwarf,Neutron stars or even black holes).The objects of most interest to gamma ray astronomy are the binaries that contain a neutron star. Most of these are found in massive systems in which the mass of the companion star is greater than $10M_0$. Supernova remnant is also found to be UHE gamma ray emitter which is expected.A brief discussion about the observation of the sources are described below.

Table 1.2.1

(UHE gamma ray source catalog)

Source	Type	Hemisphere	Co-ordinates Dec	RA	Distance from earth	Periodicity
Cygnus X-3	Binary X-ray source	N	40.9	307.8	> 11.4 kpc	4.8 hour
Hercules X-1	Binary X-ray source	N	35.4	254.0	~ 5 kpc	1.7 day, 1.24 s
Vela X-1	Binary X-ray source	S	-40.6	135.4	~1.4 kpc	8.96 day , 283 s
Crab nebula	Supernova Remnant	N	22.0	82.9	~ 2 kpc	Steady (33 ms ?)

Cygnus X-3 :

Cygnus X-3 is a very interesting astrophysical object.Cyg X-3 located at least 11.4 kpc away from the solar system , is a low mass x-ray binary system with a well known period of 4.8 hours which is normally interpreted as binary orbital period.Recent observations also indicate the presence of a fast pulsar of 12.6 ms pulsation in the TeV gamma range (4). The radio emission from Cyg X-3 is of particularly interesting as Cygnus X-3 displays flaring activity and occasionally exhibits large radio flares.

Cyg X-3 was first observed as x-ray source in the Cygnus constellation by a rocket borne x-ray telescope (5).The object has not seen at optical wavelengths.Cygnus X-3 was first observed as a TeV gamma ray source by Crimea astrophysical Laboratory (6) and subsequently observed by a number of other observations.

First attempts to observe UHE gamma rays from Cygnus X-3 were unsuccessful (7,8). The first report of successful detection of PeV gamma ray emission from any source came from the University of Kiel group (1). This result has a great importance in the UHE gamma ray astronomy.

The Kiel air shower array was consisted of 28 scintillation counters each of area $1m^2$.The sensitive area of the array was about 3000 m^2.Timing information were obtained from 11 fast timing detectors . The arrival direction was determined in this array with high accuracy (angular resolution better than 1^0).Showers with zenith angle less than 30^0 only were accepted for the analysis.The arrival direction of each showers was sorted into bins of right ascension and declination.They found a 4.4σ excess in the Cygnus X-3 direction compared to the background among the showers with age parameter greater than 1.1 (the mean age value in the Kiel observation) i,e, among the earlier developing showers. More significantly they found that event time exhibited a periodicity with peak emission at a phase 0.35 .They used P=0.1996814 d and P = 0 at an epoch t_0 = JD 2440949.9176 given by Parsignault et al (9) based on their x-ray data. The Kiel group also gave time average flux (integral flux) of $7.4 \pm 3.2 \times 10^{-14}$ photons $cm^{-2}s^{-1}$ above energies 2 PeV.For a distance to Cygnus X-3 of 11.4 KPc , this would corresponds to a luminosity of 2×10^{37} erg s^{-1}(considering the absorption effect due to interaction of UHE gamma rays with the 2.7^0 K black body radiation).They have also observed muons in the showers.When the data in the Cygnus X-3 bin were examined in terms of its muon to electron ratio this is found to be almost same ($0.67 \pm .09$) that obtained for a normal air showers initiated by a charged nuclei whereas the expected ratio would be ~0.10 (10).The detection of PeV signal from Cygnus X-3 was confirmed by Haverah Park group (11) within a few months of the publication of the Kiel results.Later positive evidence of UHE signal from the direction of Cygnus X-3 is reported by several groups (12,13,14,15) however negative results are also reported. Although the performance of the detectors improved with time, the significance of most of the published positive detection remained at a 3σ level.All the positive observation of Cygnus X-3 above TeV energy shown an excess close to two phases of the 4.8 hour orbital period at ~0.2 and ~0.6. However recent reports confirm only the emission at the second phase.Early observations of Cygnus X-3 provided the hope that the nature of the UHE radiation from this and similar sources could be studied regularly.However

most recent observations have been unable to confirm the existence of such emission. A summary of the results of some recent observations is presented in table 1.2.3.

Table 1.2.3

A Summary of some recent observations for UHE gamma-radiation from Cygnus X-3

Array Reference	Database	Observation
HEGRA EAS array (Located at the Canary Island La Palma 28.8°N 17.9°W,790 g cm^{-2}) (16)	Nearly 100 million events had been collected during 1989-91.Energy threshold of the array was 50 TeV.	No steady emission was observed but few short term excess was noticed . The largest short term excess on the 20 th January,1991 coincides with the huge radio flare. Phase analysis of the arrival times of the events of that day into the 4.8 hour phasogram shows enhancement of signal at a phase .2-.3. SOUDAN2 collaboration claims the detection of an increased muon flux from the direction of Cyg X-3 for the same day.
Chicago Air Shower Array (CASA) (17) (Located at Dugway Utah,USA .40.2° N, 112.8° W ,870 g cm-2)	About 1300 million events were collected by the array during 1991-93. 410 million events were taken for the analysis.	Search was made for steady and sporadic nature of emission with and without a cut on the muon content of the shower. No statistically significant excess was found.
EAS-TOP (18) (2005 m a.s.l., 42.45°N 13.56°E)	The database used in this analysis was taken during 1989-1990.	A search for possible periodic and sporadic emission had been performed.No significant excess was

		observed in any search.The upper limit to the DC flux was estimated F (>200 TeV) < 10^{-13} $cm^{-2}s^{-1}$
Ohya EAS array (19) (36.59° N,139.84°E)	A total number of 2.5 x 10^6 shower events were taken in the period 1986 - 1993.	Muon less EAS from Cyg X-3 had been searched. A 4σ excess has been observed in the data set with the muon cut(R_μ<.2) and size cut less than 10^5.
GREX EAS array (20) (Located at Haverah Park,UK)	Between March 1986 and December 1990 21.3 million events were collected.	No positive observation.The upper flux limit(95% CL) was estimated as 5 x 10^{-14} $cm^{-2}s^{-1}$ (>900 TeV).
CYGNUS EAS array (21) (Located in Los Alamos New Mexico ,35.9° N)	Over 200 millions air shower events was recorded.	Negative results reported.The estimated upper flux limit is 4 x 10^{-14} $cm^{-2}s^{-1}$(>70 TeV).
Akeno Giant Air Shower Array(AGASA) (22)	Data collected during 1990-1991.	The array Looked for steady excess in EeV energy range. A 3.4σ excess has been found from the direction of Cygnus X-3 .The flux limit from the observation was estimated as F(>3 x 10^{17} eV) = (3.4 ± 1.0) x10^{-17} $cm^{-2}s^{-1}$.

One of the most striking feature of recent observation is the detection of EeV radiation from the direction of Cygnus X-3 by the Fly's Eye group (23) .The result is confirmed by the Akeno group (24) and also by Akeno Giant Air Shower Array (25) although such emission was not seen on Haverah Park data (26).

All these results make Cygnus X-3 a very interesting astrophysical object.

Hercules X-1 :

Hercules X-1 is considered to be the prototypical binary x-ray pulsar.The x-ray flux displays periodic variations with time scales of 1.24 s , ~1.7 d and ~ 35 d.The two shorter periodicities are interpreted as being due to rotation and occultation of an accreting neutron star that is located in a close binary system.The unusual 35 day flux modulation has an x-ray light curve that is composed of an 11 day high intensity state and a 19 day low intensity state that is interrupted midway between the 11 day high state by an intermediate high state (intensity ~40% of main high state) of 5 day duration.Hercules X-1 is not a radio source like Cygnus X-3.

Pulsed TeV gamma radiation from Hercules X-1 was discovered by the Durham group in 1983 at the array in Dugway(27) and subsequently observed by the Whipple observatory . Several observations of TeV gamma-ray emission have been reported (28) . One highlight was the observation of of a 42 sigma excess with the Pachimarhi Cherenkov detector in April 11 , 1986 in India (29). UHE pulsed gamma-ray emission was first observed at the Fly's Eye array (30).Observations at both PeV and TeV energies indicate the possibility that Hercules X-1 may be characterized by occasional transient blue-shifted emission of gamma-rays (14). No statistically significant long term steady PeV radiation from Hercules X-1 has been reported so far. Results of some recent observations are given in table 1.2.4.

Table 1.2.4

A summary of some recent observations for UHE gamma-radiation from Hercules X-1

Array Reference	Database	Observation
KGF EAS array (31)	The data was from about 400 days during 1985 - 1987.	There is a 2.8σ DC excess with a zenith angle cut of >28° but the orbital phase distribution of the excess is not uniform.
Ohya EAS array (32)	Five years of data(1986-1991) with large muon detector had been analyzed.	A slight muon cut (R_μ<1.0) was made and a 4.2σ excess at the pulsar period of 1.236 sec was observed.

CASA & MIA EAS array. (33)	Data collected during 1990-1991.	No evidence was found for any excess.
GREX EAS array (34)	A database of over 30 million events recorded during 1988-90 .	No sign for any excess.
Ooty EAS array (35)	A total of 6.9×10^6 events collected during 1984-87 .	Positive evidence was found for episodic emission from the source.
HEGRA EAS array (36)	During 1989-91 the array collected more than 100 million events.	No statistically significant excess was observed.
CYGNUS EAS array (37)	Over 200 millions EAS events were recorded.	No evidence for any steady or spo-radic emission .

Vela X-1 :

Vela pulsar is the strongest GeV gamma ray source detected by the *COSB* satellite . This is a massive x-ray binary system, located comparatively close to the solar system (~1.9 KPc). It is believed to consist of a neutron star and a companion B-supergiant of 24 solar masses. Vela X-1 is originally discovered by the UHURU satellite experiment. It has been extensively studied at x-ray wavelenghts. Vela X-1 has a pulsed period 282.9 s and an orbital period 8.96 d. The orbital motion of the system is such that the pulsar is eclipsed for 20% of the total orbital period of 8.96 d. Being located in the southern sky it is accessible for observation only from sites in southern latitudes or near the equator.

Gamma radiation of UHE from Vela X-1 was first observed by the Bucland Park EAS array in Adelaide (38). The small array of 12 scintillation counters was operated at sea level. The muon density are not measured by the array. Background was discriminated using the value of age parameter. In the search for a flux from Vela X-1 only showers within 2^0 of source direction and

having s>1.3 were selected.These events were folded with the 8.964 days orbital period into bins of width 0.02.In one of the phases (~0.33) there was 8 events where 1.5 are expected.The gamma ray flux (>3 PeV) was estimated as $10 \pm .3 \times 10^{-4}$ photons $cm^{-2}s^{-1}$ which implies a luminosity of 4×10^{34} erg s^{-1} of the source.Later the observation was supported by BASJE collaboration at Mt Chacaltaya after reanalyzing their data collected between 1963-64 (39).At TeV energies Vela X-1 would appear to be reasonably well established gamma ray source. At PeV energies the evidence is however not so compelling still now.

Crab nebula :

In the year 1054 AD a supernova explosion took place which is well documented in ancient Chinese records .The result of this explosion is a supernova remnant,the Crab Nebula.The Crab nebula is one of the most studied source in high energy astrophysics.

A 33 ms pulsar (PSR 0531 + 21) was discovered in the remnant by Staelin and Reifenstain.The discovery of the the pulsar PSR 0531 +21 in the Crab nebula confirmed the connection between Supernova explosions and pulsars and supported the suggestion that pulsars are rotating neutron stars.The Cab nebula is located about 2 KPc away from the solar system.

First detection of VHE gamma rays from the direction of Crab nebula was reported by Smithsonian Astrophysical Observatory group (40) after three years of observation.Further evidence for the detection of TeV emission from the Crab nebula was reported by Whipple observatory collaboration (41).Now Crab is firmly established as TeV gamma-ray source.

Using the database accumulated by the Lodz EAS array , Dzikowski et al (42) reported first detection of flux of gamma radiations of energy >10 PeV from the Crab pulsar.Support for the Lodz identification of the Crab nebula as a UHE gamma-ray emitter came from Fly's Eye experiment (43) and also from Tien Shan EAS experiment (44).However the serious conflict with the Lodz group claiming to have detected the Crab nebula as UHE gamma-ray emitter, came from the observations at Haverah Park (45).Alexeenko et al (46) first reported the observation of PeV burst from the direction of the Crab nebula during the period 14:00 - 19:00 on 23rd Feb ,1989 with their EAS array at Baksan.Latter TIFR group (47) and Gran-Sasso collaboration (48) reported observation of same PeV transient burst.Though none of the three detections individually correspond to transient emission of exceptional intensity however the three independent but correlated detection strongly suggest that the effect is real.

There is yet no clear conclusion about the PeV emission from Crab.Because of the importance of Crab nebula as an astrophysical laboratory ,these results must be verified.

Other potential UHE gamma-ray sources :

Besides these sources already discussed ,there exist a small number of galactic as well as extra-galactic objects which have attracted the attention of UHE astronomers in recent years.Several groups have reported for positive evidences of UHE gamma-ray emission from these sources.However the results are yet to be firmly confirmed. Observations relating to a number of these sources are summarized here.

Scorpius X-1(SCO X-1) :

This source is a galactic x-ray binary object at a distance of 500 Pc. The source is known to exhibit quasi-periodic x-ray oscillation.There has been a report by Matano et al (49) of impulsive emission at PeV energies observed in hadron poor showers with the SYS array at Mt. Chacaltaya .They have observed a significant excess in the number of hadron less showers arriving from within 7^0 of SCO X-1 during May 1986 over time scales of few weeks.In an independent experiment Ooty group (50) also observed similar kind of excess.These observations indicate SCO X-1,like Cyg X-3,is emitting PeV radiation with variable flux over a time period of few weaks.No significant evidence for continuous emission at UHE is observed from SCO X-1 till now.

4U 1145 -619 :

The South Pole Air Shower Experiment(SPASE) has observed (51) a 4.9σ steady excess of events from the direction of 4U 1145 -619 based upon analysis of 9.3 million showers detected between May and Sep 1988.TeV observation of this source have been made by Durham group during 1987-88 (52).The independent TeV and PeV observation of this source appear to suggest that 4U 1145 -619 be considered as a strong candidate of gamma-ray source.

PSR 1957 +20 :

This source is first observed in radio observation made at the Aricibo observatory (53) which is an eclipsing millisecond binary pulsar.The orbital period is 33000.9 s.The companion star is presumably a white dwarf which is being highly ablated as a result of intense energy transfer from the pulsar.KGF group reported (54) observation of 53 events against a background of 34 events amounting to a 3.3σ signal in the orbital phase interval 0.2-0.3 during the period 1984 to 1987.The Potchefstroom group have claimed a steady emission from this source at a 10^{-3}

confidence level (55).Ooty group (56) also looked for emission from this object during the same period (1984-1987) but no excess was found. There is no compelling evidence so far that PSR 1957 + 20 is a UHE gamma ray source.

Geminga :

The high energy gamma-ray source Geminga (2CG 195 +4) is the second strongest source in the COS-B catalog of sources.It was discovered by the SAS-2 satellite (57). Search for PeV radiation from Geminga is of particularly interest since the x-ray and gamma-ray detections indicate that it is similar to the Crab and Vela pulsar.Especially appealing for UHE experiments are the reported detection of periodicity at TeV energies (58,59). Observations with the GRAPES 1 array at Ooty during 1984-87 has shown evidence for emission of UHE radiation during one week interval in Oct 10-16,1986 (60).

Centaurus A :

This extra-galactic object is one of the brightest active radio galaxy located at a distance of nearly 6 MPc. As a source this is only visible in the southern hemisphere . Cen A was observed as a TeV radiation emitter by the Narrabri observatory (61). It is also visible in the x-ray region. Analysis of three years of operation of the Buckland Park at Adelaide shown a slight excess (2.7σ) in the box containing Cen A for energies > 1PeV (62).JANZOS collaboration (63) have reported observation of an excess over background between 14 April 1990 and 3 June 1990.The duration (48 days) and luminosity ($\sim 10^{43}$ erg s^{-1}) of the excess are similar to observed previously from x-ray outburst from Cen A. Further study is required to confirm the observation of UHE emission by Cen A.

LMC X-4, M 31 and few other extragalactic objects are also very appealing for UHE experiments. But there have been no reports of the detection of PeV gamma-rays from these extragalactic objects yet.

Problems regarding the nature of UHE radiation from discrete point sources :

Even if the sources are accepted as detected , it is not possible to conclude that the sources are emitting UHE gamma rays. Observation of excess flux of EAS was reported by several groups from the direction of *Cygnus X-3* , *Hercules X-1* and some other sources.The properties of the initiating particles of the detected excess showers are very tightly constrained.

The initiating particle should be neutral,stable ,rest mass at most a few MeV and interacting very much like a nucleon in the atmosphere. Charged particles could not travel such a long distance (~12kpc) without being deflected by the galactic magnetic field , neutrons can not survive such a long time required to travel such a long distance. So UHE gamma photons have to be assumed as primaries of such EASs. In the most of the positive observations the excess EASs from the direction of *Cygnus X-3* and *Hercules X-1* are observed in phase with the orbital motion of the respective systems and it appears that the excess EASs are due to gamma-ray photons.The main indicator of a photonic origin for a shower is the relative low *muon content* in that shower.However there are a number of detections of gamma-ray (?) sources in which showers from the source direction appear to have high muon content,close to that expected for hadron initiated showers.

Muon content of gamma-ray initiated showers :

The first idea of a search for showers initiated by UHE gamma-rays was based on the fact that these showers should contain much fewer muons than normal ones.The muon component in hadron initiated showers originate from decay of charged pions created in interactions of hadron with the atmospheric nuclei.There are two types of process involve in generation of muons in electromagnetic showers,direct creation of muon pairs and photoproduction.The direct production of $\mu^+\mu^-$ pairs by photons is analogous to the creation of e^+ e^- pairs and in the asymptotic case of full screening of the nucleus field by the atomic electrons

$$\sigma_{\mu^+\mu^-}/\sigma_{e^+e^-} = (m_e/m_\mu)^2$$

which is very small.In the photoproduction muons are generated through production and subsequent decay of pimesons ($\pi^\pm - \mu^\pm\nu_\mu\tilde{\nu}_\mu$) . The cross section for photoproduction is very small compare to Bethe-Heitler pair production ($\gamma - e^+e^-$) cross section.As a result gamma-ray initiated showers should be muon poor.*Wdowczyk* (2) first made detailed theoretical calculation and conclude that muon content in gamma-ray initiated showers should be more than one order of magnitude lower than that of normal showers.Monte carlo simulation results (64,65,66) also indicate that the muon content should be ~ 0.1 of that of proton initiated showers.From the simulation result Mckomb et al (67) concluded that only at energies around 10^{18} eV the photoproduction will significantly contribute to the number of low energy muons.However a number of experimental evidence from UHE gamma-ray observations of different point sources suggest that gamma-ray initiated EAS's are no means deficient in muons.*Samorski and Stamm* used the Kiel array to investigate the

muon content in the excess air showers from the direction of Cygnus X-3.A neon hodoscope of effective area 21.5 m^2 under 880 gcm^{-2} of concrete was used as a muon detector for muons of energy > 2 GeV. They reported (1) that the muon content at the excess showers from the direction of Cygnus X-3 is only slightly less (67 %) than that obtained from a typical proton shower. Similar conclusions have been reached by the Los Alamos group (14). SOUDAN (68) and NUSEX (69) groups reported observations of 4.8 hour modulation in the flux of high energy muons arriving from the direction of *Cygnus X-3*. On the other hand, signals from *Cygnus X-3* detected by the Akeno group during 1986 depend upon the application of a muon poor cut(70).Ohya group (19) also observed UHE radiation from *Cygnus X-3* on the basis of muon poor cut.So it appears at least some of the showers from *Cygnus X-3* have much higher muon content than expected.Hence the situation is very confusing.

To resolve the discrepancy several proposals have been made so far.

i) Incomplete shielding of the muon detectors in the Kiel array allowed some photons *'punch-through'*.

ii) The observed excess EAS's was initiated not by gamma-rays but a new kind of particles (*Cygnet* ?).

iii)The cross section for hadronic interaction of photons is increasing in unexpected way with their energy.

Stanev et al (71) suggested that some of the penetrating particles in 'gamma-induced' EAS from *Cygnus X-3* observed by the Kiel group using a single layer of flash bulbs under 880 gcm^{-2} concrete may be 'punched-through' photons rather than muons.However they concluded that only 30 % of the muon density might be explained in terms of *'punched through'* photons assuming an overall detection efficiency for gamma-rays of 40 % for the neon flash bulbs.

Several authors (72,73 ,74) proposed that the experimental data require the introduction of a new particle. The properties of the initiating particles of the detected excess showers are very tightly constrained as discussed above.The Los Alamos experiment has seen a signal from *Hercules X-1* having a period of 1.24 s .Further the showers came in bursts and arrival time within each burst has periodicity that is characteristics of the period of *Hercules X-1*.This periodicity restricts the rest mast of the particle within few MeV.If the neutral particles are not photons then such low mass particles should have been seen at accelerators.

One possible explanation of the phenomena would be that the cross section for hadronic interaction of photons is increasing with their energy. Except for the differences in the magnitude of the cross-section , the photon-hadron elastic and inelastic reactions behave very similarly to the corresponding pion-hadron reactions at accelerator energies. This behavior can be well explained by theoretical model known as *Vector Meson Dominance* model of photon.The model assumes that photons interact with hadrons by first changing into neutral vector mesons ρ^0, ω^0 , ϕ^0 ,ψ^0 etc.Then the vector mesons that are created interact with the hadrons.The model is usefill in explaining the experimental photon-hadron interactions data.On the basis of the model Beznukov (75) approximated the energy dependence of the cross-section of photo-absorption of real photon by proton which is given by

$$\sigma_{\gamma p}(s) = 114.3 + 1.647 \ln^2(0.0213\ s)\ \mu b$$

where s is substituted in GeV.The photo-nuclear cross-section is in general extrapolated at the air shower energy using the above or similar expressions and used to predict the muon content in a EAS initiated by a gamma-ray photon of primary energy 10^{14} eV or more.But it may happen that gamma-rays have unexpectedly high photo-nuclear inteaction cross sections. A possible mechanism for that has been given by *Drees and Halzen* (76). According to them gluon structure of high energy photons can be the origin of large photoproduction cross section.*Wdowczyk and Wolfandale* (77) have studied the consequences of adopting this hypothesis for EAS. They found no experipental objection against the validity of the hypothesis and in certain cases the description of the experimental data is even better.However still at energies 10^{14} to 10^{16} eV the photoproduction cross section will remain very much small than that of pair production and as long as cross section of photoproduction is very much less than that of pair production the basic features of gamma-ray initiated showers will be unaltered (78). Recent *HERA* (79) results demonstrated that 100 TeV gamma ray initiated showers should in fact be muon poor.

The shower '*age*' is another possible distinguishing feature between gamma-ray initiated showers and hadronic showers.Though a number of authors opposed this idea.

Shower 'age' in gamma-ray initiated showers :

The shower '*age*' parameter, s,is used to characterise the shape of the lateral distribution of photon-electron component in EAS.It is usual to fit the same form of lateral distribution to all EAS's without regarding the nature of the primary particle.Showers that develop early in the atmosphere have on the average larger 'age' than late developing showers of equal primary energy. The energy in an electromagnetic cascade, as it penetrates the atmosphere is attenuated much faster (radiation length 37gmcm^{-2}) than that in a nuclear-electromagnetic cascade in which the energy is carried forward through the relatively stable hadrons (interaction length ~80 gmcm^{-2}).So it was thought that gamma-shower would look much older than normal showers.This philosophy was adopted in numbers of observations and also worked in many of those cases.The Kiel Group observed (1) that the signal from *Cygnus X-3* only in the high (.1.1) 'age' showers.Ooty group (13) obtained a 3.4σ excess in the *Cygnus X-3* direction only when a cut is made at s>1.4 (rejecting 66 % of the data). By selecting showers of age >1.3 an excess over background of 3.8 σ is observed by the MSU group(80) .The Adelaide group (38) made a similar 'age' cut and found the signal from Vela X-1. However no 'age' cut was used in the successful search by the Haverah Park group (11) for evidence of UHE emission from *Cygnus X-3*.

Fenyves (81) from his simulation results opposed the idea of making 'age cut' to discriminate gamma-induced showers from normal showers. *Hillas* (82) and *Cheung and Mackeown* (83) also reached at similar conclusion from their monte carlo simulation results.Thus making 'age cut' to differentiate gamma-ray initiated showers from large background of hadron initiated showers is a controversial question.

Thus a serious problem regarding the nature of the primaries of the observed excess EASs from the discrete point sources arises.

1.3 Aim of the present work :

The aim of the present work is twofold

i) an investigation on the muon component and electro-magnetic component of the EAS to study the nature of the initiating primary particles of the excess extensive air showers from the direction of celestial point sources as observed by several EAS groups.

ii) a search for celestial discrete UHE sources by the EAS technique.

As discussed in the previous section the nature of the radiation emitted by several observed discrete UHE point sources is very confusing. UHE gamma photons are assumed as primaries of such EAS but the excess EAS did not have the photonic signature.The muon content of the excess showers found to be comparable with that of the normal showers and those showers are characterised by high shower 'age' value.Since shower 'age' represents a measure of the longitudinal development of the EAS and muon number does not change much with the atmospheric depth after the maximum development of shower reaches while shower size decreases rapidly with the increase of shower 'age' there is a probability that the high muon content of the observed excess showers from point sources is due to high shower 'age' value.Considering this possibility the variation of the ratio muon density to particle density with shower age at particular radial distance from the shower core for a fixed shower size will be studied.

Monte carlo simulation results (1,2,3) show that 'ages' for gamma-ray initiated showers are nearly same as that of charged cosmic ray initiated showers though in many observations it is found that the signal from different discrete sources is contained only in high 'age' showers.In most of the observations the EAS from point sources were observed at large angles during most of the observation time due to high angle of transit of the sources at the arrays.With the increase of zenith angle the atmospheric thickness increases , so it may happen that the high 'age' values of the excess showers from the direction of point sources is due to high zenith angle of the showers.Taking this possibility into consideration a variation of shower 'age' with zenith angle will be examined.

The present situation of the observation of the discrete UHE sources is also very confusing as discussed in the last section.A number of observations indicate the presence of UHE radiation from some point sources while negative evidences are also reported.Initial observations indicate a steady flux of EAS from the direction of Cygnus X-3 and few other sources.But most of the recent observations unable to detect such emissions. Some of the observations reported the nature of the

emission as sporadic.The flux of emission of radiation from the point sources, particularly from Cygnus X-3 is reported to change by considerable amount during last fifteen years.The Cygnus X-3 is appeared as a variable source.To clearly understand the nature of emission from these sources it is necessary to observe the potential UHE point sources by a large number of EAS arrays spread over the surface of the earth .The NBU EAS array is capable (latitude 26.7^0) to observe the potential UHE point sources of northern hemisphere like Cygnus X-3 , Hercules X-1 , Crab nebula etc very effectively.In the present investigation a search has been carried out to observe continuous emission of UHE radiation from four potential UHE sources - Cygnus X-3 , Hercules X-1,Crab nebula and Geminga.The emission of flux from Cygnus X-3 and Hercules X-1 that has been observed previously as modulated by the orbital periods of the respective objects which are nearly 4.8 h for Cygnus X-3 and 1.7 day for Hercules X-1 has been reexamined.

*** Chapter 2 ***

2.1 Experimental Set-up :

Extensive air shower (EAS) is an unique means for the study of cosmic rays of energies greater than 10^{14} eV. From the fifties the study of extensive air showers using large arrays of particle detector has been made for the interest of high energy physics in the region not accessible in accelerators and also for the study of the characteristics of primary ultra high energy (UHE) cosmic rays. Since the convincing discovery of UHE gamma radiation from Cygnus X-3 by the Kiel group air shower arrays are extensively used in the search for point sources of cosmic rays.

The air shower initiated by a cosmic ray particle or a gamma ray photon in the energy range 10^{14} to 10^{16} consist of about 10^4 to 10^6 particles at sea level. The particles present in an EAS may be classified into three groups, electromagnetic component or soft component which consists of electrons,positrons and photons, muon component and hadronic component.The particles of the electromagnetic and muon components are spread over a large area with density of particles decreases rapidly as the radial distance from the shower core increases. The shower front can be sampled with a large number of particle detectors regularly spread over a wide distance range.

The NBU EAS array :

The small air shower array at North Bengal University campus (latitude $26^0 42'$ N, longitude $88^0 21'$ E , 150 m a.s.l., atmospheric depth 1015 gcm^{-2}) , INDIA , operating since 1982. At present it is composed of nineteen plastic scintillation counter, each of area 0.25 m^2, for the measurement of density of electronic component of air shower, eight fast timing counters to determine the arrival direction of primary cosmic ray particles and two magnet spectrographs of maximum detectable momentum 220 GeV/c. The scintillation counters are arranged in a radial symmetric patern around the centre of the array with a spacing of about 8 m near the array centre and a spacing of about 16 m at the edge of the array. The plan of the array is shown in fig 2.1.1 . The total area covered by the array is about 1600 m^2. The array is designed to observe showers of energies 10^{14} - 10^{17} eV. Timing informations are obtained from eight fast timing detectors, four of them located near the centre of the array while the rest four are placed at the edge of the array. Two magnetic spectrographs , each of an area 0.5 m^2 ,under a concrete shielding absorber are also

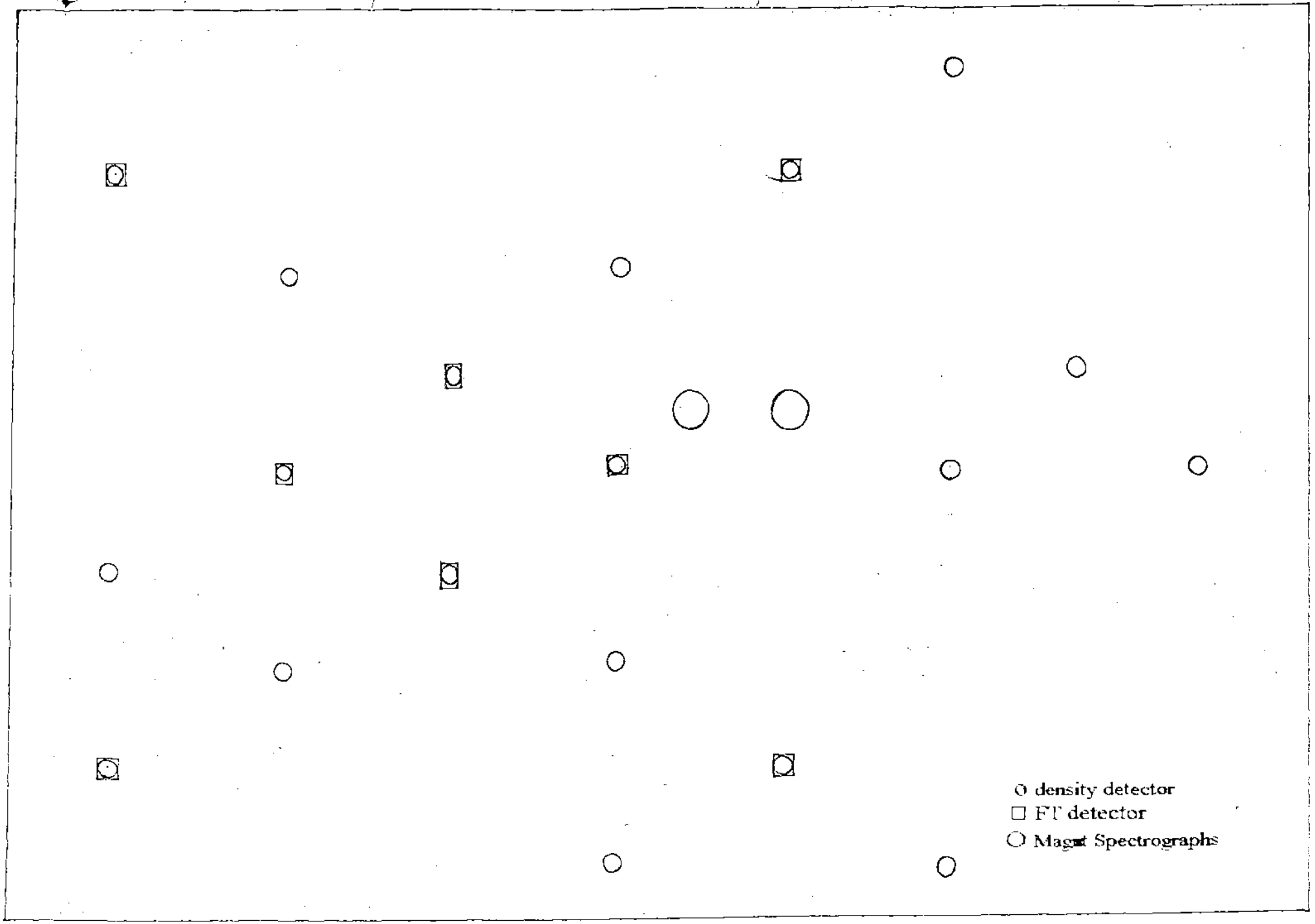

Fig 2.1.1 The NBU EAS array

operated in conjunction with the air shower array for the study of muon component of EAS.

Electron density detectors :

In the NBU air shower experiment plastic scintillation counters are used as particle detector for obtaining the density information of the soft component of the EAS. In each detector a 50 cm x 50 cm plastic scintillator with thickness 5 cm is housed in a pyramidical light tight enclosure made by galvanized iron sheet and viewed from below by a photomultiplier (Philips XP 2050 / Dumont 6364 / RCA 5819) from a vertical distance of about 39 cm (Fig.2.1.2). The inner surfaces of the enclosure are painted with high reflection efficiency material composed of Titanium dioxide (TiO_2) . The photomultiplier tubes are operated in the voltage range 850 - 1200 volt. Different voltages have to be applied to different counters to ensure that the single particle pulse height in different counters are nearly same. The detectors were calibrated for cosmic ray muons. This was done by placing each scintillation counter within a telescopic arrangement of three GM counters , two of which were placed above the detector with their axis mutually perpendicular to each other and the third GM counter was placed below the detector. The variation in the detecting efficiency of the scintillation detectors from the centre of the detector to its edge found small (< 8 %) ,probably due to small size of the detectors.

Fast timing detectors

Fast timing system is one of the important part of the NBU air shower array in order to determine the arrival direction of primary cosmic ray and to investigate the characteristics of EAS at various inclinations. Eight timing detectors are employed in the NBU array to get the timing information of shower front. The shape and size of the scintillator and the enclosure of these timing detectors are the same as electron density detectors. But Philips fast photomultiplier tubes (XP 2020 , rise time ~ 1.5 ns) are used instead of relatively slow photomultipliers(rise time ~ 20 - 30 ns) used in the electron density detectors. These photomultipier tubes are operated at negative voltages of 2000 - 2200 volts to minimise the noise generated from the high voltage power supply.

The magnet spectrographs :

Two magnetic spectrometers are operated in conjunction with the NBU EAS array to study

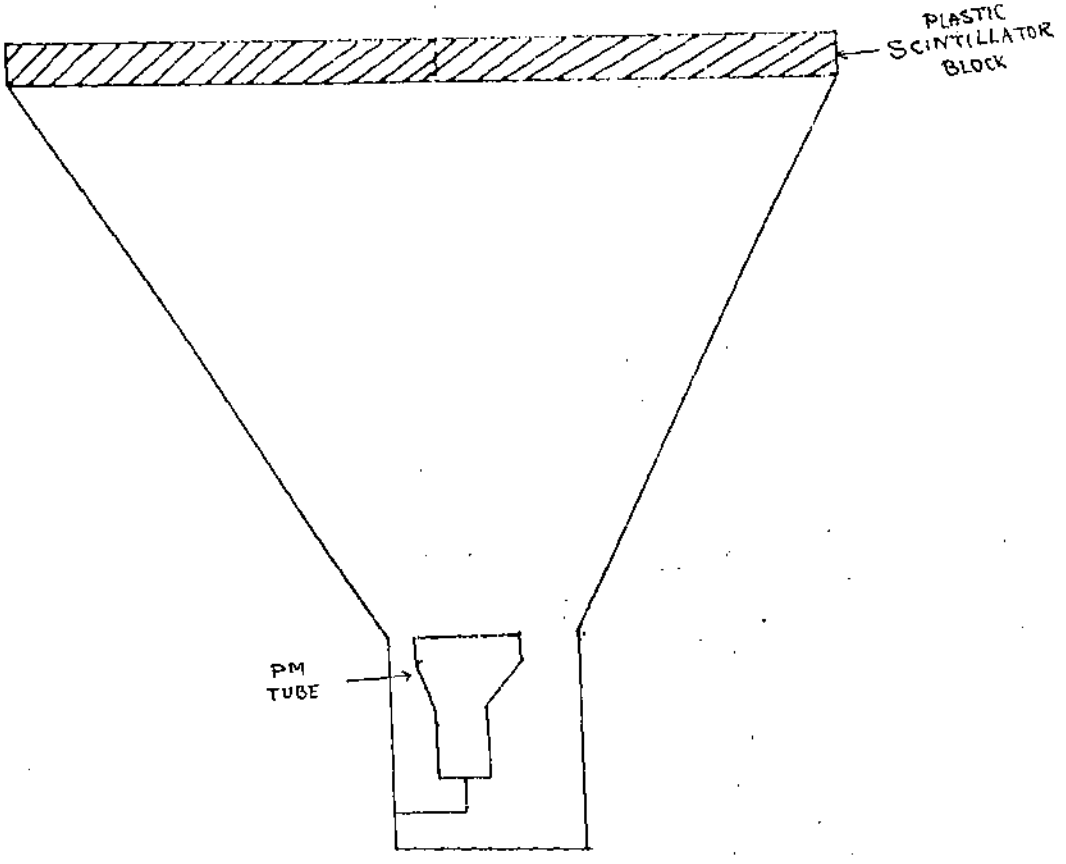

Fig. 2.1.2. SCINTILLATION DETECTOR ASSEMBLY.

the muon component of the EAS. The spectrographs consistsof a solid iron magnet in between four neon flash tube trays. The solid iron is built by placing 80 low carbon content steel plates (180 cm x 125 cm x 1.25 cm) ,having a rectangular hole (35 cm x 19 cm) at the centre, one above another. The height of the iron yoke of the spectrometers (the maximum path of a muon in magnetic field) is 1 m. the magnetic induction in iron is B = 16 Kgs. To filter out the electromagnetic component the spectrograph is shielded by concrete absorber.Additional lead absorber of about 5 cm thickness is placed above the top tray of the neon flash tubes to increase the absorbing capability of the electronic component. The solid iron magnet itself acts as a absorber . As a result the lower energy cut-off for the incident particle is set at 2.5 GeV.The neon flash tubes are placed in a hodoscopic arrangement which are used as muon track detectors. Two flash tube trays are placed above each magnet while two are placed below in such a way that if a muon is detected by the system then the muon have to pass through all the four neon tube hodoscope. The accuracy of locating a muon trajectory is within $\pm$ 0.14 cm. Four cameras are used for recording the muon trajectories from the flashes of the muon tubes. The muon energy is determined on the basis of muon deflection in magnetic field. The magnetic spectrographs limit the zenith angle of acceptance of the incident muons to a few degrees from the vertical.The detailed of the spectrograph is available in (1).

Data Acquisition System :

Data acquisition system is an essential part of any EAS array. In the NBU setup data acquisition system plays a very important role. It first selects an air shower event and when an air shower event occurs it records the event time ,the density information in each particle detector and timing information in each fast timing counter. It also records the muon trajectories in magnetic spectrographs if spectrographs detect muons in coincidence with the air shower trigger. The whole data handling system may be divided into four main parts, a EAS selection system (coincidence circuit) , timing data handling system, density data handling system and muon data handling system.

1.EAS selection system :

In the present experiment an air shower event is selected only when a minimum of four particles per square meter incident within 50 ns in each of the four triggering detectors located near the centre of the array. An EAS selection or trigger circuit is used to generate a fast trigger pulse

whenever the arriving shower satisfy the shower selection criteria.

2. Timing data handling system :

The output pulses from the all first timing detectors are brought to the control room which is located near the centre of the array by means of nearly equal length coaxial cables (RG 58) . Then these pulses are given to a *Lecroy fast discriminator* (Lecroy octal discriminator 623 B). The width of the discriminator output pulse is adjusted to 50 ns which ensure that a coincidence always takes place between timing pulses from four cental detectors when a shower having size greater than the threshold size, is incident within the effective area of the array. The bias of the discriminator is set at half particle level. The fast discriminator outputs are given to a fast coincidence circuit and this coincidence output pulse is used as the start pulse for the eight channel *Lecroy TDC* modules (Lecroy 2228 A) . Outputs of the each discriminator channel is delayed by 172 feet RG 174 cables (total delay nearly 258 ns) and these delayed pulses give the individual TDC stop. From the TDC data the relative arrival times of the shower particles at various points are obtained.

3. Density data handling system :

From each particle density counters essentially the pulse height information is obtained. Knowing average single particle pulse height the number of charged particles traversing the counter can be calculated. To digitise the analogue pulses carrying the information of charged particle density in EAS at various points a *Wilkinson* type *Analogue to Digital Convertor* (ADC) (2) is used.

The output pulses from each particle detector are brought to the main control room through RG-58 co-axial cables using preamplifiers which sit below the photomultipliers of the scintillation counters. These preamplifier outputs are amplified in the control room and fed to the *Sample and Hold* (S/H) (3) circuits. The *sample and hold* circuit holds the peak of the pulse normally for about 3 μs by charging a capacitor. At the end of 3 μs duration the capacitor is discharged and the S/H circuit is ready to accept the next event. Whenever an air shower hits the array and the trigger condition of the array is met a master trigger pulse is generated. This master pulse triggers the *Master Control Unit* (MCU) of the data handling system which in turn generates a set of instructions. It gives a hold command to all the S/H circuits , switches off the input data lines by

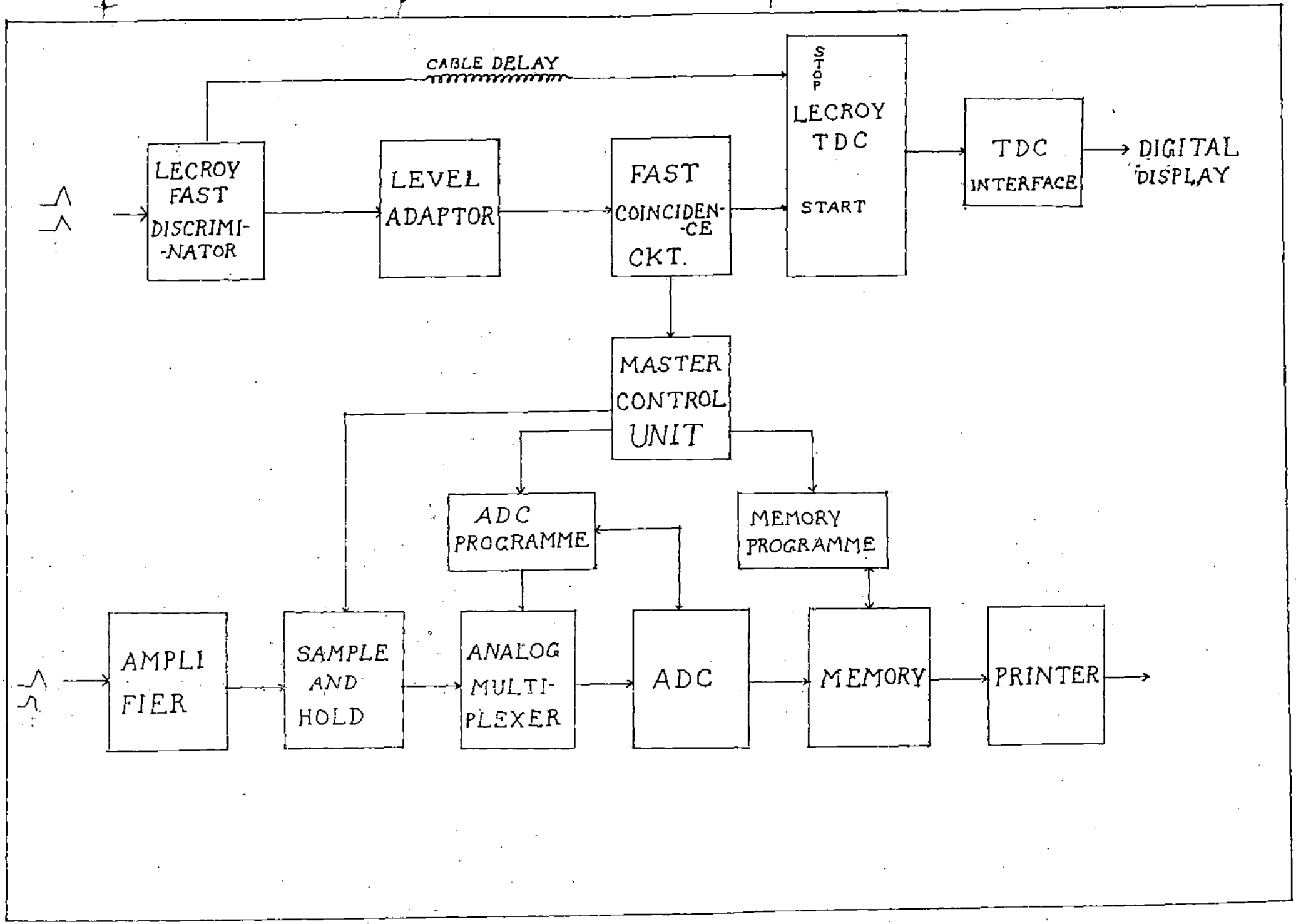

Block Diagram of the Data Handling System.

analogue switches and triggers the ADC programme circuit simultaneously.The muster pulse is also used for the veto of the coincidence circuit. The veto is withdrawn only after the recording of the event time ,the timing informations and the density informations. According to the instruction the S/H circuits hold the input informations at that instant till the the hold command is withdrawn. Now the ADC programme unit connects all the output pulses of the S/H circuits by an analogue multiplexer to the ADC system one after another. It first selects the first channel of the analogue multiplexer and connects it to the ADC system for digitization of the analogue pulse . Once the conversion is over the digitised output of ADC is read into the memory unit. Next the second channel of the *analogue multiplexer* is selected and the same process repeat. The total time required to scale all the density channels is about 8 ms. After the storage of all the density information for all the density detectors in memory unit these data are transfered to the printer for printing on a paper tape.

4.Muon data handling system :

For the detection of muons a telescopic arrangement of scintillation counters are used. Each spectrographs unit is placed in between the two scintillation counters . When a muon passes through the telescope a two fold coincidence pulse is generated. If this twofold coincidence pulse occurs in coincidence with the air shower trigger a high voltage pulse of about 4.5 KV/cm of rise time .75 μs (μs) is applied to the aluminum electrodes placed between the layers of the Neon flash tubes within the 5 μs of the passage of the muon. In the influence of the high energy muon that passes through the spectrographs the Neon flash tubes on its trajectory are ionised and glow with the application of high voltage pulse.Four cameras are used for recording the muon trajectory from the flashes of the Neon tubes.

All the detectors of the array and the data handling system are monitored daily and sequentially.

Modernisation and extension of the existing NBU array has been completed . In the present form the old data handling system is replaced by a fast computer interfaced data handling system. The accuracy in measurement of event time has been improved a lot .Computer hard disks and floppy disks are now used instead of paper tape as storage device of the EAS events.

2.2Data treatment and analysis:

Recorded EAS events are analysed to obtain astrophysical and nuclear physical informations associated with the EAS data. There are a number of observable shower parameters which provide various information about the primary cosmic rays and about the shower development.Estimation of shower parameters is a necessary preliminary in shower analysis. In the current analysis the following routine for estimation of shower parameters has been used.

1. Initial estimation of arrival direction of showers.
2. Estimation of four basic shower parameters viz. core location (x_0,y_0) ,shower size (N_e) and shower age parameter(s).
3.Re-estimation of the arrival angle of shower considering the shower front curvature and the thickness of the shower disk.

Muon data are analysed separately.

Showers are selected for the current analysis if they have

(i) core location within thirty meter from the array center (approximately the array boundary)

(ii) at least five detectors with particle density greater than four per square meter

and (iii) at least four timing measurements of the shower front.

1.Estimation of arrival angles of incident EAS :

An exact determination of arrival direction of showers is important to identify the ultra high energy point sources.The accuracy of the arrival angle determination mainly depends on the capability of accurate measurement of the relative arrival times of the shower particles. The uncertainty in the timing measurement causes by several factors , time spreads of the shower particles in the shower disk, curvature of the shower front ,Instrumental uncertainty of the time measuring instruments ,time offsets etc.

Instrumental uncertainty in timing measurement :

Due to the finite precision of the time measuring instruments used in making the arrival time measurements of the shower particles an uncertainty is introduced in the final directional results. This inherent uncertainty is known as Instrumental uncertainty and is an important

parameter in the directional study.In the present experiment the Instrumental uncertainty is measured in the following way.

The fast timing detector under study is placed above another fast timing scintillation detector thus forming a telescope. Coincidence is taken between the two detectors and this coincidence pulse is used to start the TDC. The pulses from the individual detectors are fed into Discriminator and the output pulses of the Discriminator are given same amount of cable delay. These delayed pulses are used to stop the individual channels of the TDC. If t_d is the time recorded by the detector under study when a particle passes through the telescope , t_0 is the time measured by the other fast detector of the telescope for the same event and d is the vertical distance between them then in ideal cases the quantity $\delta = t_d - t_0 + d/c$ should be zero but in practice only the average of δ for a large number of observations is ~~appeared~~ found to be nearly zero. A distribution is formed for the quantity δ which is shown in fig 2.2.1 . The standard deviation σ for the Gaussian fitting of this distribution gives the uncertainty in the arrival time measurement. Since the uncertainty for two detectors combine (quadritically) in the estimation of σ the uncertainty in the timing measurement for a single detector is $\sigma / 2^{.5}$ which is in the present case $1.22 \pm .03$ ns.

Time offsets of the time measuring instruments :

There may be a finite but constant difference in the actual time of arrival of a shower particle in a fast timing detector and the measured time by the detector. This difference in time is known as time offset of the timing detector. The amounts of offsets are different for different time measuring instruments. Since the actual arrival times of shower particles are necessary to obtain true arrival direction of showers, the measured times have to be corrected for the time offsets before they are used for the directional analysis. The arrival direction of an air shower event is normally determined by the fast timing technique. Using this technique the arrival directions are practically determined by the relative arrival times of the shower particles on each fast timing detector.So only the relative time offsets between the different timing instruments are necessary, not the actual time offsets of the instruments.During the experiment different voltages have to applied to phomultipliers of the different fast timing detectors. This causes different photomultiplier transit time in different detectors. There may be a small difference in the response time of the scitillators and/or photomultipliers of the different detectors. A small difference in cable delay between different channels may exist due to unequal cable length (which is obviously very small)

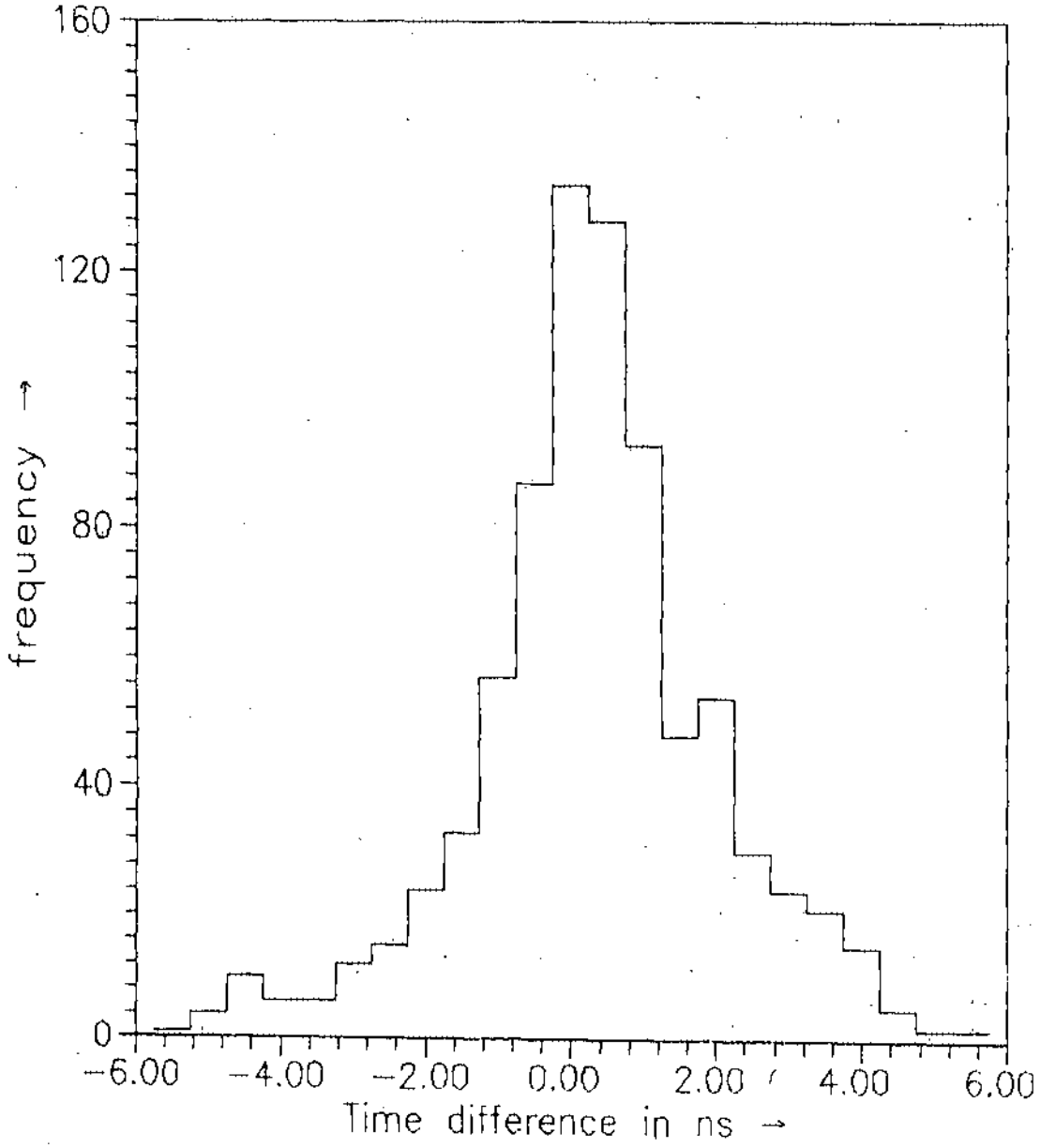

Fig. 2.2.1 Distribution of the deviations in arrival times between two fast timing detectors.
(Average = .34 ± .06 , St. Deviation = 1.73 ± .04)

or any manufacturing differences of cables. There might be a small difference in electronic propagation delay between different time measuring channel. These factors are responsible for the relative time offsets of the time measuring instruments. In the present experiment the relative time offsets are determined in the following way.

Suppose t_i is the true arrival time of a shower particle in the ith detector.Time response delay of the detector,electronic propagation delay , cable delay etc causes a total to_i amount of delay , so that time measured by the detector will be $t^m_i = t_i + to_i$. Here to_i is the true time offset of the ith time measuring instrument.Similarly time measured by the jth detector will be $t^m_j = t_j + to_j$.

Therefore

$$t^m_i - t^m_j = t_i - t_j + to_i - to_j$$

$to_i - to_j$ is the relative time offsets between the ith and jth timing instruments. The summation of the quantity $t^m_i - t^m_j$ is taken for a large number of events. For a large number of events the quantity $\Sigma (t_i - t_j)$ should vanish provided the observed events have azimuthal isotropy (which is expected because of the highly isotropic nature of the cosmic rays) . Hence for each pair of detectors we get

$$\Sigma (to_i - to_j) = \Sigma (t^m_i - t^m_j)$$

or

$$(to_i - to_j - t^m_{ij}) = 0$$

where

$$t^m_{ij} = 1/n \Sigma (t^m_i - t^m_j)$$

n is the total number of events considered.There are eight such equations for eight detectors. Solution of these equations gives the relative time offsets between different detectors.

Initial estimation of EAS direction :

Initial estimation of shower direction is found by a unweighted least square fit of a plane shower front to the timing data. If a detector is not fired in a shower event it will make no

contribution to the calculation of the shower directions. The plane shower front is given by

$$l x_i + m y_i + n z_i + c (t_i - t_0) = 0 \qquad \cdots \quad 1$$

where x_i , y_i , z_i are the coordinates of the ith detector , t_i is the arrival time of a shower particle on the ith detector, l,m,n are the direction cosines and t_0 is a reference time which is actually the time of arrival at a fictitious detector at the origin of the coordinate system. The direction cosines are constrained by the relation

$$l^2 + m^2 + n^2 = 1 \qquad \cdots \quad 2$$

The quantity

$$\chi^2 = \Sigma w_i \{ l x_i + m y_i + n z_i + c (t_i - t_0) \}^2 \qquad \cdots \quad 3$$

where the summation is over all the detectors producing time information of the shower front for that particular event, is minimised to determine the free parameters l, m, n and t_0 . The w_i's are the weight factors all of which are taken 1 in the initial estimation of shower direction. The conditions of minimization of χ^2 with respect to l, m, n and t_0 are given by

$$\delta\chi^2 / \delta l = 0$$

$$\delta\chi^2 / \delta m = 0$$

$$\delta\chi^2 / \delta n = 0$$

and

$$\delta\chi^2 / \delta t_0 = 0$$

Solution of these equations along with the constrained condition of direction cosines (equ. no. 2) gives the values of l, m, n and t_0 in terms of spatial coordinates of the timing detectors and the arrival times of the shower particles at different detectors . The measured arrival times of the

shower particles are corrected for the offset of the corresponding detector before analysis of arrival direction.Thus the direction cosines and hence zenith angle (z) and azimuthal angle (A) of each shower event is determined.

2. Determination of shower parameters :

Estimation of basic shower parameters is a necessary preliminary in shower analysis. The shower core (x_0, y_0),shower size (N_e) and shower age parameter (s) are normally treated as basic shower parameters. The shower core is a point in the shower plane having maximum shower particle density . The shower size gives the total number of shower particles present in the shower at the observation level and the shower age parameter describe the longitudinal development of electromagnetic cascade. Since most of the shower particles are electron and photons , basic shower parameters are determined by the electromagnetic components . There is no direct way of determination of these shower parameters. These parameters are usually estimated in an indirect way by fitting the experimentally observed shower particle densities to a lateral distribution function (ldf) of shower particles. Thus ldf of the soft component of the EAS plays a very important role in the study of cosmic ray air showers. The shape of the distribution is also important by itself since it gives information about the model of shower development.So knowledge of the ldf of the soft component of the EAS is a prerequisite for the analysis of showers detected with scintillation counters.

Different authors proposed different functional forms of the lateral distribution of the electromagnetic component of EAS but till now there is no one functional form of general acceptance.Basic analytical work in this field is due to Moliere(1) .However Moliere distribution is only applicable near the maximum development of the cascade. Nishimura and Kamata (2) extended the earlier work and obtained a distribution for all stages of development. Greisen (3) put forward an empirical relation representing the Nishimura and Kamata distribution which is the well-known NKG function and is given by

$$\rho(r) = c(s)\, N_e\, (r/r_m)^{s-2}\, (1 + r/r_m)^{s-4.5}$$

where $\rho(r)$ is the density of shower particles at radial distance r from the shower core , s is the shower age parameter , N_e represents the shower size, r_m is the Moliere radius and $c(s)$ is the normalisation constant which is given by

$$c(s) = 1/(2\pi r_m^2)\ \Gamma(4.5 - s)/\{\Gamma(s)\ \Gamma(4.5 - 2s)\}$$

The NKG function has been widely used in the analysis of electron density data of air showers. However for several years, a number of authors has pointed out that the NKG function does not give a good description of the electron lateral distribution of air showers. Now there is consensus among the researchers of the field that the correct lateral distribution is substantially narrower than the NKG function. But the NKG function as a whole seems better than the other lateral distribution functions in interpreting the experimental data. Moreover most of the cosmic ray groups are using NKG function to analyse their air shower data in connection with the search for UHE radiation from discrete point sources.To compare the results of the present experiment with the results of other EAS experiments it is necessary to use the same lateral distribution function of electrons for estimation of the shower parameters. So considering the above factors, in the present analysis we use NKG function as lateral structure function for electronic component of air showers.

The main parameters of individual EAS were determined using a computer. The density informations of shower particles at different detectors are obtained from the ADC readings. The shower parameters i,e, the core location (x_0,y_0) , shower age (s) and shower size(N_e) have been determined by minimising a weighted chi-square (χ^2) which is defined as follows

$$\chi^2 = \Sigma W_i (\Delta^o_i - \Delta^o_i)$$

where Δ^o_i is the observed density in the ith particle detector which is related to the corresponding ADC reading D_i by the relation

$$\Delta^o_i = D_i / (A_i \times C_i)$$

A_i is the area of the ith detector and C_i is the callibration factor obtained from the single particle pulse height measurement. Δ^e_i is the expected density in the ith detector which is calculated by

substituting the estimated shower parameters in the NKG function and W_i is the statistical weight factor which is taken as

$$W_i = (1/ \sigma_{poisson}^2)$$

The condition of minimisation of χ^2 with respect to shower parameters is given by

$$\delta\chi^2 / \delta Q_i = 0$$

where i = 1 to 4 and Q_i 's are four shower parameters. The above equations are highly non linear and difficult to solve analytically. So independent estimation of the shower parameters are not possible from the above equations. Hence an iterative procedure is applied to estimate the parameters. An iterative process of determining the shower parameters is to adjust the value of shower parameters such that the value of χ^2 becomes minimum. In the present analysis the quantity χ^2 is minimised by using the standard method of steepest descent and the values of x_0 , y_0 , s and N_e for each shower are determined.

Study on shower front curvature :

It is well known that the leading particles in the shower front do not lie on a plane and the time spreads of the shower particles in the shower front increases with core distances (4). Due to the nearly cone like shape of the shower front a systematic inclination of the fitted shower direction is expected if the shower front is approximated by a plane and if sampling of the time information are not systematic around the shower core. Shower disk thickness is also a function of the core distance and as a result the spread of the time distribution increases with core distance.In the present experiment an attempt has been made to determine the shower front curvature and the variation of time spreads of the shower particles in the shower front with core distances the following method.

A preliminary arrival direction of the shower is determined by fitting an unweighted plane to the arrival time of shower particles of those detectors which are within 15 m from the shower core provided number of such detectors in the shower event are at least four. The plane approximation of the shower front may be used for small core distances. The deviation of arrival

times from the plane front for the remaining detectors are calculated and the mean measured delays of the shower particles at different core distances are estimated. The mean delays from the plane approximation of the shower front as a function of core distances is shown in fig 2.2.2 . It is found that the mean deviation increases with the increase of core distance, consistent with the results of the Haverah park group (4) and the monte carlo simulation results of Hillas (5) , but the observed variation is not very smooth. This is probably because a small number of timing detectors are used in the present experiment to get the timing information of shower particles. The variation can be expressed by a linear relation of the type

$$dt = a r + c$$

The least squares fit of the results to a straight line gives the value of a = 0.19 and c = -2.12 .

The r.m.s. deviation of arrival times with the core distance is shown in fig 2.2.3 for two different shower sizes. It is observed that the time spread increases with the increase of core distance but decreases with the increase of shower size. The observed spread is compared with the Linsley's formula (6) (a dashed line in the fig 2.) which is given by

$$\sigma_t = \sigma_0 / n^{.5}(1 + r/r_t)^b$$

with σ_0 = 2.6 ns ,r_t = 30 m and b = 1.5 , n is the number of particles that hit the detector . In the Fig 2. n is taken as the particle density corresponding to a shower of Ne = 2.5×10^5 and 'age' 1.3. The observed spread is found slightly greater than that given by the Linsley's formula.

3. Re-estimation of the arrival direction :

The shower core position is used to refit the timing informations for all the detectors. Using conical shower front and radial distance dependent weight factors the arrival directions of each shower event are recalculated. The weight factor used in the analysis is given by

$$w_i = 1/\sigma_{total}^2$$

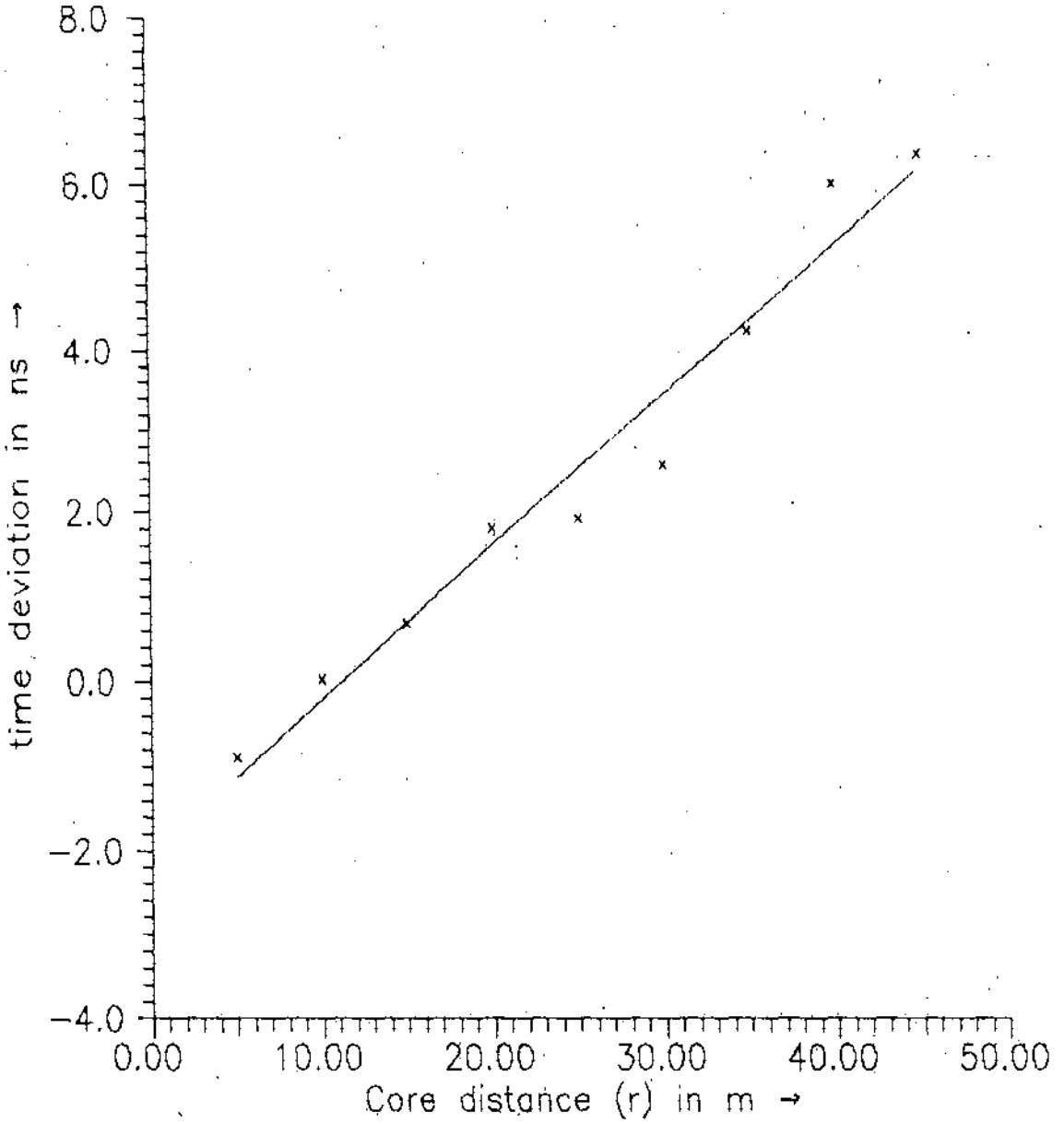

Fig 2.2.2 Variation of mean deviation of arrival times from a plane shower front with core distances. The solid line is the least square fit of the data to a straight line.

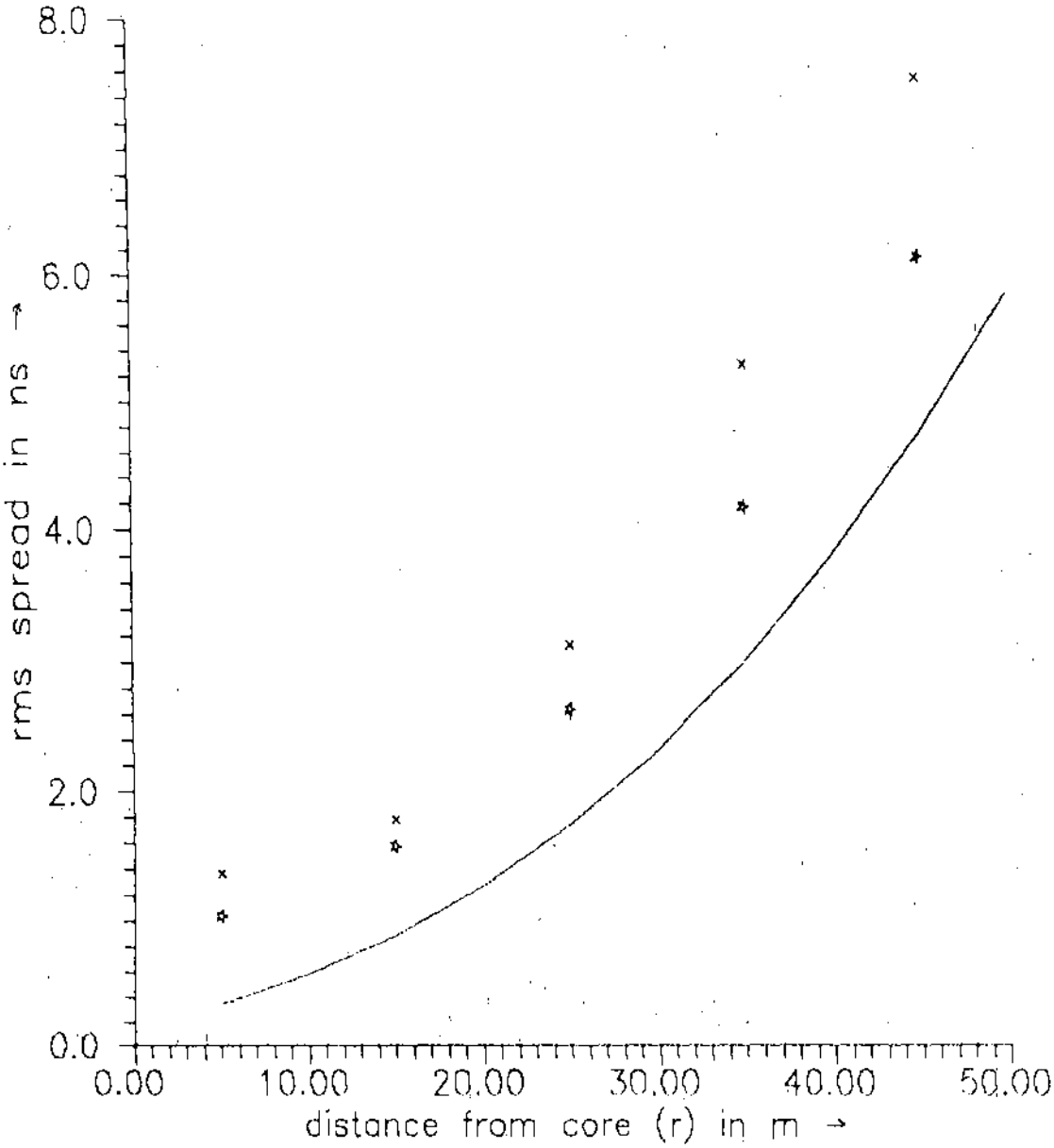

Fig 2.2.3 Variation of rms spread of arrival times with core distances for two shower size range, x – $Ne < 2 \times 10^5$, * – $Ne > 2 \times 10^5$. The solid curve represents linsley's formula (for shower size $Ne = 2.5 \times 10^5$, and shower 'age' $s = 1.3$) .

where $\sigma_{total}^2 = \sigma_t^2 + \sigma_{inst}^2 + \sigma_{electronics}^2$

An accepted timing fit to a shower front is judged by the value of the quantity

$$\chi_t^2 = 1/(n-3) \Sigma w_i (t^0_i - t^e_i)^2$$

where t^0_i , t^e_i are the observed and expected time at the ith detector respectively , n is the number of timing detectors fired in the shower event .and is also judged by the deviation of the measured times , $dt_i = t^0_i - t^e_i$, of different detectors. If $\chi_t^2 > 5$ or any $dt_i > 3$ then events are reanalyzed after rejecting the most deviant detector. The process is repeated until $\chi_t^2 < 5$ and all $dt_i < 3$ or if the events have not remained in four time- measurements of the shower front.

Examples of observed shower data and reconstructed shower parameters from the observed data for two typical observed EAS events are shown in Fig.2.2.4 and Fig. 2.25.

Arrival direction in equatorial co-ordinate system :

During the diurnal motion of a heavenly body its altitude and azimuth continually changes. Also even at the same instant , at places of different latitudes the same body has different altitudes and azimuths. However right ascension and declination of a heavenly body remain the same during their diurnal motion. So 'equatorial co-ordinates' are normally used to define the position of a star.

If the observer's latitude is ϕ and the z and A are the zenith and azimuth of a heavenly body then its declination is given by

$$\delta = \mathrm{Sin}^{-1}(\mathrm{Sin}\phi\, \mathrm{Cos}z + \mathrm{Cos}\phi\, \mathrm{Sin}z\, \mathrm{Cos}A) \quad .....$$

and if h be its hour angle then

$$h = \mathrm{Sin}^{-1}(\mathrm{Sin}z\mathrm{Sin}A/\mathrm{Cos}\delta) \quad .....$$

If a heavenly body is observed at local siderial time lst and h is the hour angle of the body then the

Event No 6064

The event time = 3 hr 12.4 minute(Local Siderial time) , Date = 22.03.94
Zenith angle = 18.6° Declination = 19.4°
Azimuthal angle = 250.7° Right Ascension = 209.5°
Chi-square/degrees of freedom = 1.05 (for timing data fit)

Shower Core Xo = 6.0 m Shower Age (S) = 1.64
Yo = 13.5 m Shower Size Ne = 2.0 x 105
Chi-square/degrees of freedom = 0.80(for density data fit)

Core distance (r) in m	Observed density in particles/m2	Fitted density in particles/m2
11.2	16.0	13.3
6.2	16.0	19.3
28.8	4.0	5.7
15.7	8.0	10.9
10.5	16.0	13.9
5.6	20.0	20.4
15.2	8.0	10.6
8.1	16.0	16.4
18.3	8.0	9.0
20.2	8.0	8.3
34.1	8.0	4.7

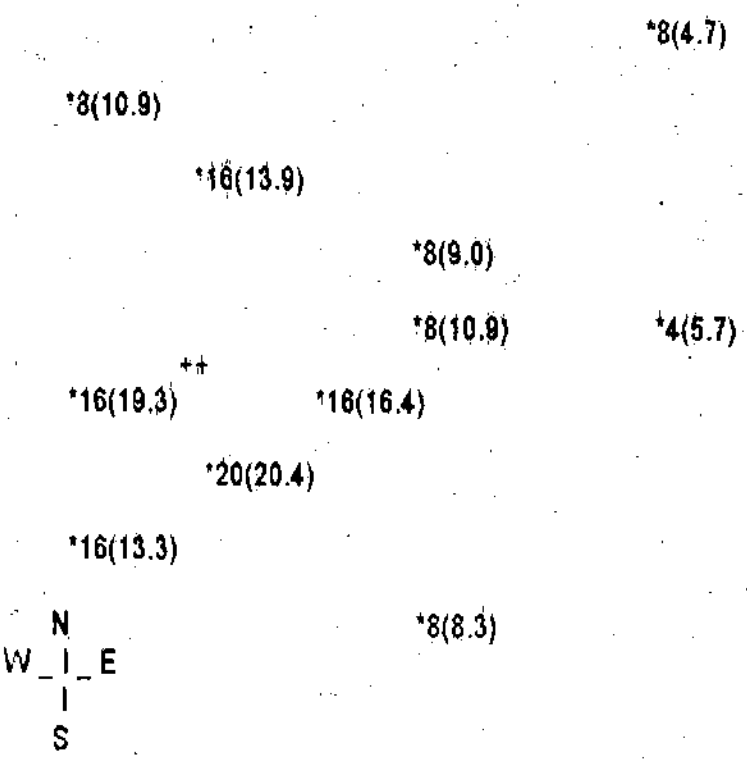

Fig 2.2.4a. Observed shower data and reconstructed shower parameters from the observed data

Event No = 1700
Event time = 1 hr 40.4 minute(Local Siderial time) , Date = 27.01.94
Zenith angle = 28.4° Declination = 47.9°
Azimuthal angle = 36.4° Right Ascension = 49.3°
Chi-square(/degrees of freedom) = 1.03 (for timing data fit)

Shower Core Xo = 28.0 m Shower Age s = 1.18
Yo = 13.0 m Shower Size Ne = 1.1 x 105
Chi-square(/degrees of freedom) = 2.12

Core distance (r) in m	Observed density in particles/m2	Fitted density in particles/m2
28.0	4.0	6.4
7.3	36.0	38.7
31.8	4.0	5.1
14.6	16.0	16.9
7.6	40.0	37.2
14.0	16.0	17.8
15.7	12.0	15.4
11.5	28.0	22.9
13.2	16.0	19.3
13.0	8.0	19.6
17.5	8.0	13.2
14.8	16.0	16.7
9.0	32.0	30.8
20.1	20.0	10.8

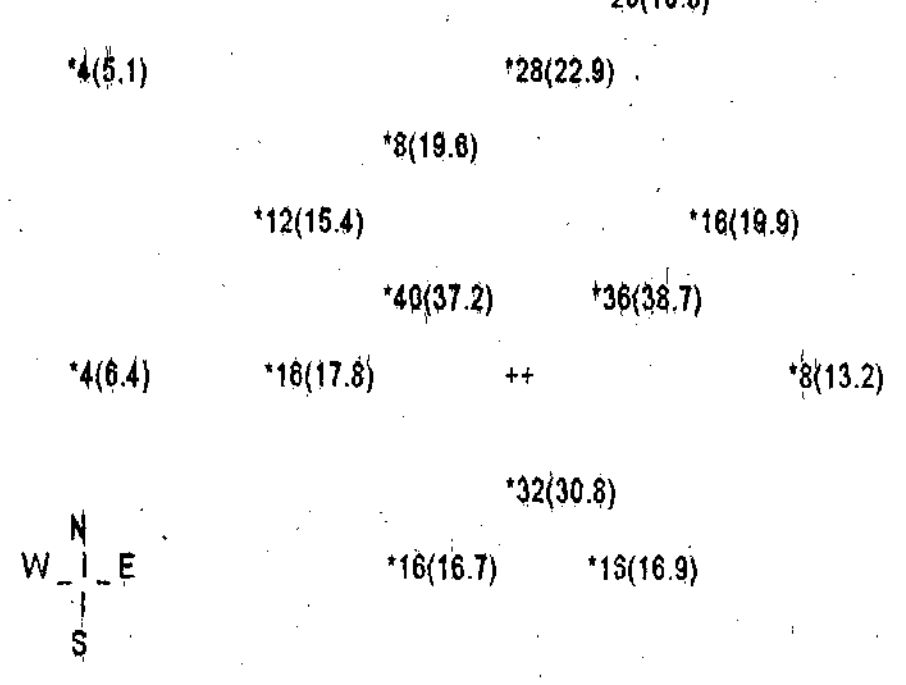

Fig 2.2.5b. Observed shower data and reconstructed shower parameters from the observed data

right ascension of the body α is given by

$$\alpha = lst - h \qquad \ldots\ldots\ldots$$

2.3 Precision of the measurements:

It is evident that any feature of EAS will be affected by the errors in estimation of the shower parameters.In order to estimate the errors in shower parameters as measured by the array and to ascertain any systematic biases in the analysis of air shower events artificial air shower events are simulated and then the simulated data are analysed with usual analysis programme.By selecting random shower sizes from an incident power law shower size spectrum ($N^{-2.5}$) with zenith angle modulated of Cos^7z in the size range 10^4 - 10^7 showers have been simulated and randomly projected over an area (a circular area of radius 40m with centre in coincidence with the array centre) approximately twice that of the array. The charged particles of EAS are expected to follow NKG distribution function.Poission fluctuation on recorded particle numbers have been incorporated.These simulated events are then analysed and interpreted using the same methods and criteria that are employed with genuine data.From the simulation study it is found that there is no systematic biases in the analysis procedure employed in the experiment.The distribution of differences between the simulated parameters and fitted parameters are shown in fig.2.3.1 . The width of these distributions give the error in the estimation of the corresponding shower parameters which are as follows

i) Uncertainty in Core location (a) $\delta x_0 = 2.04 \pm .05$

(b) $\delta y_0 = 2.16 \pm .05$

ii) Uncertaity in shower size $\delta N_e/N_e = (15.6 \pm .3)$ %

and iii) the value age parameter is uncertain by $\delta s = .109 \pm .002$

The χ^2 distribution for the experimentally observed that and that obtained from the analysis of the artificial shower data are shown in fig.2.3.2 .

Angular Resolution of the NBU EAS array :

An exact determination of arrival direction of shower is especially important to identify point sources.Some error is introduced in the estimated arrival direction due to instrumental uncertainty of the time measuring instruments, time spread of shower particles in shower disk, finite number of time measuring detectors etc . The accuracy in the measurement of angular co-ordinates

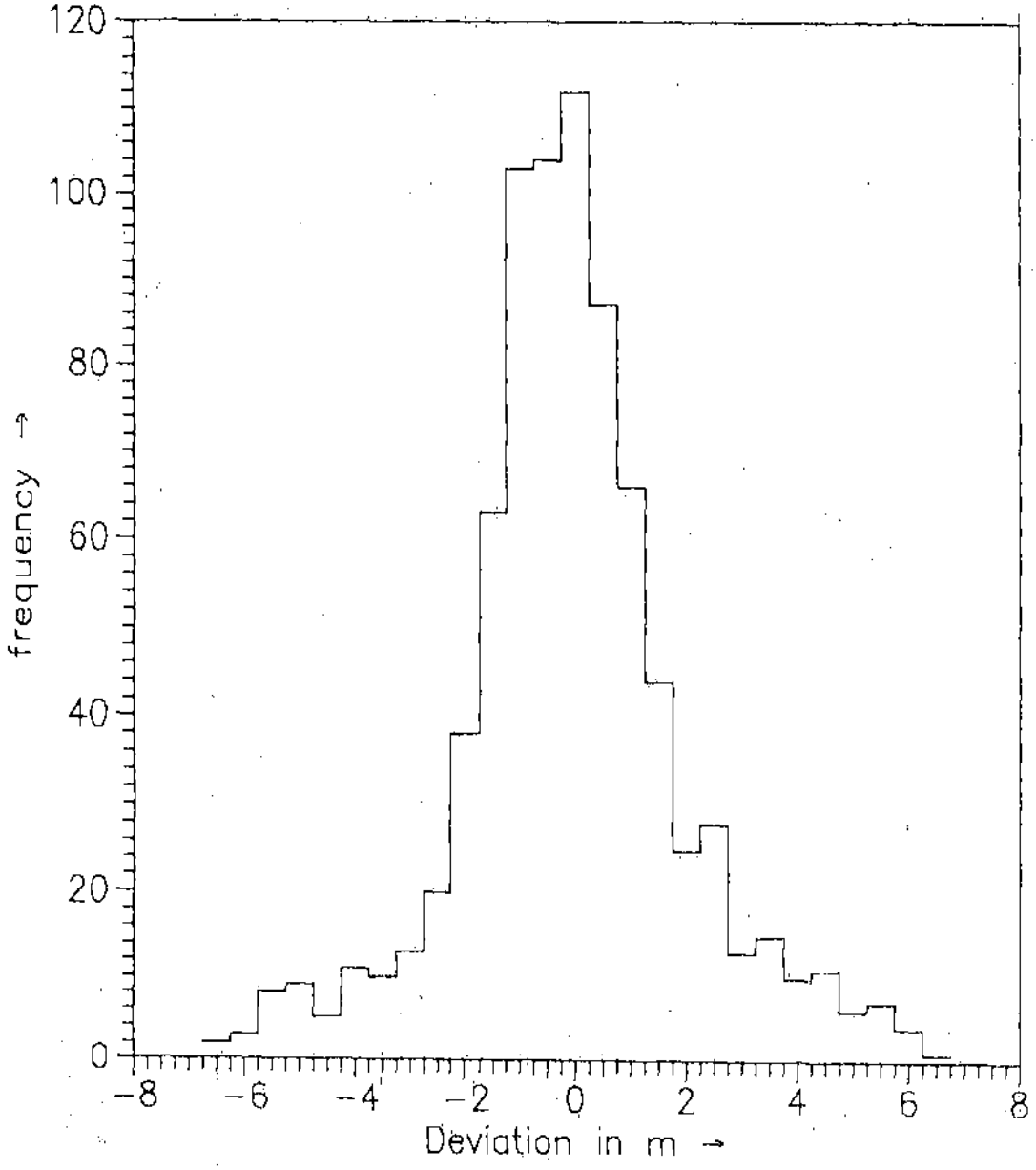

Fig 2.3.1a Distribution of deviations of the estimated core (x) from the true core position (from simulation results).

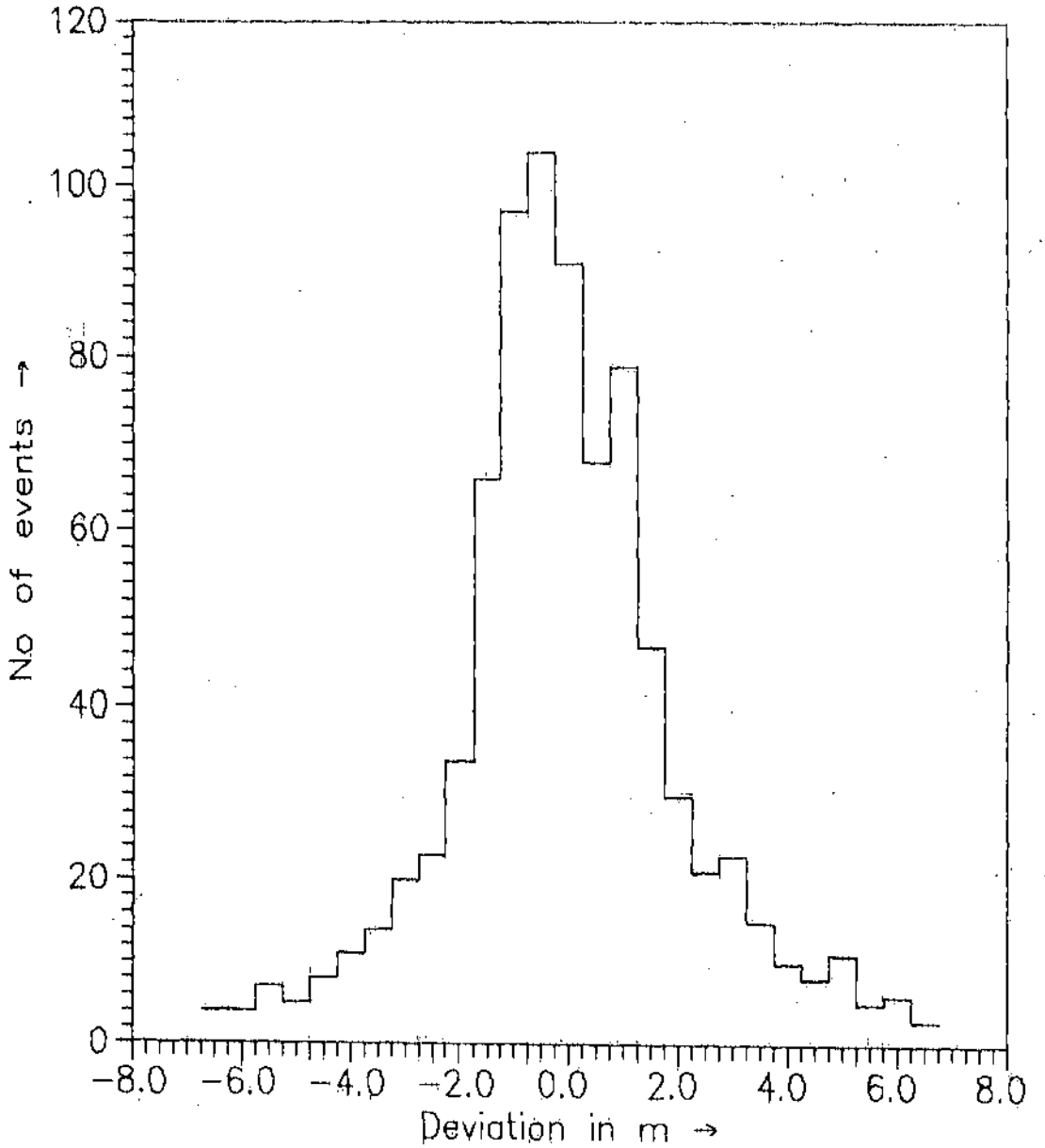

Fig 2.3.1b Distribution of deviations of the estimated core (y) from the true core position (from simulation results).

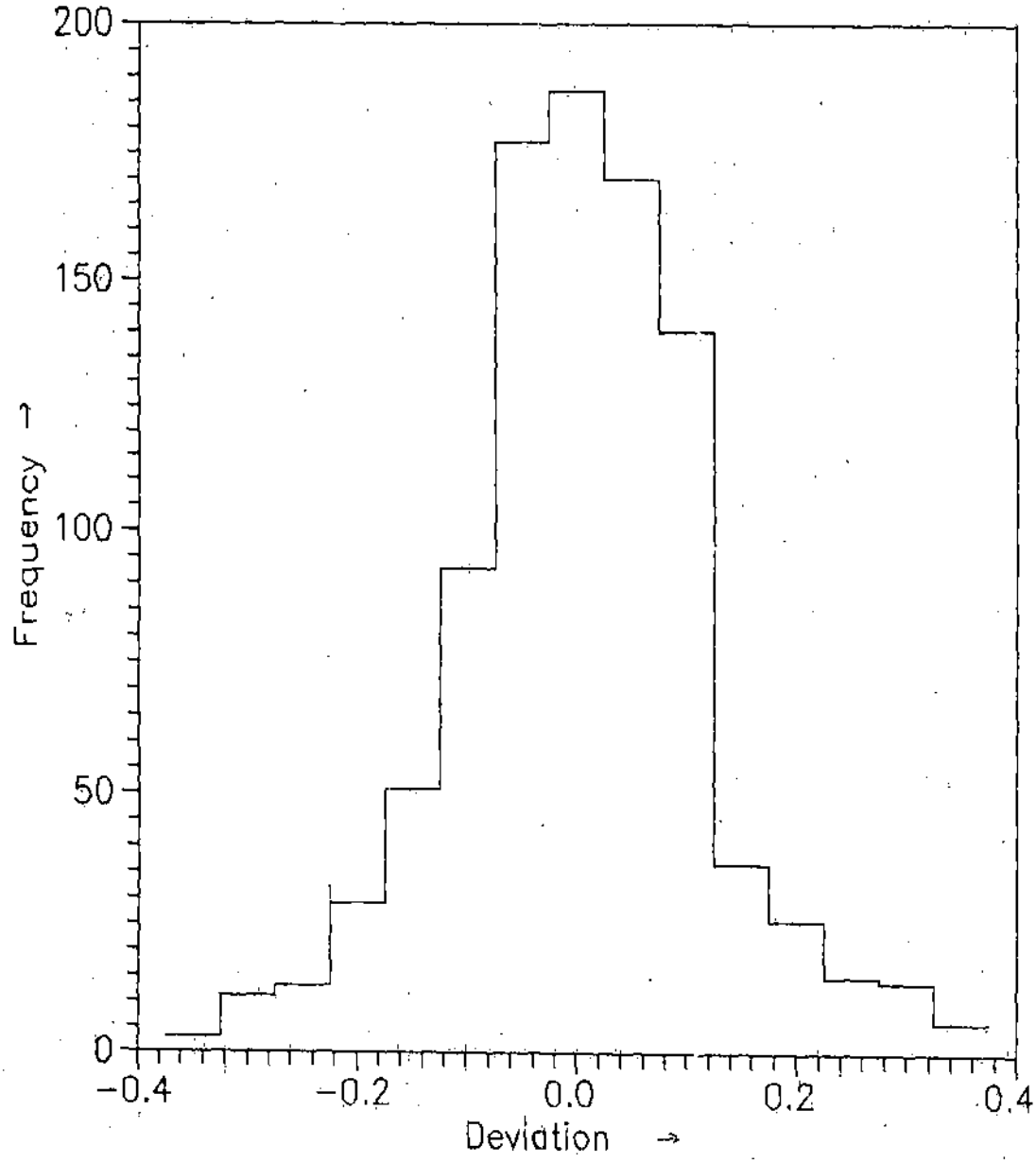

Fig 2.3.1c Distribution of deviations of the estimated age (s) from the true age (from the simulation results).

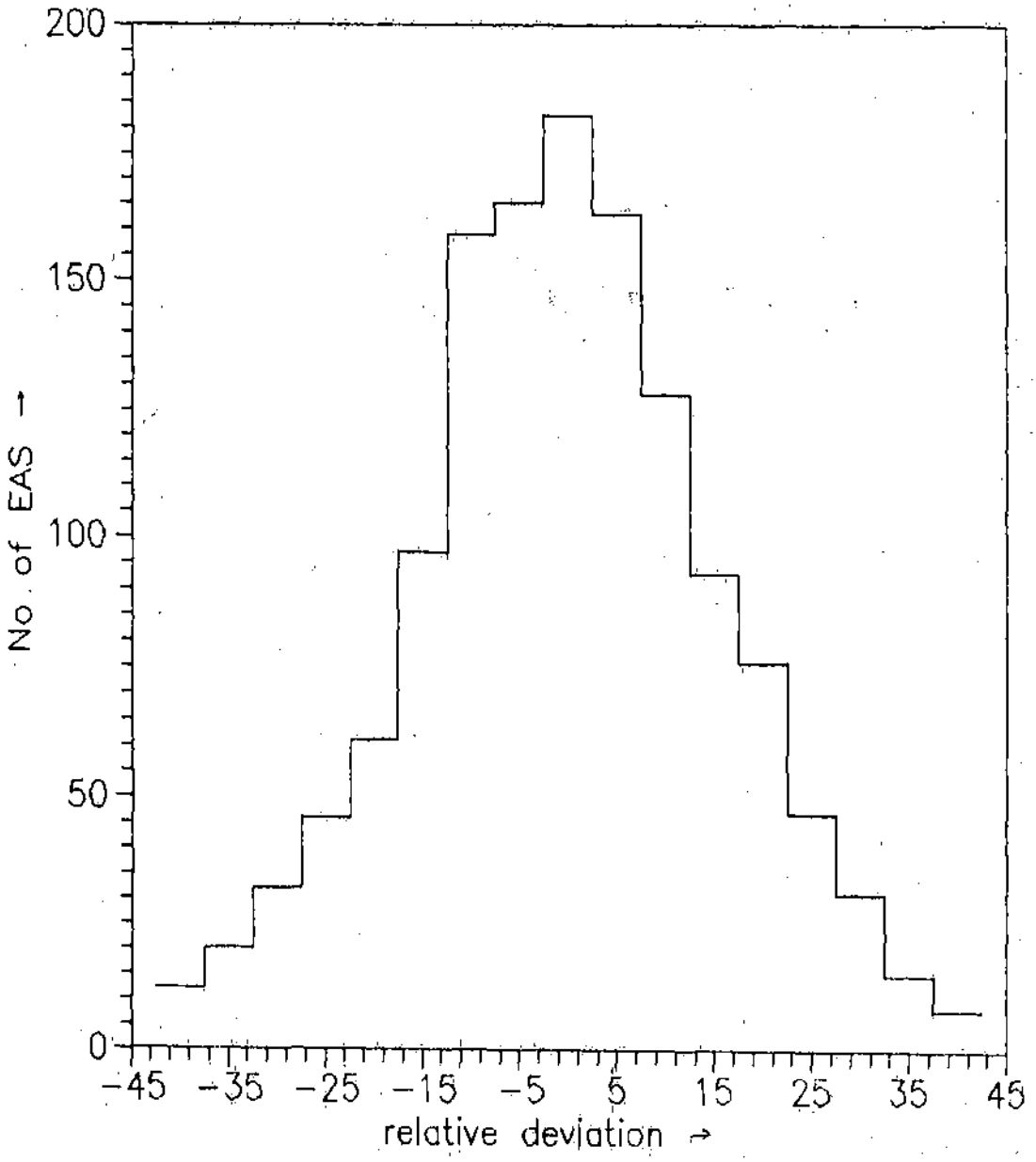

Fig 2.3.1d Distribution of rediative deviations of the estimated size (Ne) from the true shower size(from simulation results).

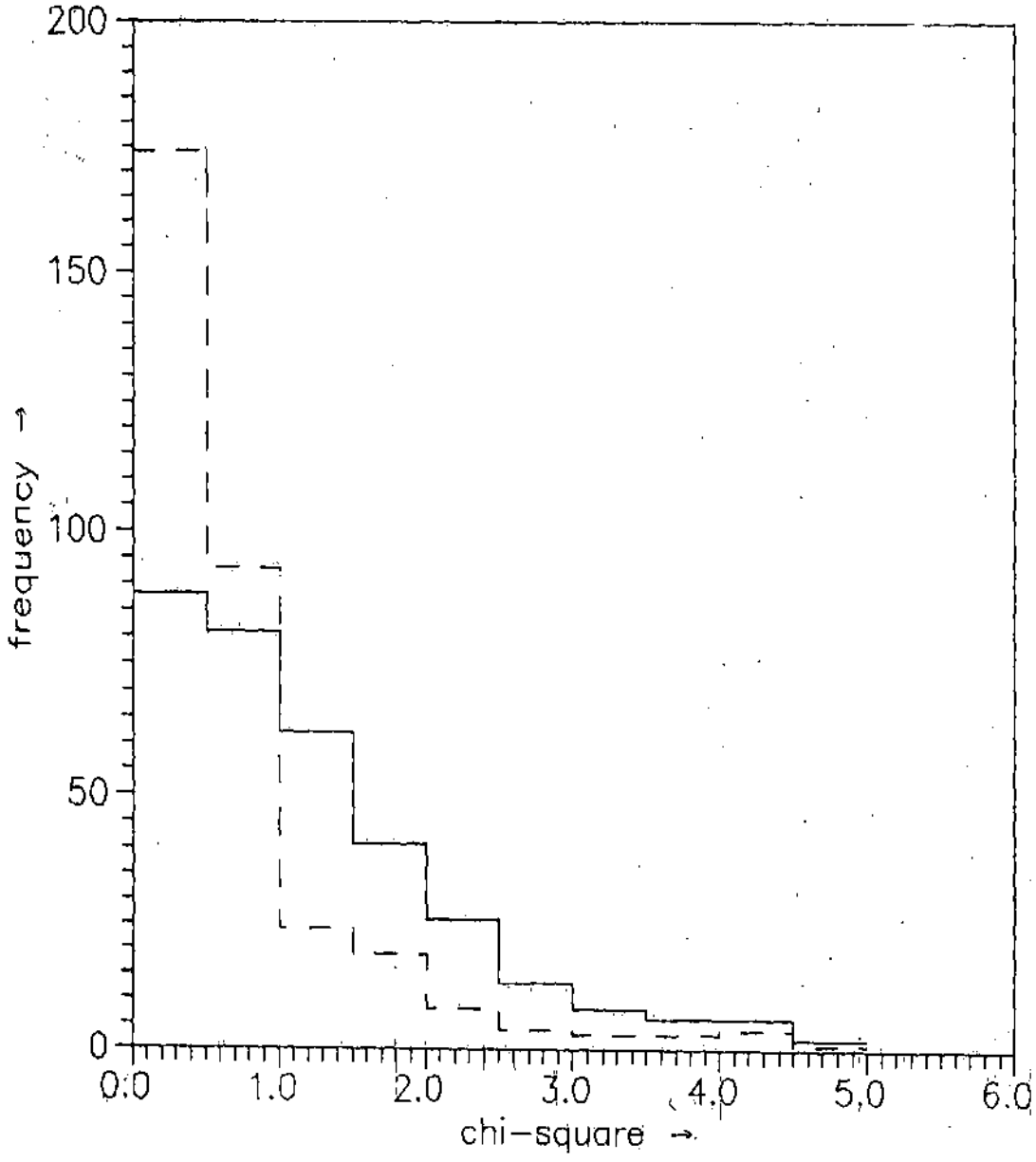

Fig 2.3.2 Chi-square distributions for experimentally observed shower data (solid line) and for artificial shower data(dashed line).

i,e, angular resolution of an air shower array is thus a very important parameter to estimate.In the absence of a point like source in UHE range which can serve as a steady candle the angular resolution of the NBU EAS array has been estimated by the conventional 'split array ' method.For the determination of angular resolution only those shower events are selected in which all the eight fast timing detectors give information about the relative times of shower front particles.The total eight detectors are divided into two sets (even and odd detectors) and two independent estimate of the arrival direction of the same event has been made from two sub-arrays. The mean space angle difference ($d\psi$) between the two arrival direction is calculated.The frequency distribution of differences ($d\psi$) is shown in fig 2.3.4 .The frequency distributions of differences in zenith angle, azimuthal angle and in equatorial co-ordinates are shown in fig.2.3.5 .The width of the Gaussian fitting of these distributions give the uncertainty in measurements of corresponding parameters.Since error in determining angular co-ordinates from the two independent sub-arrays added quadritically in the resulting distribution and there are twice as many detectors in the whole array then the individual sub-arrays so the angular resolution of the whole array will be $1/2^{1.5}$ times of the width of the distribution.The resolution of the array in different angular co-ordinates is shown in table 1.

Table 1

Angular Co-ordinates	Zenith	Azimuth	Declination	Right-ascension
Resolution from Experimental data	$1.10^{o}\pm.02^{o}$	$1.99^{o}\pm.03^{o}$	$1.10^{o}\pm.02^{o}$	$1.44^{o}\pm.03^{o}$
Resolution from Simulation data	$0.55^{o}\pm.02^{o}$	$1.65^{o}\pm.07^{o}$	$0.54^{o}\pm.02^{o}$	$1.03^{o}\pm.04^{o}$

It is found that the resolution of the array is not very good in azimuth.This is probably due to small number of detectors used for the time measurement.In order to check the resolution of the array Monte Carlo simulation have been carried out.Particle arrival times were generated using the

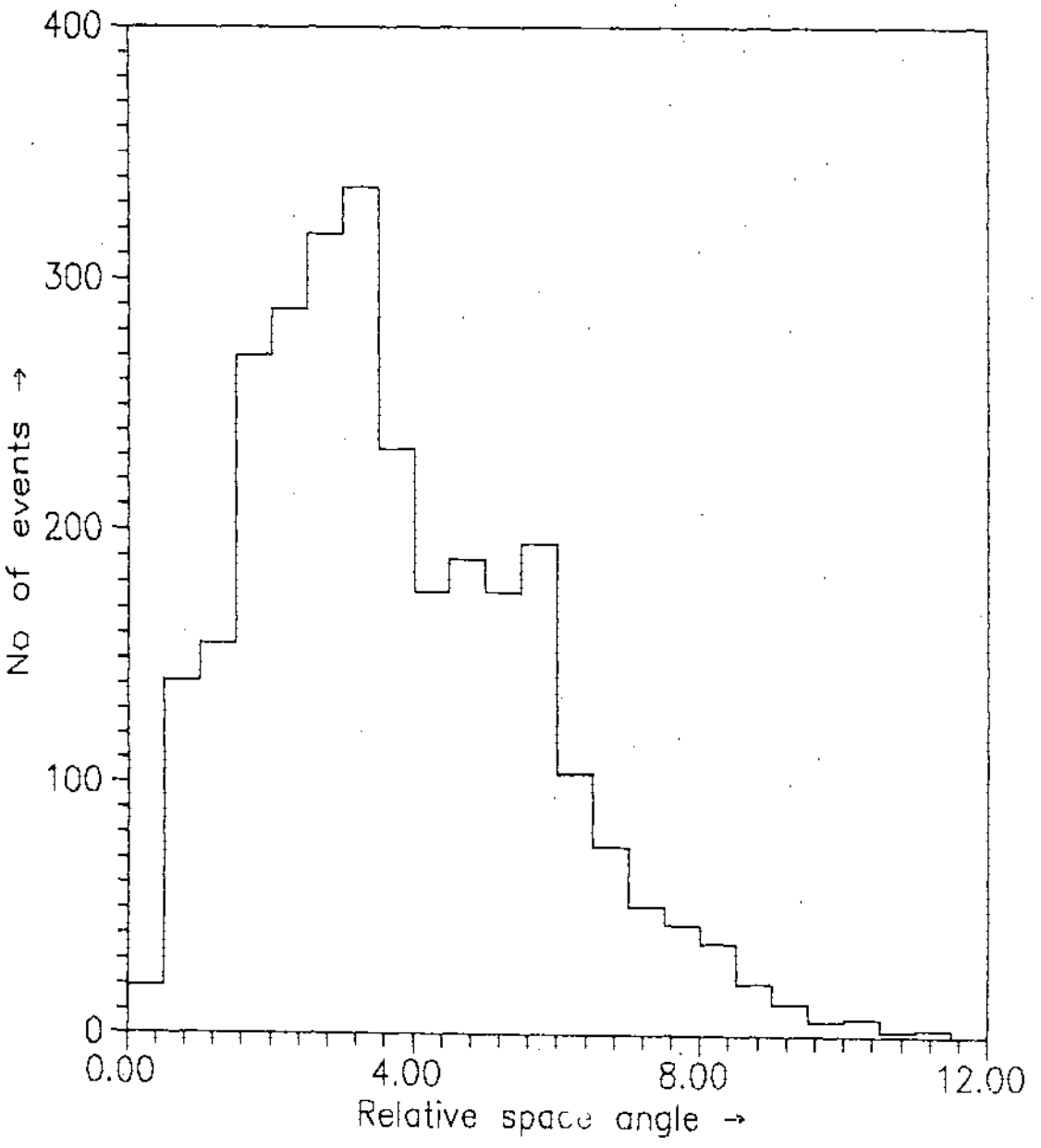

Fig 2.3.4a Distribution of relative space angle measured by two sub arrays for weigted curved shower front.

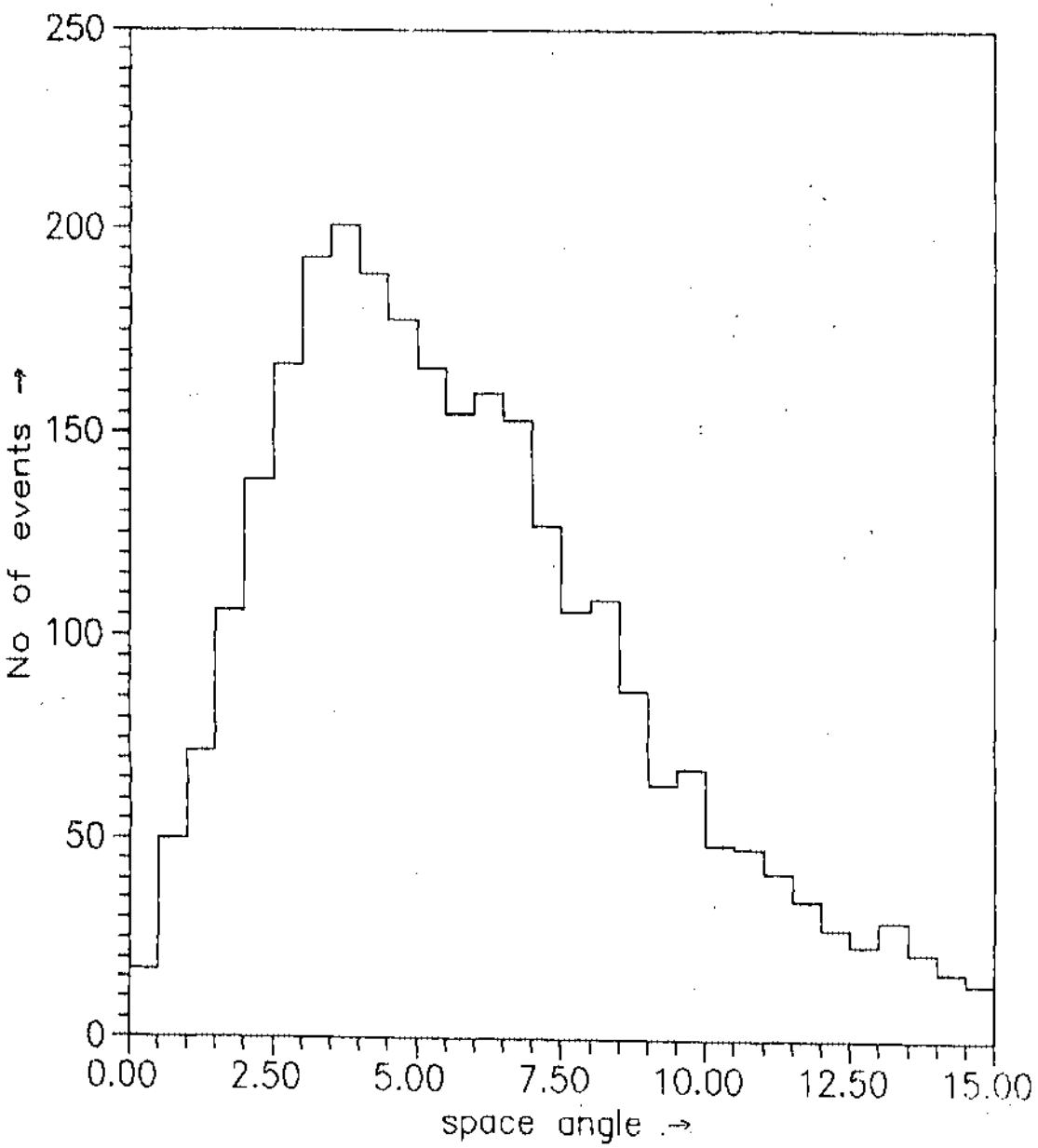

Fig 2.3.4b Distribution of relative space angles measured by two sub arrays for an unweighted plane shower front fit of arrival times.

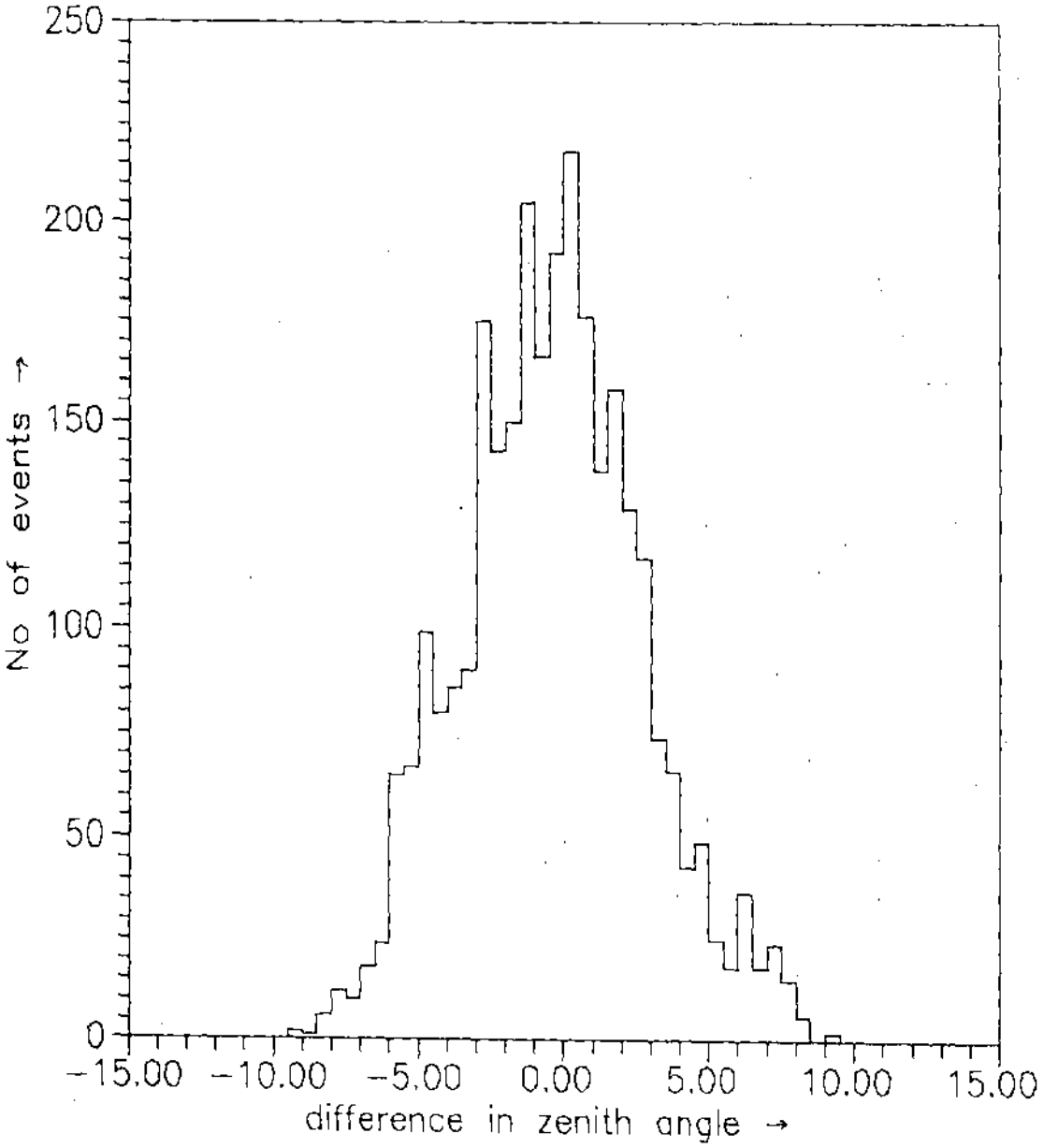

Fig 2.3.5a Distribution of relative deviations in Zenith angle.
(Average = −.37 ± .06 , sigma = 3.12 ± .04)

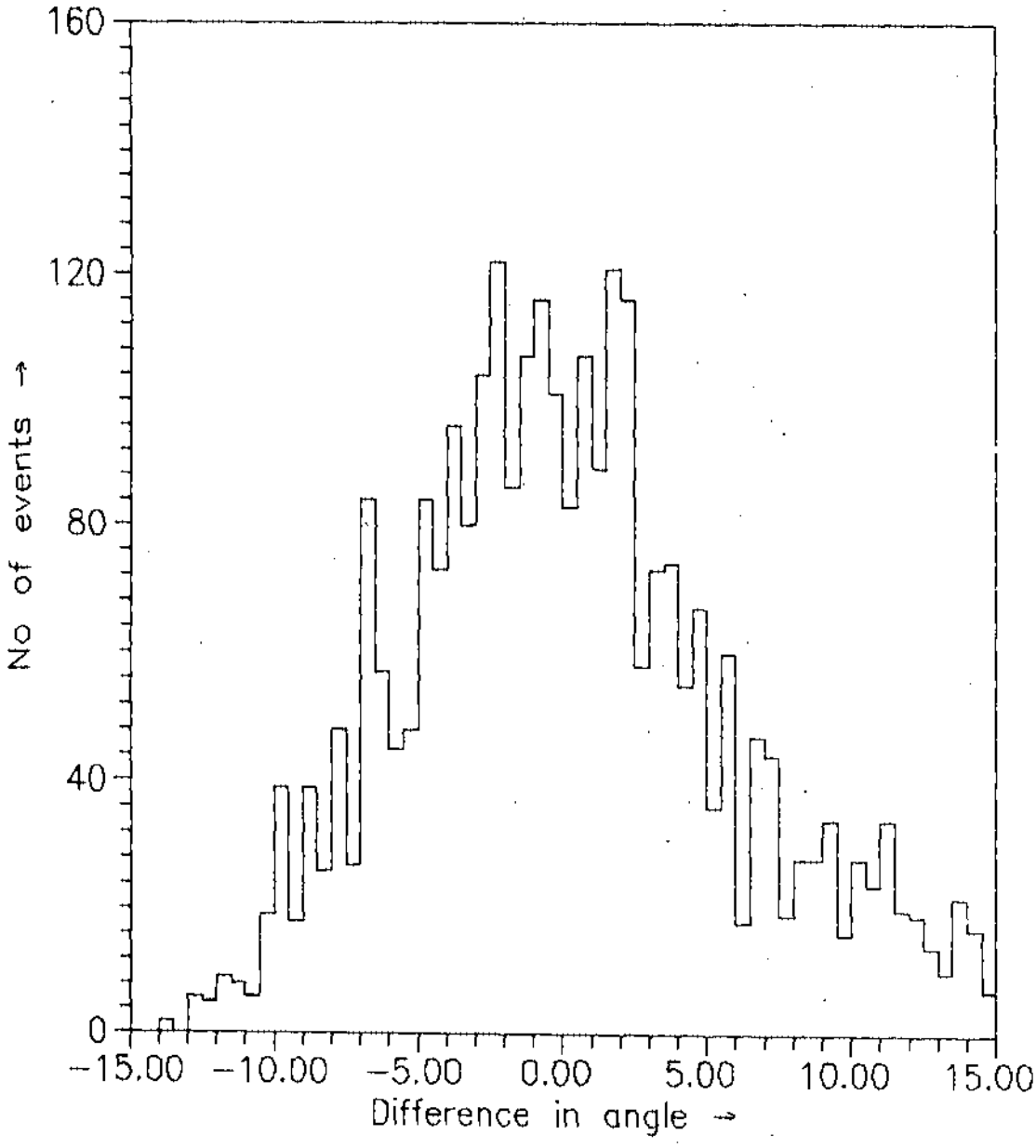

Fig 2.3.5b Distribution of relative deviations in Azimuth angle
Average = 0.2 ± 0.1 , St.Dev. = 5.64 ± .08

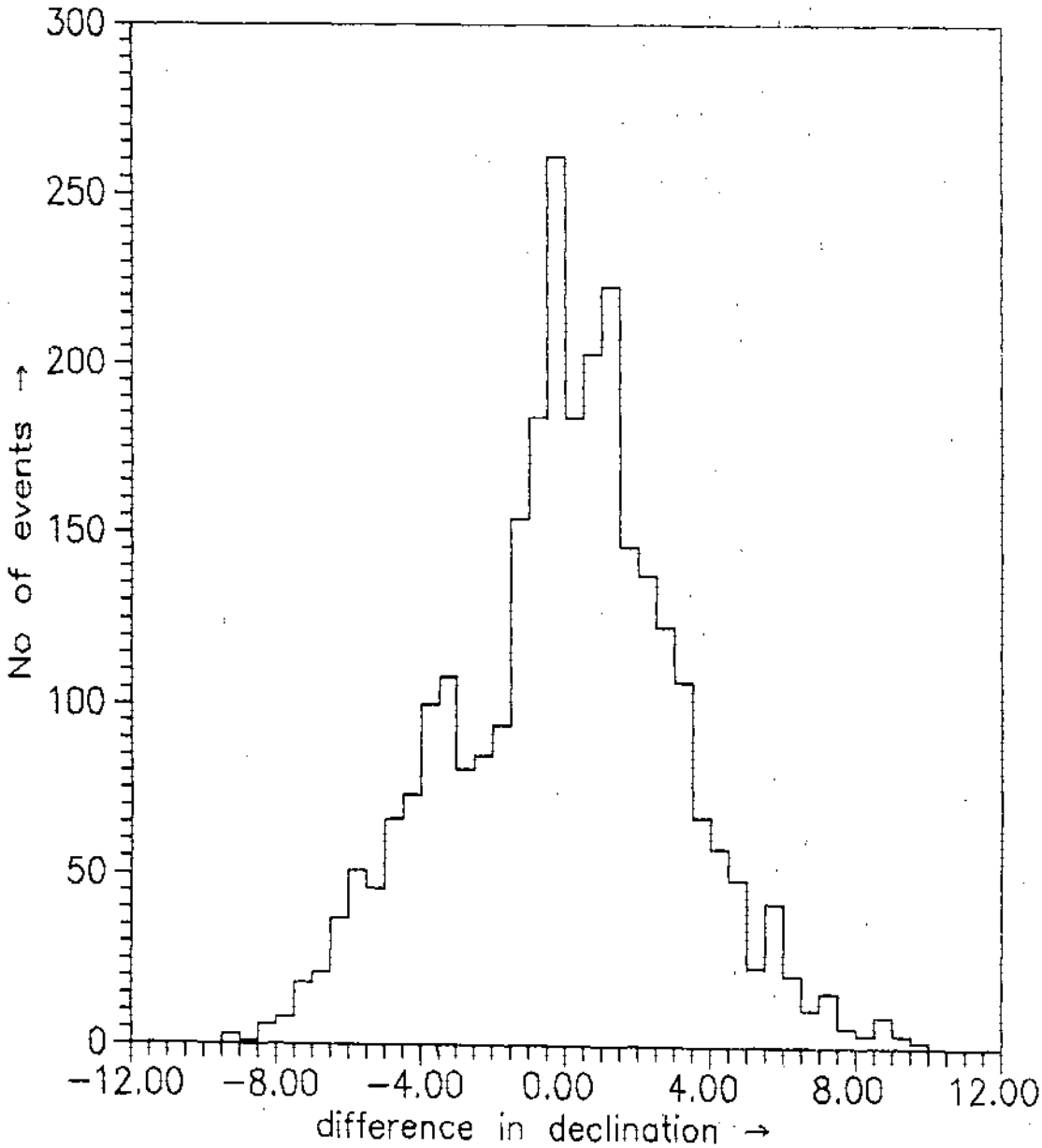

Fig 2.3.5c Distribution of relative deviations in Declination
(Average = −.05 ± .06 , St. Dev. = 3.11 ± .04)

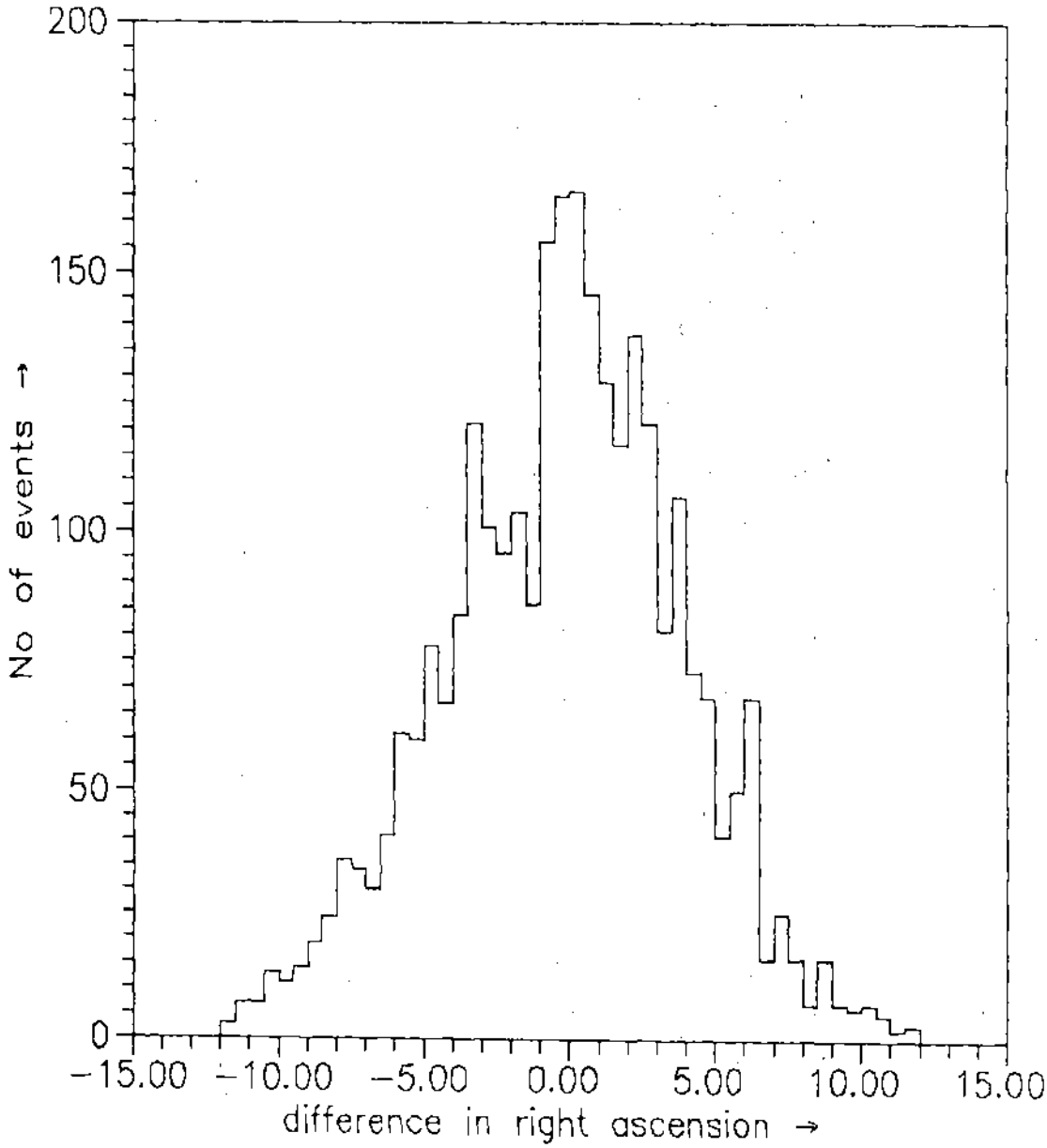

Fig 2.3.5d Distribution of relative deviations in Right Ascension.
(Average = −.20 ± .08 , St.Dev. = 4.08 ± .05)

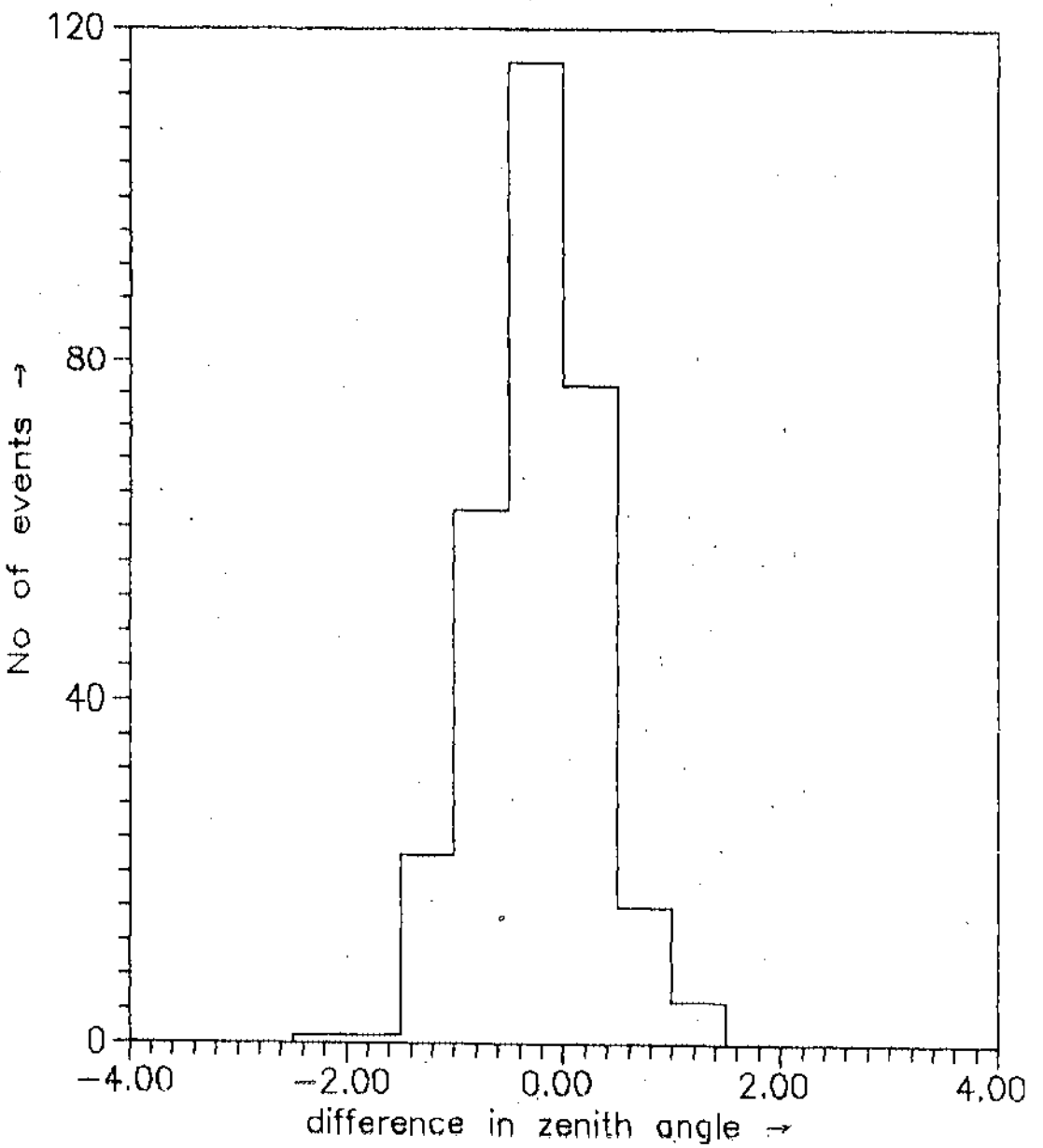

Fig 2.3.6a Distribution of relative deviations in Zenith angle (for simulated data)

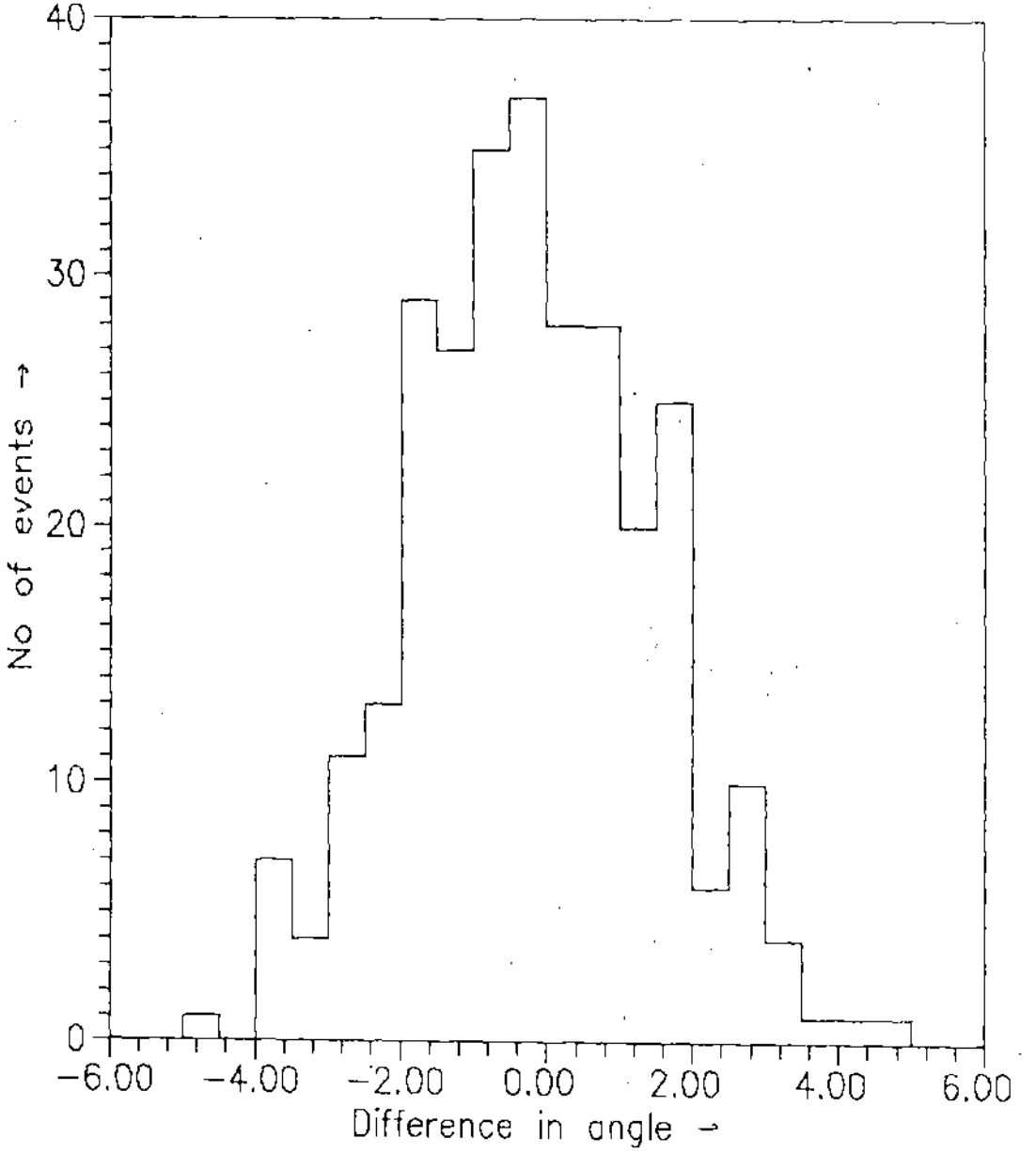

Fig 2.3.6b Distribution of relative deviations in Azimuth angle (for simulated data)

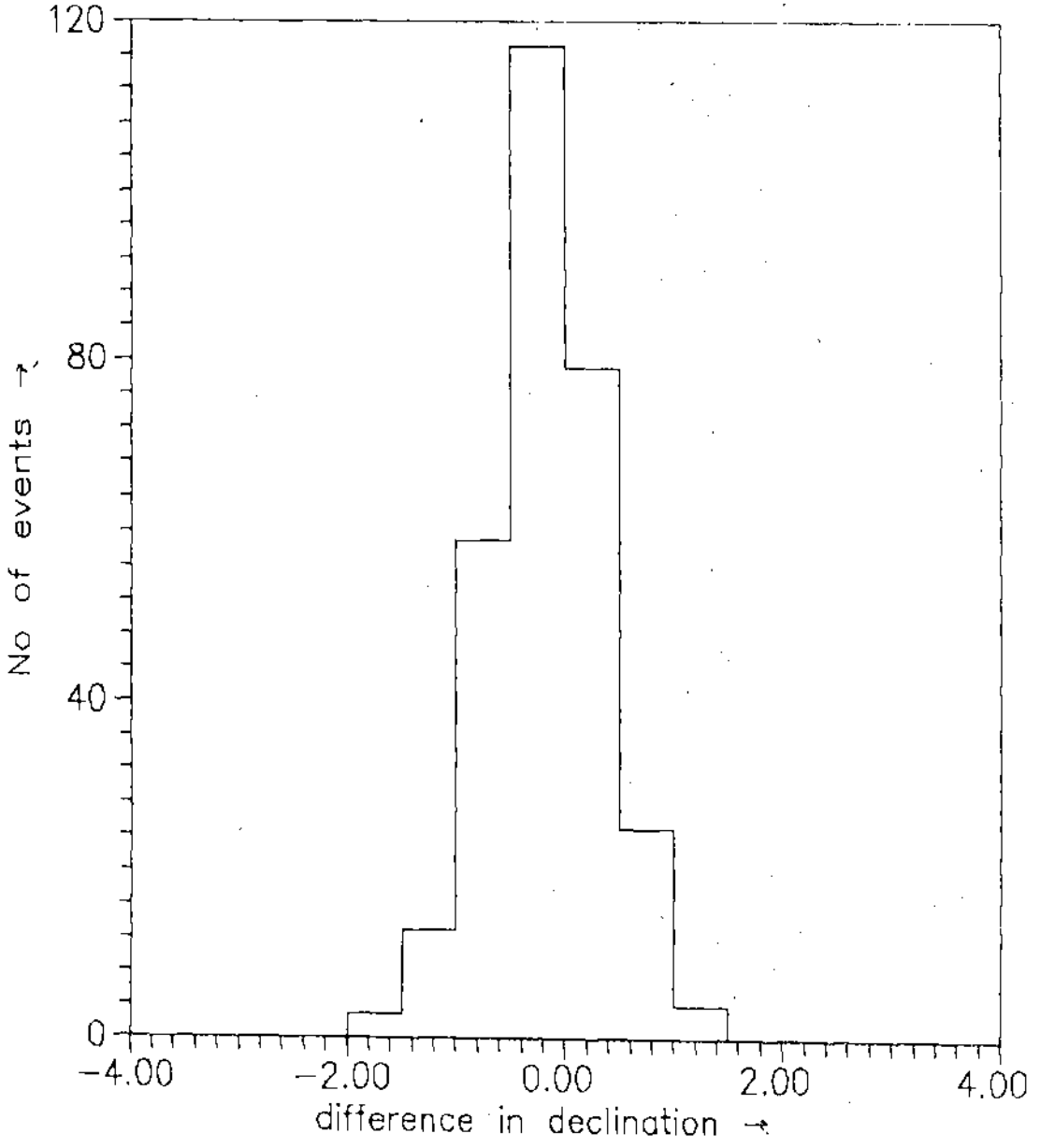

Fig 2.3.6c Distribution of relative deviations in Declination (for simulated data)

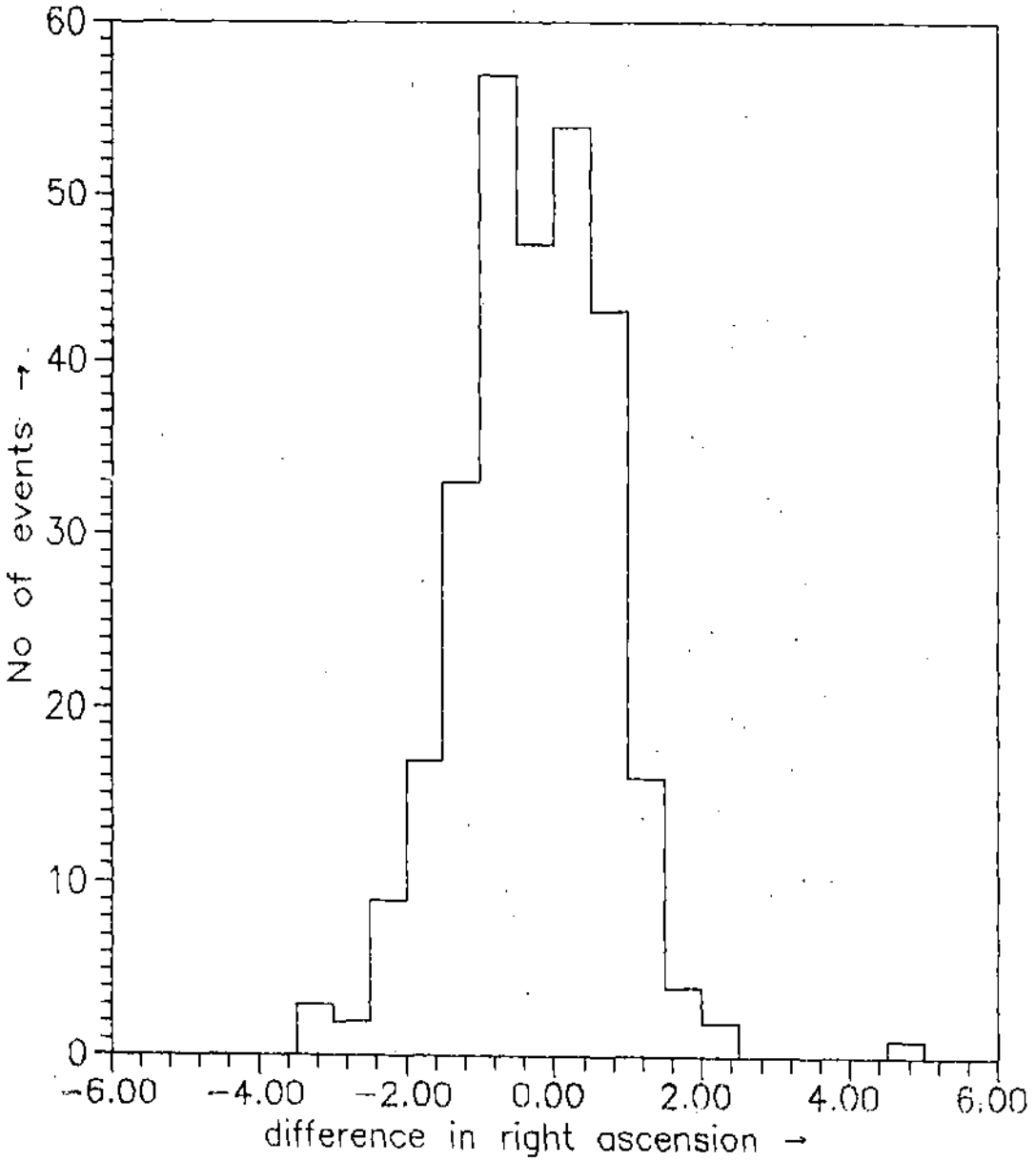

Fig 2.3.6d Distribution of relative deviations in Right Ascension (for simulated data).

observed curvature and the rms spread assuming a Gaussian distribution. The instrumental uncertainty is also included.The events times are selected randomly from the observed event times.The arrival times are then fitted to conical shower front with proper weightage and thus the resolution of the array is estimated.The resolution of the array obtained from the simulation results is also shown in Table 1. It is found that the resolution of the array estimated by the sub-array method is greater than that obtained from simulation results.

The sub-array comparison technique has been employed to compare the following shower front approximation

1) An unweighted plane shower front

2) A weighted curved shower front

The results are shown in Table 2 and fig.2.3.4 . From the results it is clear that the angular resolution of the array has been improved by a lot by introducing the weights and the curvature.

Table 2

Fit	Mean Space angle	Width
Plane(Unweighted)	$5.78^0 \pm .06^0$	$3.13^0 \pm .04^0$
Curve(Weighted)	$3.71^0 \pm .04^0$	$1.97^0 \pm .03^0$

Projected angle Distribution :

Whether the array co-ordinate system is coincident with the local horizon is checked by using the distribution of arrival angle projected on two orthogonal vertical planes. As the azimuth angle distribution of the showers is uniform, the projected angle distribution is expected to be symmetric about zero value.The observed projected angle distributions are shown in fig 2.3.6 .It is found that the distributions are symmetric about zero, having a mean close to zero and r.m.s. spread of 21.3 and 21.4 in the North-South and East-West planes respectively , consistent with the zenith angle distribution of showers.

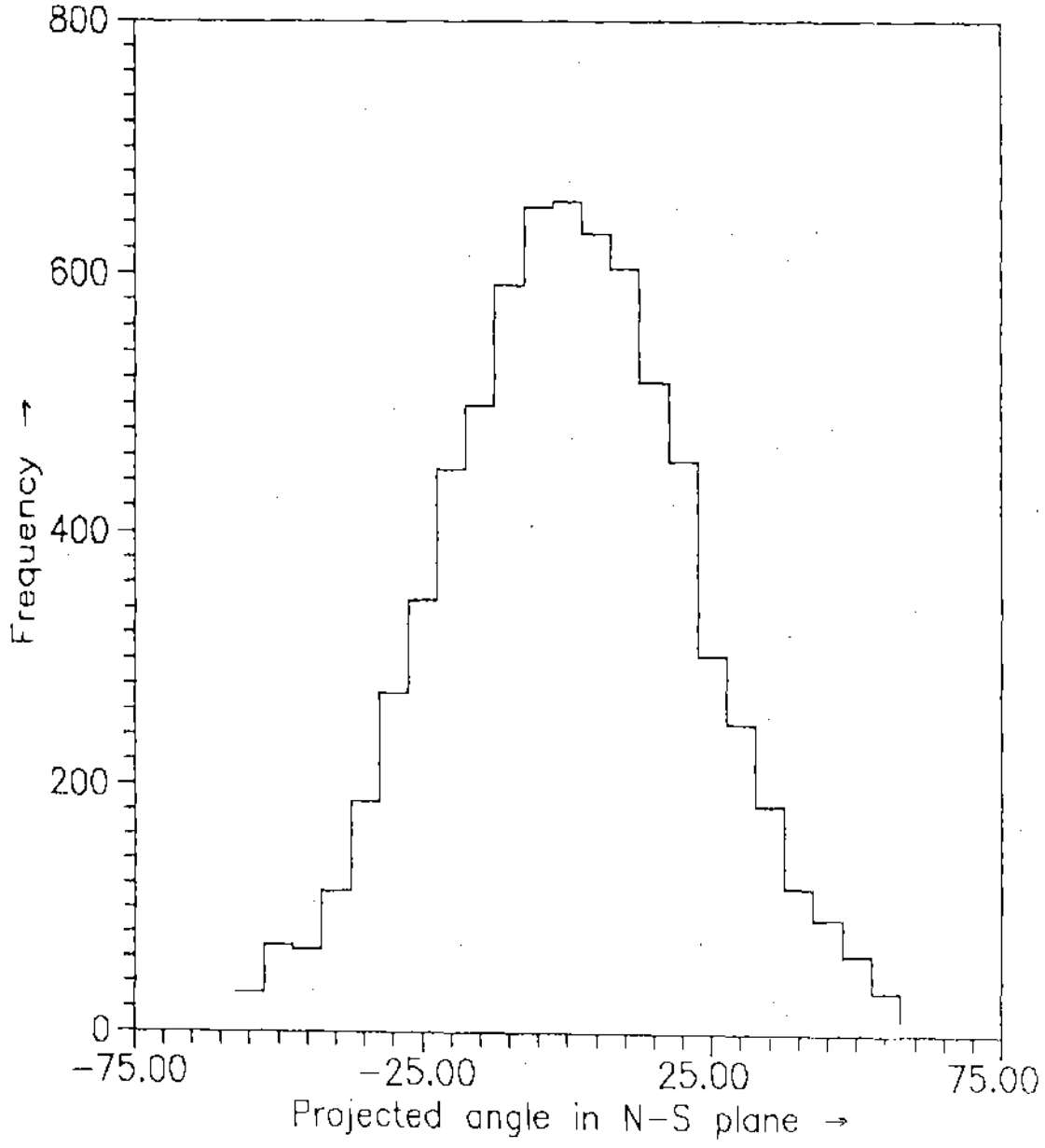

Fig 2.3.7a Projected angle distribution in N–S plane.
(Average = −.03 ± .25)

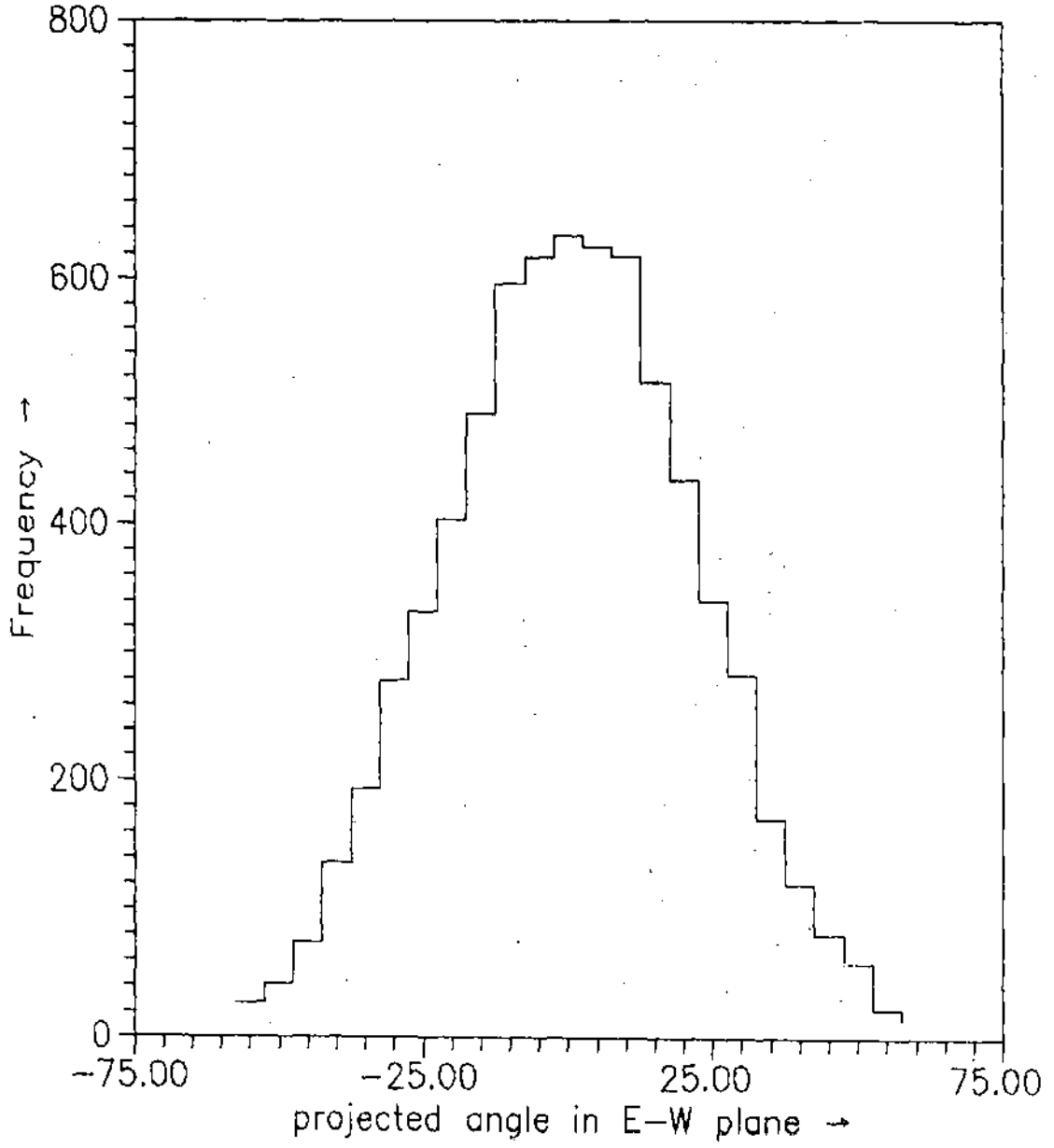

Fig 2.3.7b Projected angle distribution in E−W plane.
(Average = 0.16 ± .25)

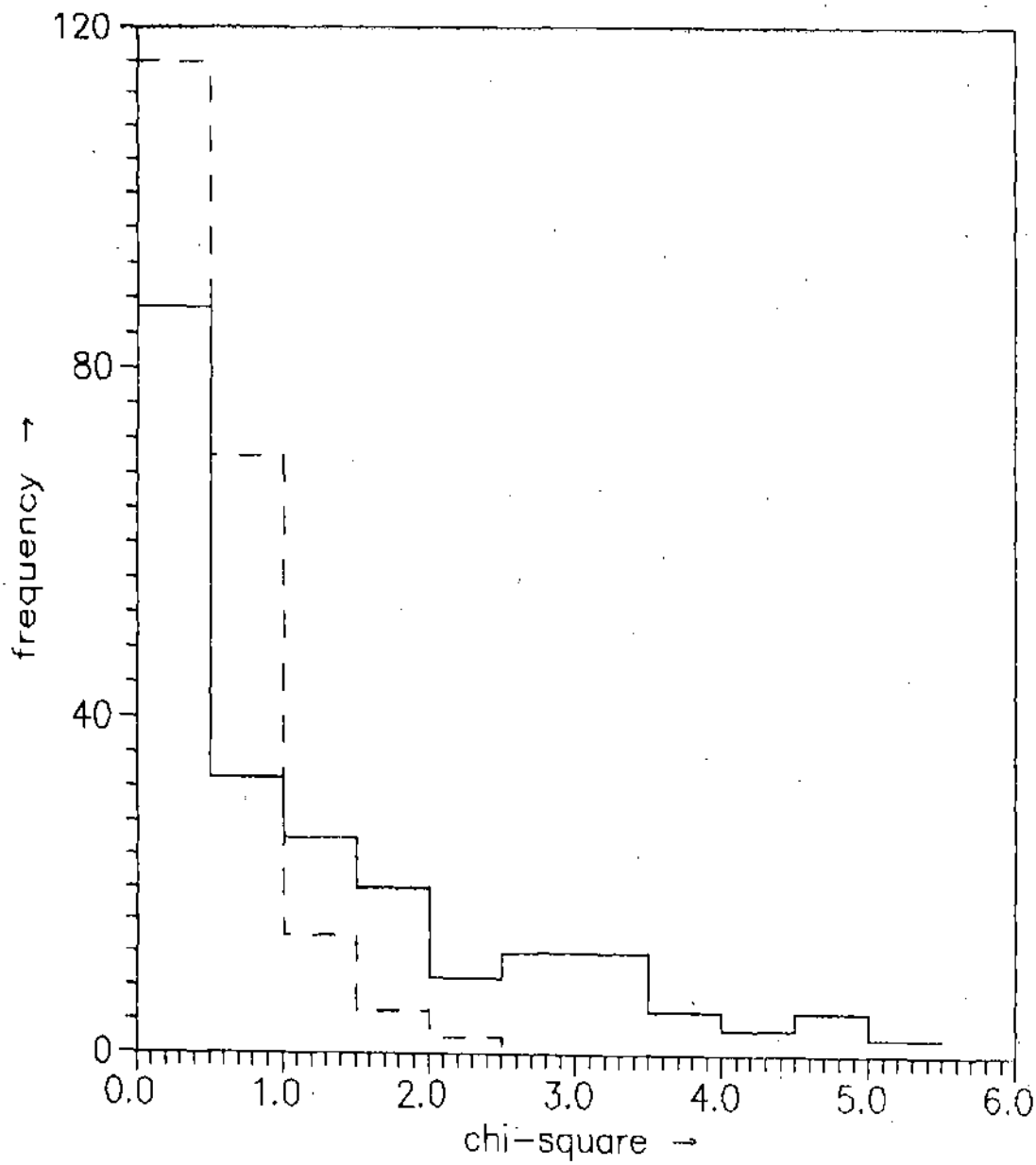

Fig 2.3.8 Chi-square distributions for timing data fit .Solid line - for experimentally observed shower data ,dashed line - for simulated shower data.

*** Chapter 3 ***

Results

The result of the present work are based on the extensive air shower (EAS) data collected using North Bengal University (NBU) EAS array. The studies of EAS detected by using NBU EAS array since 1980 have yielded results on the UHE nuclear interactions and on the composition of primary cosmic rays at the energy range 10^{14} eV to 10^{16} eV. The search for UHE discrete point sources is now the thrust of the NBU EAS project. At the first phase of investigation in this direction a sample of nearly 15,000 events ~~are~~ is taken for the present analysis which were collected by the array during the period Jan 1993 to June 1994. The total run time is 752 hours. Before discussing the main results of the present experiment,the array performance is described.If any large systematic biases involves in the measurement of the air shower observable it will surely reflect on the general characteristics of the observed air showers.The general characteristics of air showers have been studied for a long time and are quite well known.So to make sure that there is no systematic errors in the final results,the general characteristics of the air showers are studied first.

3.1. General Characteristics of the observed EAS :

The results of the present experiment are mainly derived from the density information of the electron component and the muon component of air shower and from the timing information of the shower front.

1.Particle Density data :

One of the main characteristics of EAS is certainly the lateral distribution of the electrons of the EAS. The basic shower parameters for each shower event are estimated in the usual way by fitting the NKG function for the lateral distribution of electrons to the observed densities of the particles.To check the quality of the density information the lateral distribution of electrons is studied. To construct the average lateral distributions the whole radial range is divided into small distance bins.The contribution of electron densities in the different radial distance (from the EAS core) bins for a small bin of shower size and shower age are calculated. The observed lateral distributions of electrons are shown in fig 3.1 and in fig 3.2 for two different shower sizes and shower age along with the NKG distribution curve. It is clear from the fig 3.1 and 3.2 that the

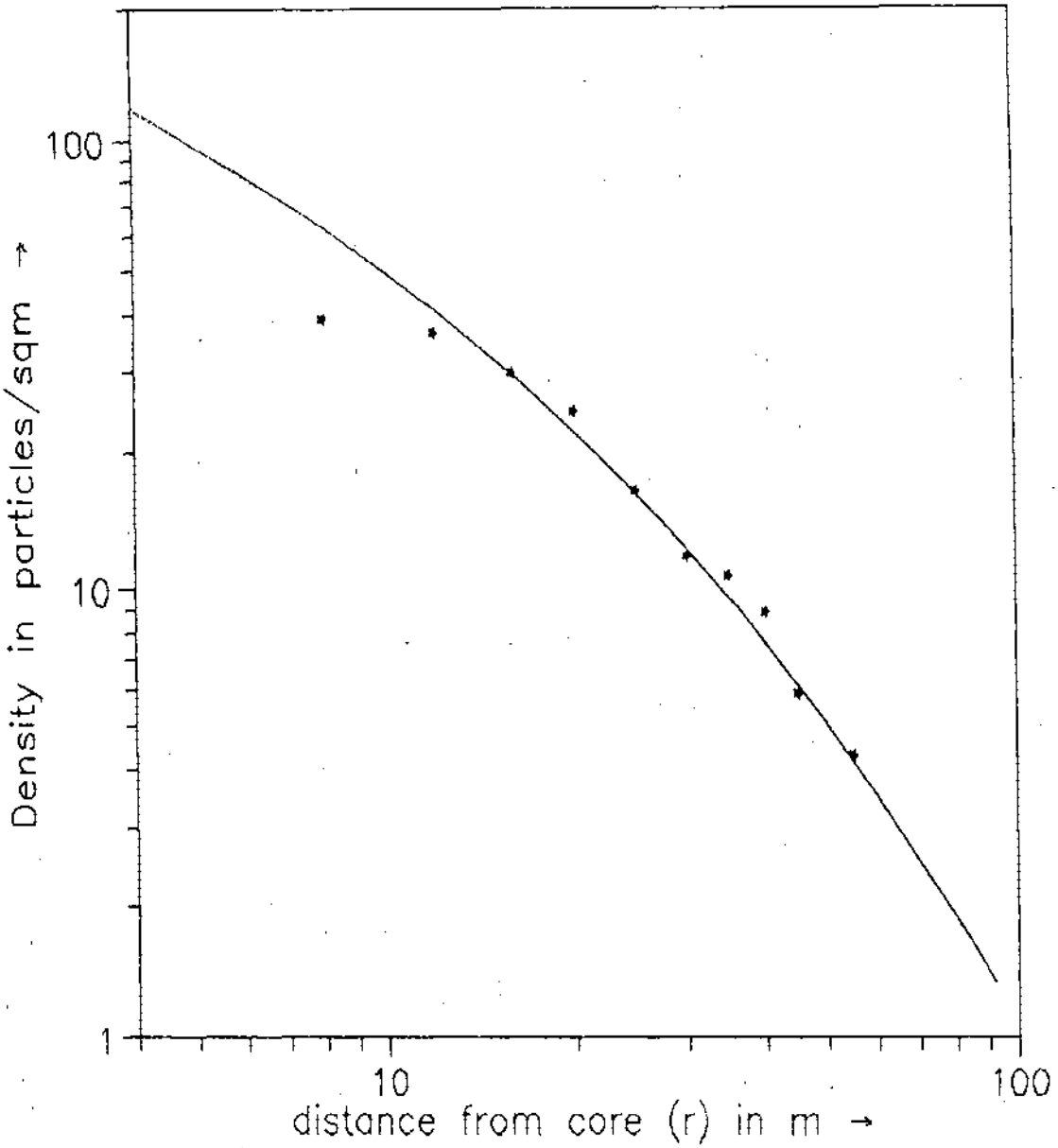

Fig 3.1 Observed radial distribution of the EAS electrons for shower size 2.5×10^5 and for shower age 1.3 compared with the NKG function(solid curve).

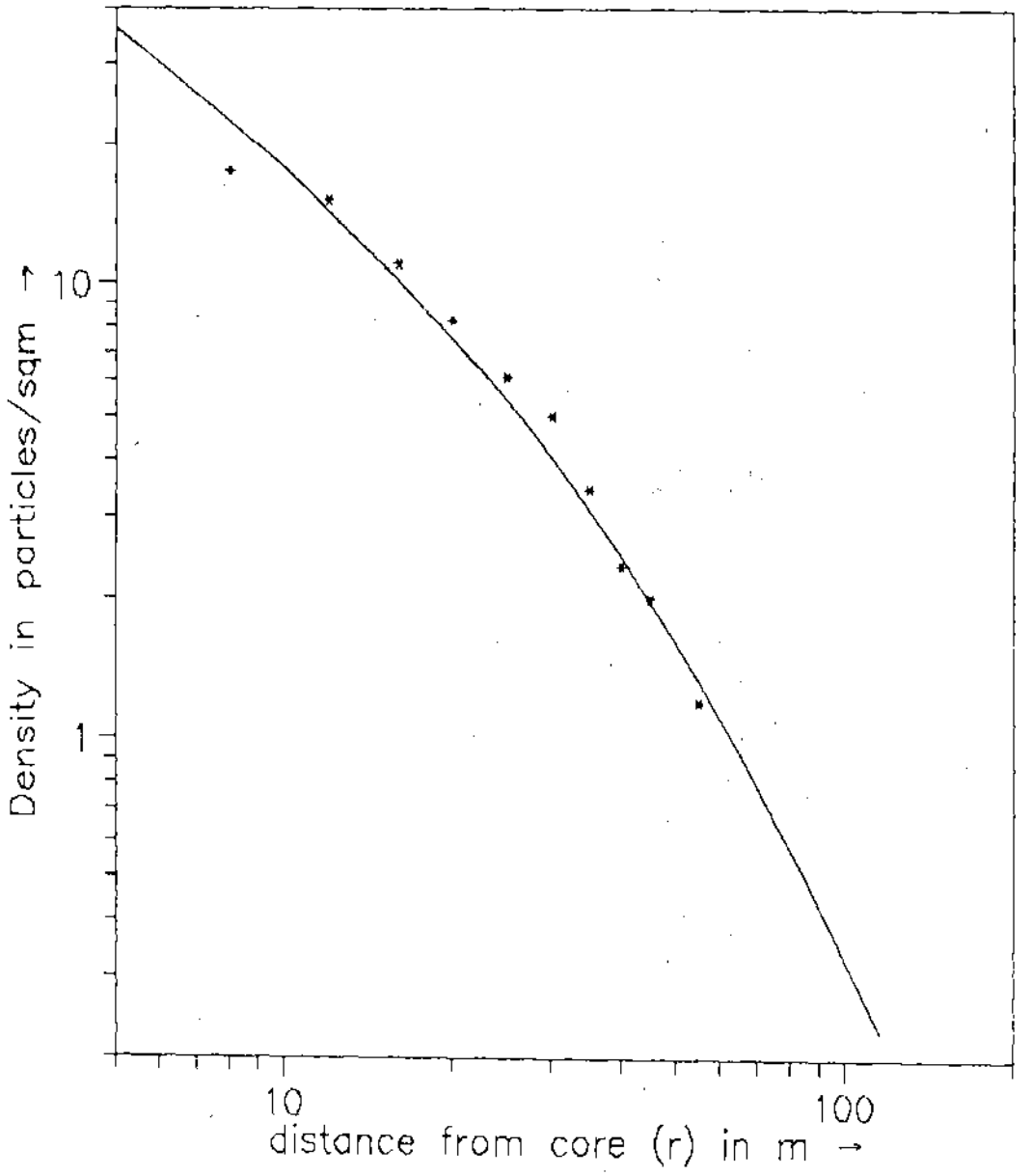

Fig 3.2 Observed radial distribution of the EAS electrons for shower size 8×10^4 and for shower age 1.25 compared with the NKG function(solid curve).

experimental data are in a satisfactory agreement with the NKG function.

The shower 'age' (s) determined by the lateral distribution of shower particles is an important parameter to indicate the stage of longitudinal development. In the fig 3.3 the age distribution obtained from the data is given. The mean 'age' of the observed showers is 1.31 which agrees well with the theoretical estimate (1.33) of Fenyves (1) .. The spread of the age distribution is 0.28. The shower size distribution of the observed showers is given in fig 3.4. Showers are detected in the shower size range 2×10^4 - 7×10^6. The median shower size range detected by the array is 2.4×10^5 - 4.8×10^5 .

2. Muon data :

Muon component of EAS provides very important information regarding the high energy interaction characteristics and about the properties of primaries. Because of the lack of interaction of muons with air nuclei muon component of EAS gives information on shower behavior at the early stage of their development. Total number of muons in an EAS is considered as good measure of the primary energy. A study on muon component of air showers in corelation with other components of the EAS can yield information about the nature of the high energy interactions. The muon size in a shower is estimated by fitting the observed muon density data to a appropriate lateral distribution function. So the lateral distribution of muons in EAS is certainly an important characteristic of EAS.

A representative example of the observed lateral distribution of muons is shown in fig 3.5 for a muon threshold energy 2.5 GeV. The observed densities are fitted with Griesen (2) function given by

$$\rho_\mu(r,N_e,>E_\mu) = \Gamma(2.5)/(2\pi\,\Gamma(1.25)\,\Gamma(1.25))\, N_\mu/r_0^2 (r/r_0)^{-.75}(1 + r/r_0)^{-2.5} \qquad \ldots 3.1$$

where N_μ is the total number of muons in a shower, r_0 is a constant estimated from the fitting which changes slightly with the change of shower size. For $N_e = 2.5 \times 10^5$, r_0 is found to be 290. In the shower size range 10^5 - 10^8 and for E_μ up to 500 GeV Greisen (3) proposed a lateral distribution

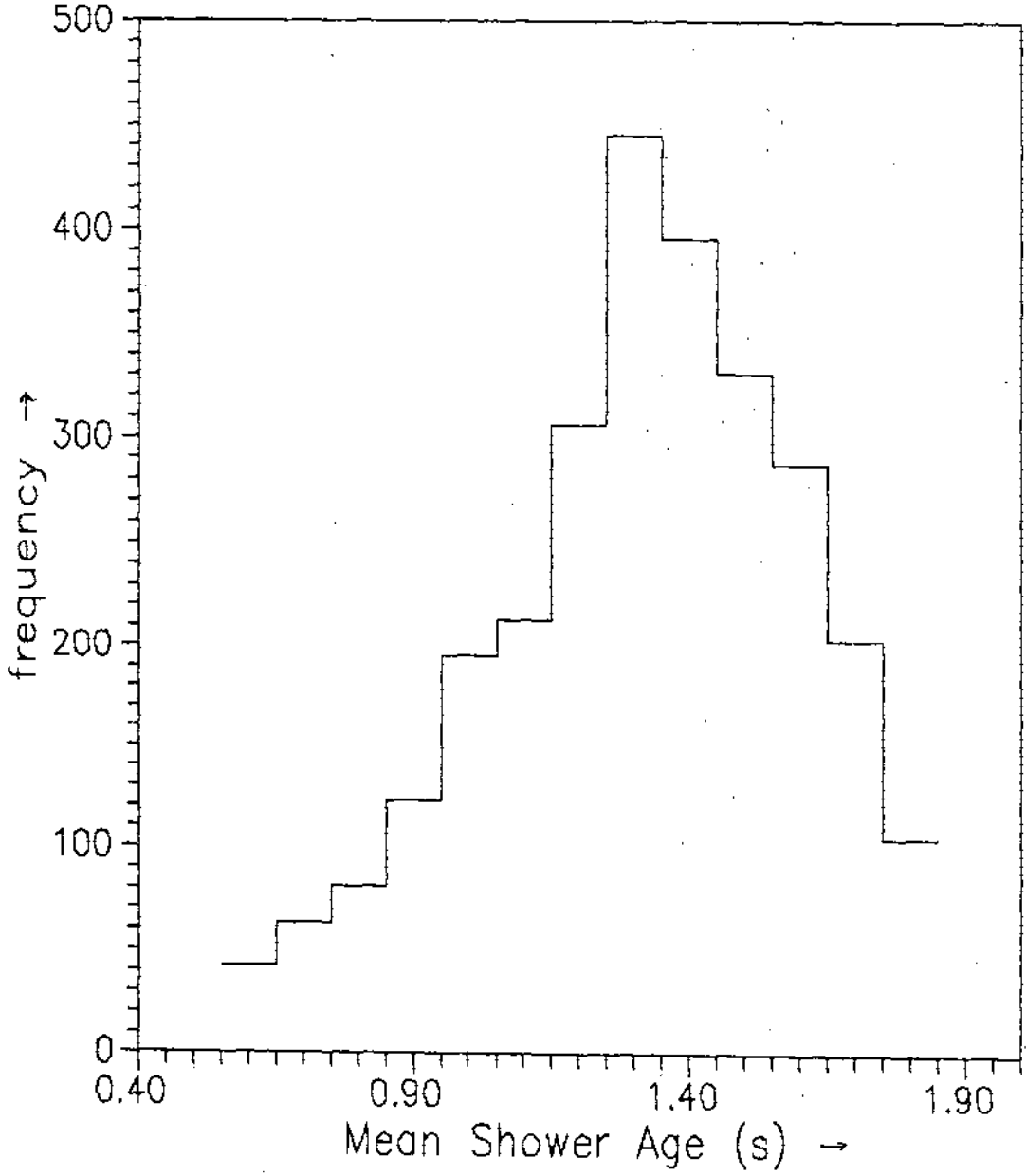

Fig 3.3 Shower age distribution for the observed shower events

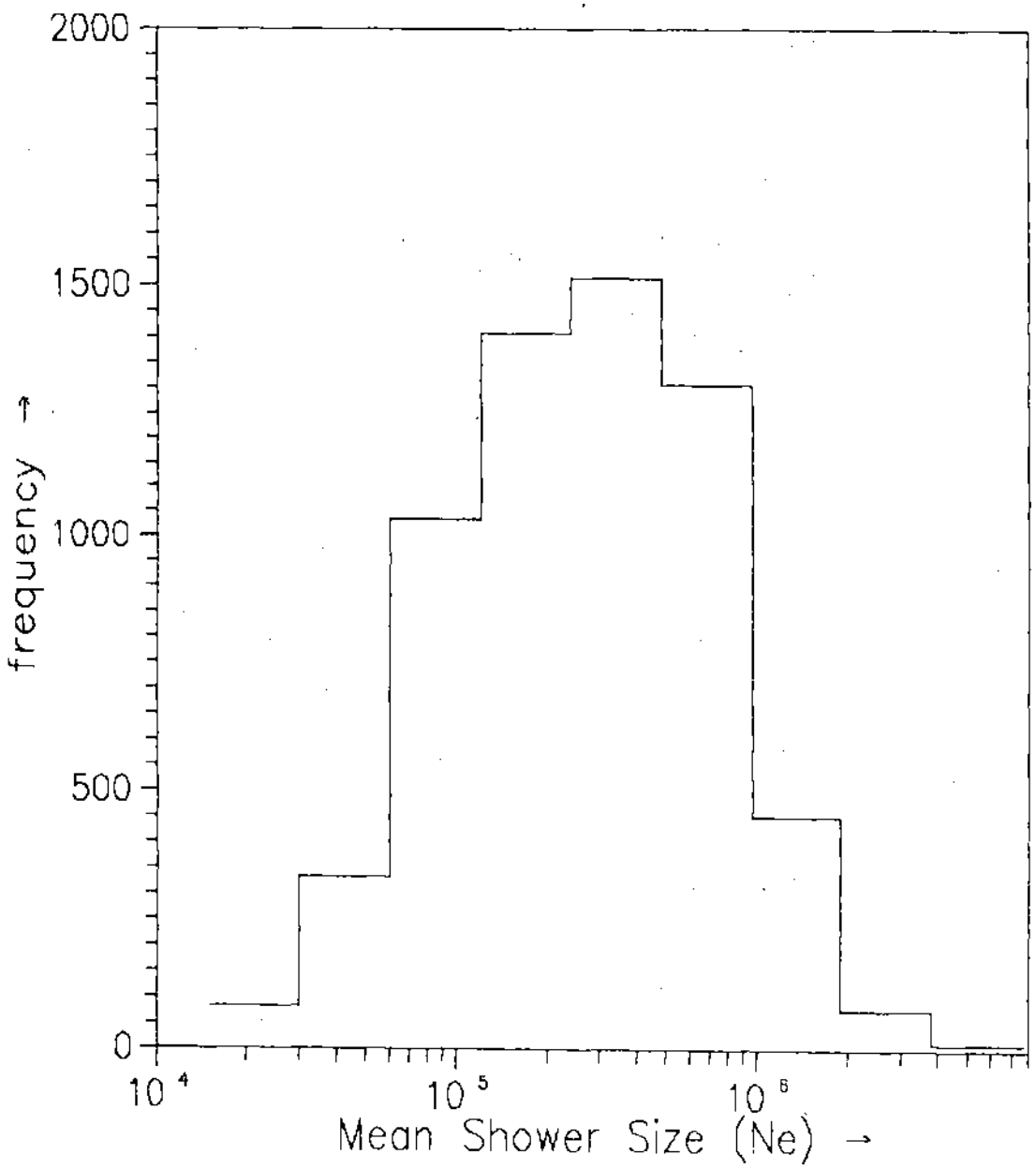

Fig 3.4 Shower size distribution for the observed air showers

formula for muons which is given by

$$\rho_\mu(r,N_e,>E_\mu) = (N_e/10^6)\,(14.4\, r^{-0.75})\,(1 + r/320)^{-2.5}\,(51/(50 + E_\mu))\,(3/(E_\mu + 2))^{0.14r} \quad .. 3.2$$

A dashed curve in the fig 3.5 represents the Griesen formula .The observed distribution is agreed well with the Griesen formula.

3.Timing information of the shower front :

Arrival direction of each EAS event is determined by usual first timing technique as described in the previous chapter. Since the ultra high energy primary cosmic rays are highly isotropic ,the azimuth angle distribution of cosmic ray air showers is expected to be uniform. The azimuth angle distribution of the observed showers is given in fig 3.6 which is consistent with the expectation. The zenith angle distribution of the EAS events is also studied to check the array performance.The errors of zenith angle measurements in individual EAS event do not exceed 1.5^0.Shower events in the size range 2×10^4 - 5×10^6 particles for zenith angles from 0^0 to 60^0 are considered.The distribution is given in fig 3.7. The zenith angle dependence of the integral flux of showers can be expressed by a power function in the form (2)

$$I(\theta) = I_o \cos^n z \qquad \ldots\ldots 3.3$$

i,e, the flux of showers monotonically decreases with the increase of zenith angle. This is due to atmospheric absorption which increases with zenith angle as the inclined showers traverse an increased thickness of atmosphere. However the number of events observed for a given zenith angle range increases with zenith angle first ,reaches a peak at around 20^0 and then falls.This is because the solid angle of acceptance increases with zenith angle as sin(z). At higher zenith angles the atmospheric absorption part dominates over the solid angle of acceptance part and as a result the number of events within a zenith angle bin falls. To remove the solid angle effect the frequency of events are divided by sin(z) and plotted against cos(z) which is shown in fig 3.8. From the figure the value of the index is found to be 7.64 .

The declination distribution of the collected showers is shown in fig 3.9.From the distribution it is found that the effective observation region in the sky by the array is within the

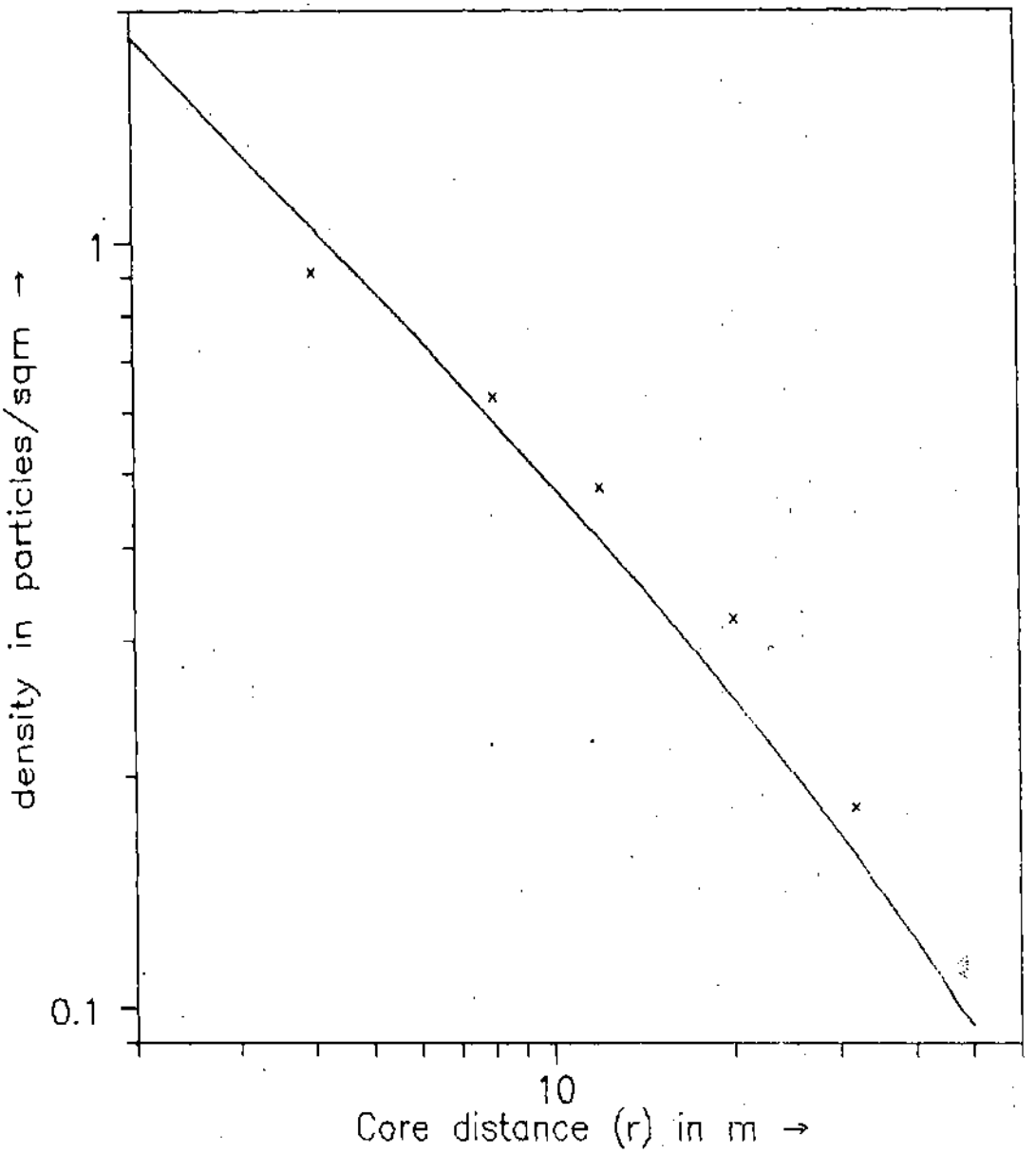

Fig 3.5 Observed radial distribution of EAS muons for the muon threshold energy 2.5 GeV for shower size, Ne $=2.5 \times 10^5$ The solid curve represents the Greisen formula.

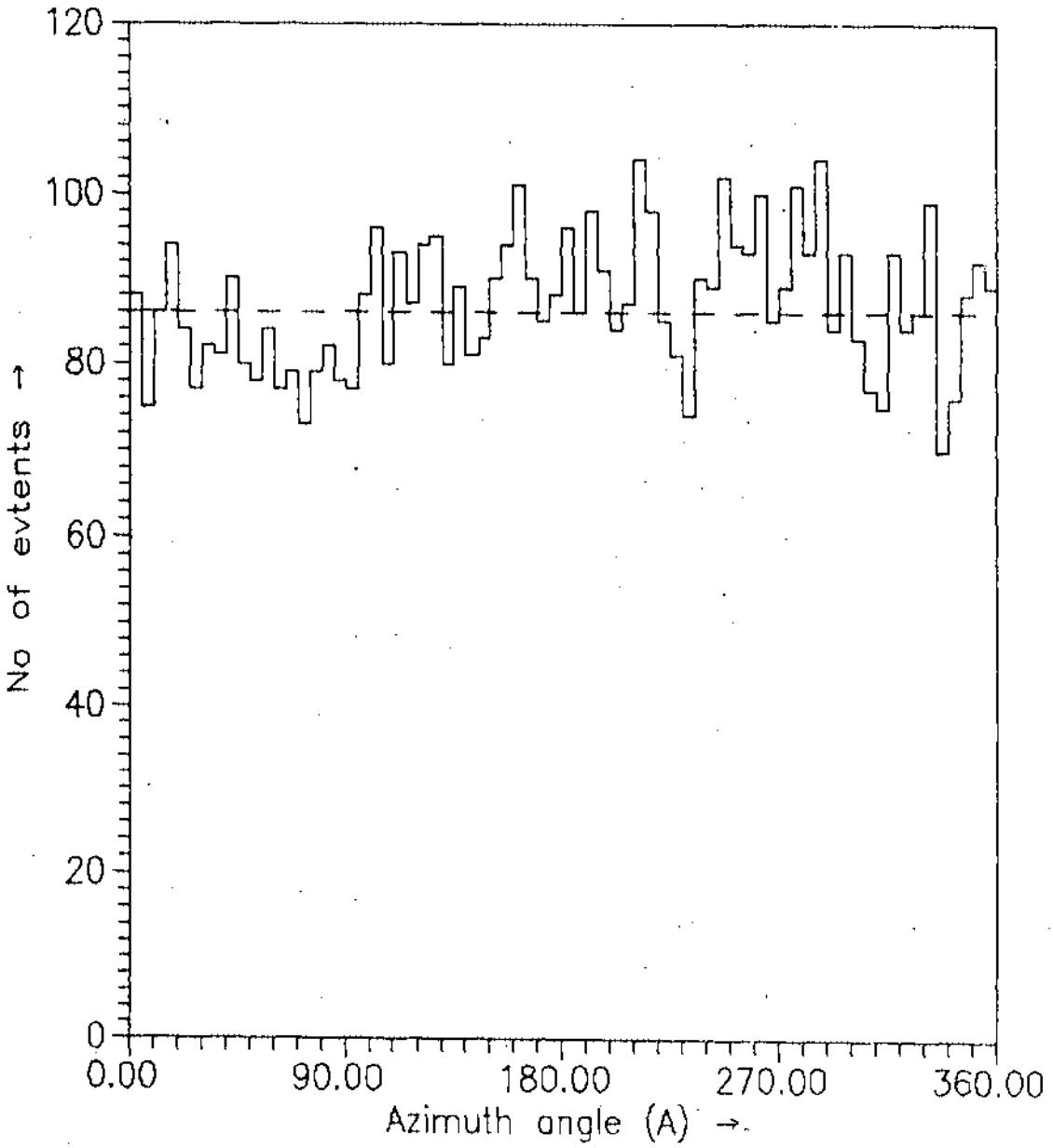

Fig 3.6 Azimuth angle distribution of the observed showers.A dashed line is the average number of showers per bin.

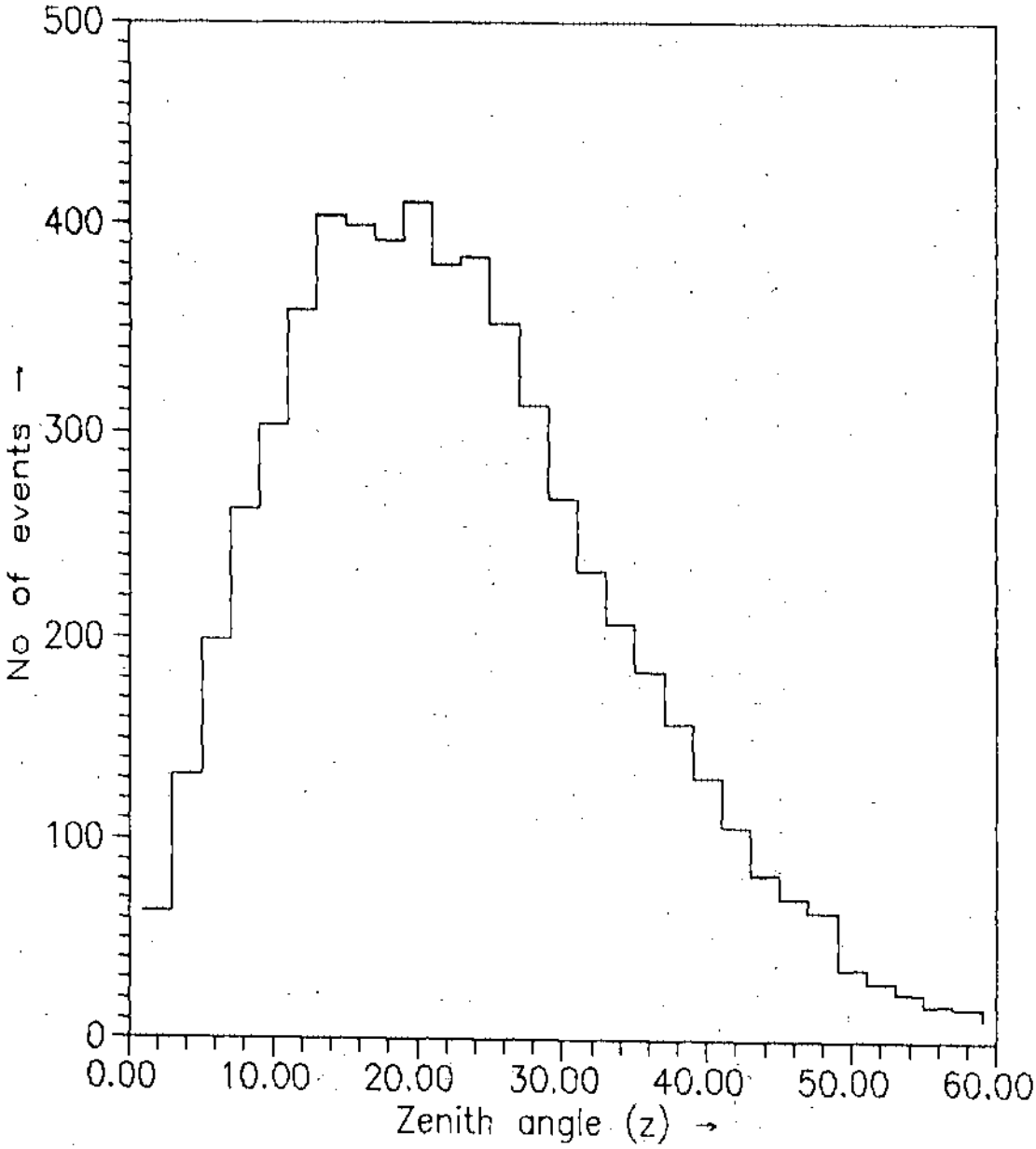

Fig 3.7 Zenith angle distribution of the observed showers

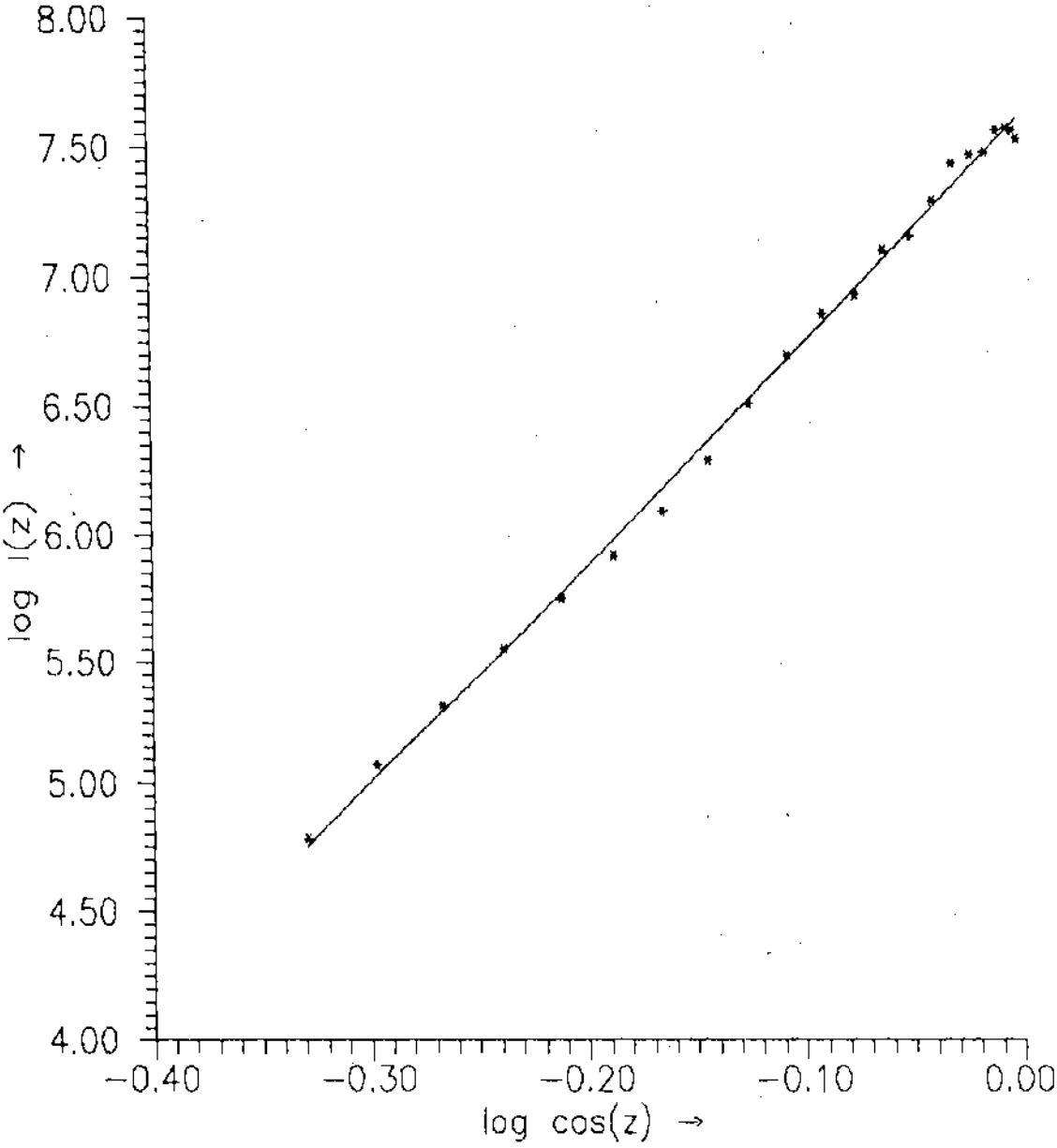

Fig 3.8 Zenith angle dependence of the observed cosmic ray flux.

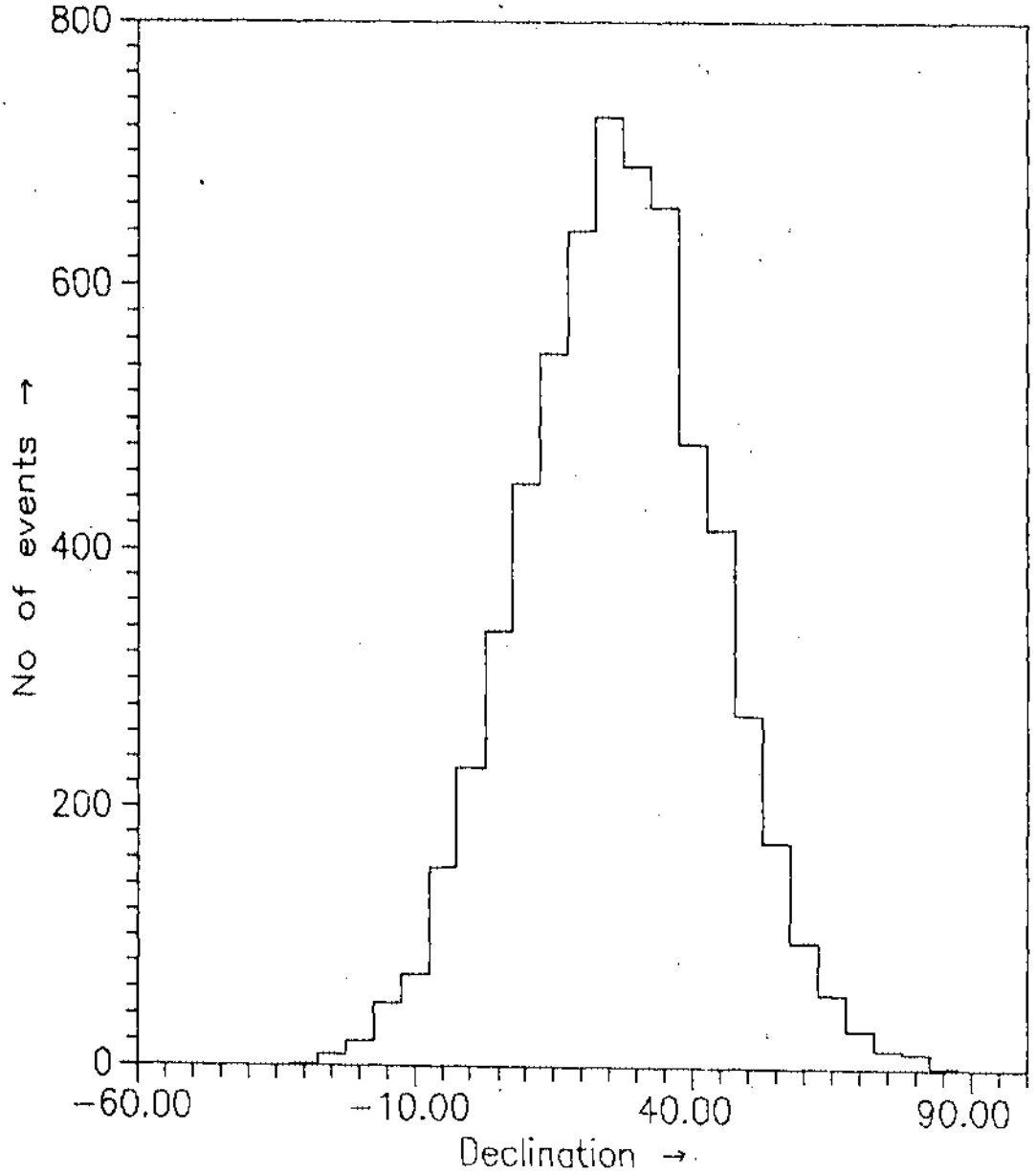

Fig 3.9 Declination distribution of the observed showers

declination range 10^0 to 50^0 . It is well known that the most of the potential sources of northern hemisphere like Cygnus X-3,Hercules X-1,Crab Nebula ,Geminga fall within this declination range.So the array can observe these sources very effectively.

The isotropic behavior of the cosmic rays should reflect in the right ascension distribution of the observed shower events.A prerequisite of any directional isotropy analysis is that the detector zenith should spend equal times in all right ascension intervals. The equalization of the operating time is implemented by random rejection of the events in each group of hourly intervals in excess of the minimum number for each hour interval.The right ascension distribution obtained using the above procedure for the observed showers is shown in fig 3.10.The distribution is consistent with the isotrpic behavior of the UHE cosmic ray particles.

So the general features of the observed air showers are consistent with the well known characteristics of air showers.

3.2. Study on shower parameters :

Muon content in a shower and shower 'age' are the two parameters which are often used to discriminate gamma photon initiated showers from the hadron initiated showers.

1. Study on shower age parameter :

The longitudinal development of EAS is an essential feature that reflects the gross feature of particle interaction at high energies. The stage of development of an air shower is described by shower age parameter (s) . The value of s equals to one when the shower is at the stage of maximum development. In the search for UHE gamma ray sources by the EAS method,several workers have made age cut to reduce the EAS background caused by primary cosmic ray charged particles. But the simulation results of Fenyves (1) ,Hillas(4) and Cheung and Mckeown (5) opposed the idea that the age parameter can be used as a differentiator of gamma ray initiated showers from hadron initiated showers, though it is an observed fact that the age cut produces results.

In most of the observations the showers from point sources were observed at large angles during most of the observation time due to high angle of transit of the sources at the arrays.As for

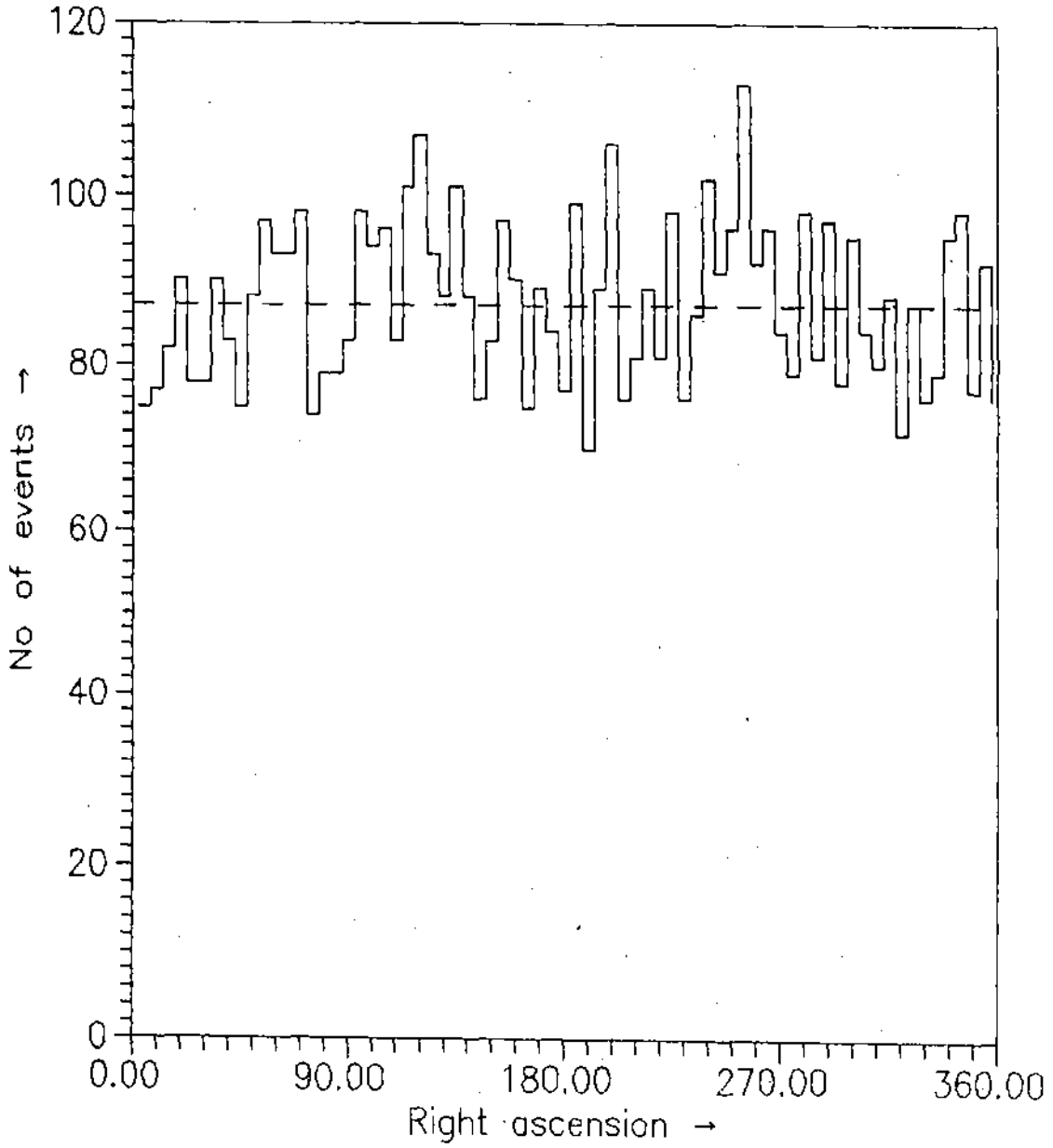

Fig 3.10 Right Ascension distribution of the observed showers.A dashed line coresponds to the average number of showers per bin.

example, Cygnus X-3 is observed at Kiel at zenith about 14^0,the same source is observed at Ooty at zenith angle nearly 26^0 at the transit.Remembering this feature, in the present experiment, the zenith angle dependence of shower 'age' parameter is studied. The variation of mean shower 'age' with zenith angle is shown in fig 3.11 for the whole shower size range (2×10^4 - 6×10^6).At the zenith the mean shower 'age' value 1.26 . The variation of s with zenith angle (z) is found slow and at $z = 60^0$ the mean 'age' reaches only 1.46 though at zenith angle 60^0 the atmospheric overburden is nearly double . In Buckland park experiment (6) and in Chacaltaya experiment (7) similar trend of variation were observed . Theoretically the variation is much faster.

The total amount of matter in the atmosphere increases in proportion to secz .The variation of 's' with secz is also plotted in Fig 3.12 . The variation of 's' with secz can be represented by the linear relationship

$$s(z) = .25 \sec z + 1.05 \quad \ldots\ldots \quad 3.4$$

The variation of shower age with shower size for the observed showers is shown in fig 3.13 . From the figure it is found that the value of average age monotonically decreases with the increase of shower size but the rate of decrease decreases with the increase in the shower size. This is probably due to the variation of effective collection area of the array with the primary energy. Similar trend of variation of shower 'age' with shower size was found in Akeno experiment (8) .

2.Study on muon component of EAS :

Results of investigation on muons with energies above 2.5 GeV arriving at the sea level are reported here .The muon component of EAS carry information regarding the high energy interaction characteristics as well as the properties of primary cosmic ray particles. Muon content in a shower is considered as a best parameter to identify gamma ray initiated showers from the hadron initiated showers. It is believed that the gamma ray showers contain less than 10% of muons of normal showers. However in a number of observations it was found that the total muon number in the excess showers from the direction of point sources is almost same as that of normal showers.To better understand the problem in the present investigation the variation of the ratio of the muon density to electron density with shower age for particular core distance at a fixed shower size is studied.

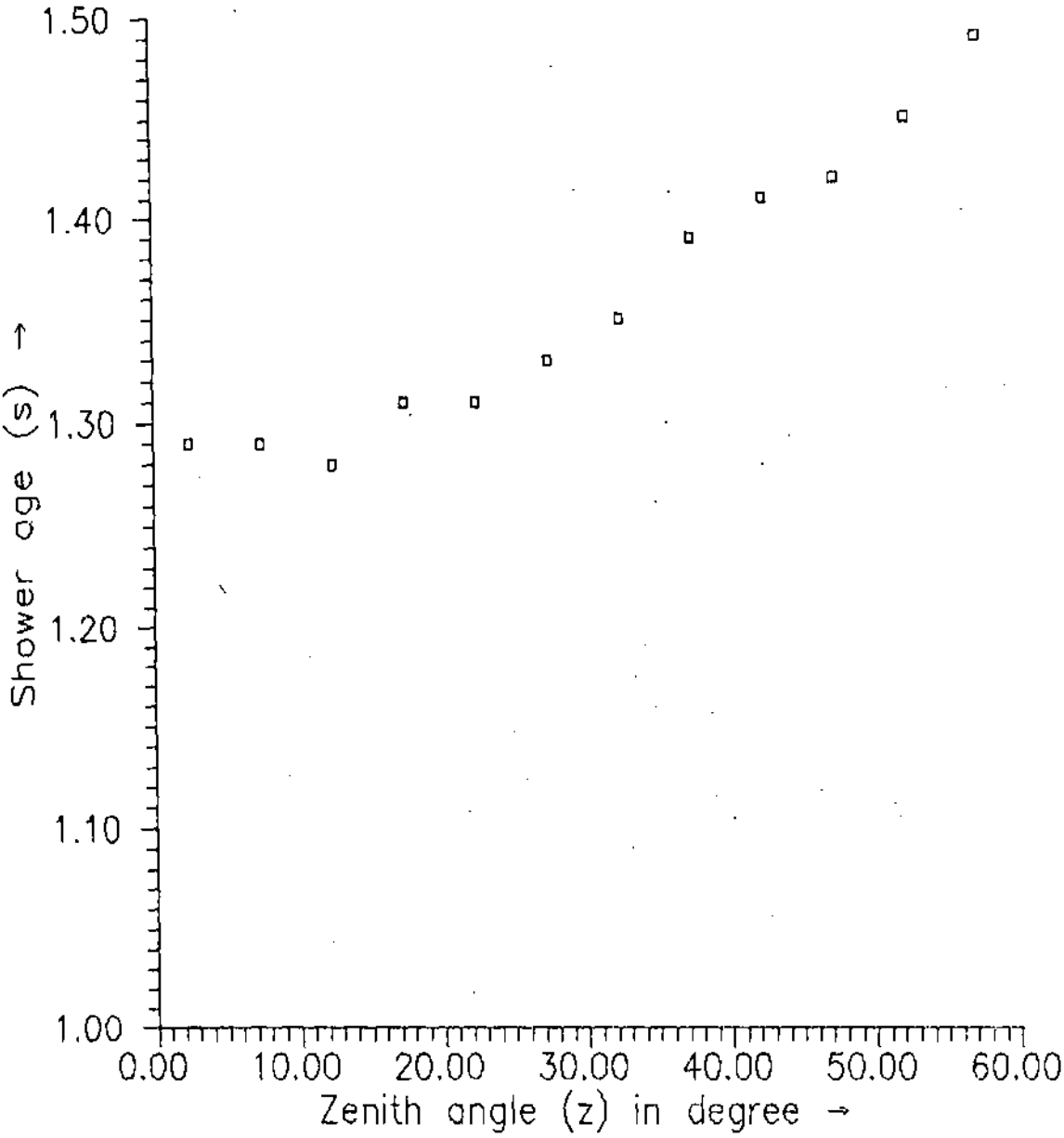

Fig 3.11 Variation of shower age parameter (s) with zenith angle (z) .

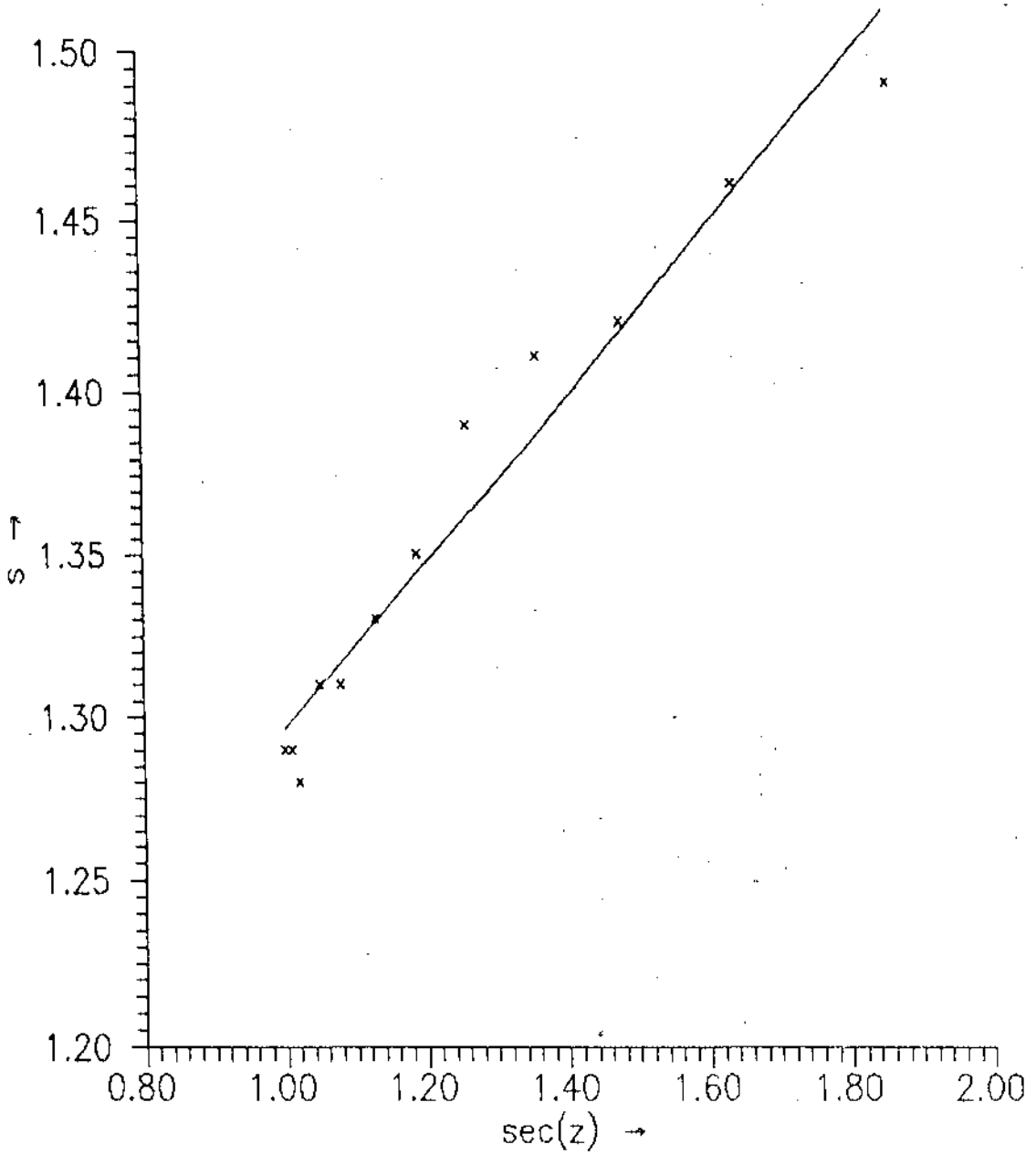

Fig 3.12 Variation of shower age with sec(z). The solid line is the straight line fitting of the data.

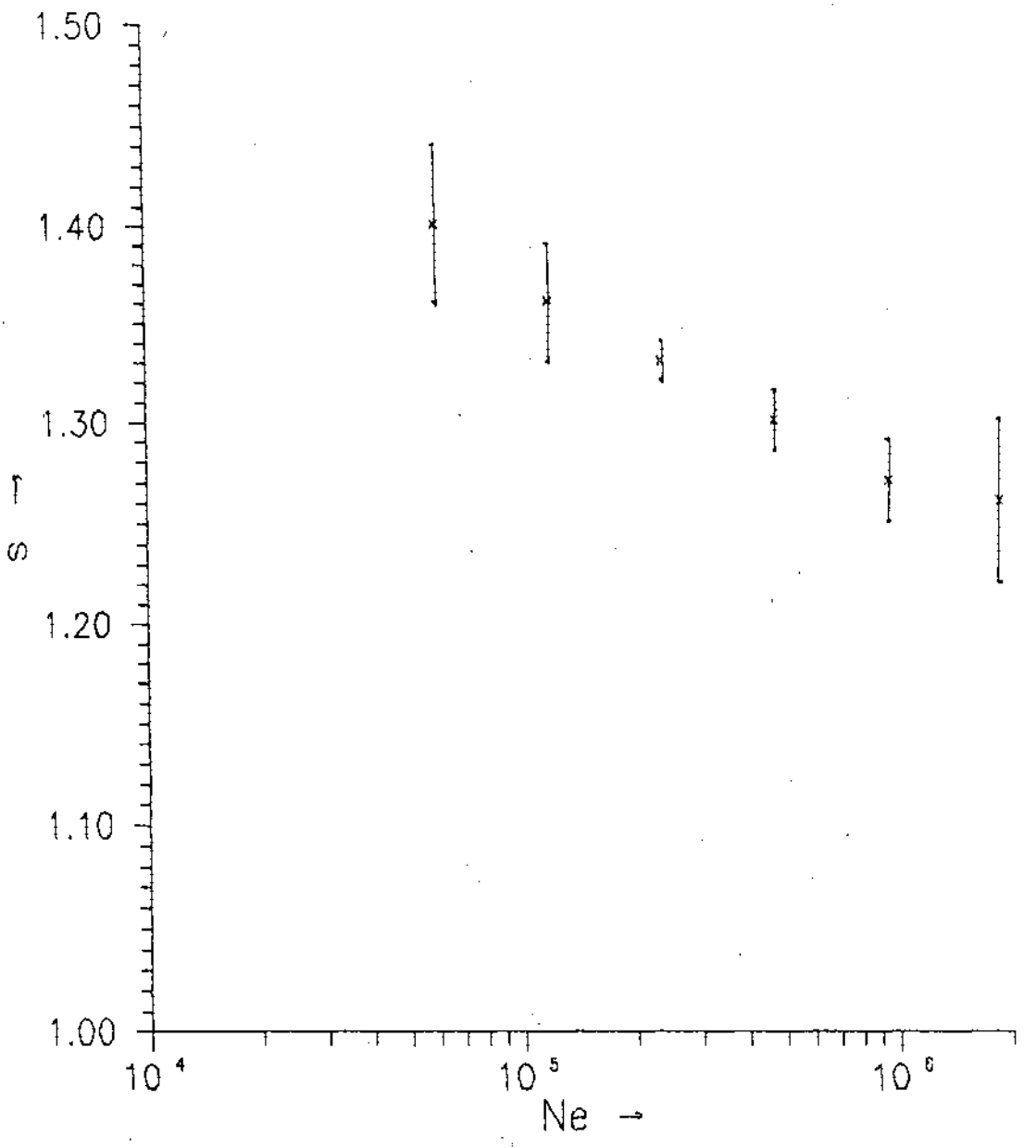

Fig 3.13 Variation of shower age parameter (s) with shower size

The variation of the ratio ρ_μ/ρ_e with shower age for shower size 2 x 10^5 at radial distance (from the shower core) 12 m and 20 m are shown in fig 3.14 and 3.15 .The radial bins are made wide enough (4m) to accommodate the error in r_μ (~2). From the figure it is clear that the ρ_μ/ρ_e ratio increases as shower age increases. This is expected because the muon number does not change much with the atmospheric depth traversed after the maximum development of shower reaches while shower size decreases rapidly with the increase of shower age. It is interesting to note that high muon content of the excess showers from the direction of Cygnus X-3 as observed by the Kiel group is also characterised by high 'age' values.

The muon size (N_μ) in a shower is obtained using measured lateral distribution of muons fitted to Griesen function

$$\rho_\mu(r,N_e,>E) = \Gamma(2.5)/(2\pi\Gamma(1.25)\Gamma(1.25))\, N_\mu/r_0^2(r/r_0)^{-.75}(1 + r/r_0)^{-2.5}$$

with the variable r_0. The variation of muon size with shower size (N_e) is given in fig 3.16 .The variation can be represented by a power law relation given by

$$N_\mu = a N_e^{\alpha} \qquad \text{.....} \qquad 3.5$$

where a is a constant. The value of the exponent (α) is found to be 0.69 .The result is compared with the simulation results of Wrotniak and Yodh (9) for the model F-Y00 for muon threshold energy 2 GeV which is represented by a dashed curve in the fig 3.14. The model assumes mean free paths for the inelastic interactions are energy independent, inelasticity is uniform in (0,1) for nucleons and (1/3,1) for mesons, inclusive distributions in x for secodaries are energy independent (scaling extrapolation of the ISR data) and secondary products are 60% charged pions, 30% nutral pions , 5% charged kaons and 5% nutral kaons. The value of exponent (α) from the said simulation result (.71) is close to the present observation.

3.3. Results of observations for UHE point sources :

The NBU air shower database has been examined for continuous emission of ultra high energy radiation from four potential sources of northern hemisphere, namely, Cygnus X-3 , Hercules X-1, Crab-nebula and Geminga . Evidences of any periodic signal with their well known orbital periods from the two sources,Cygnus X-3 and Hercules X-1,are also examined using the

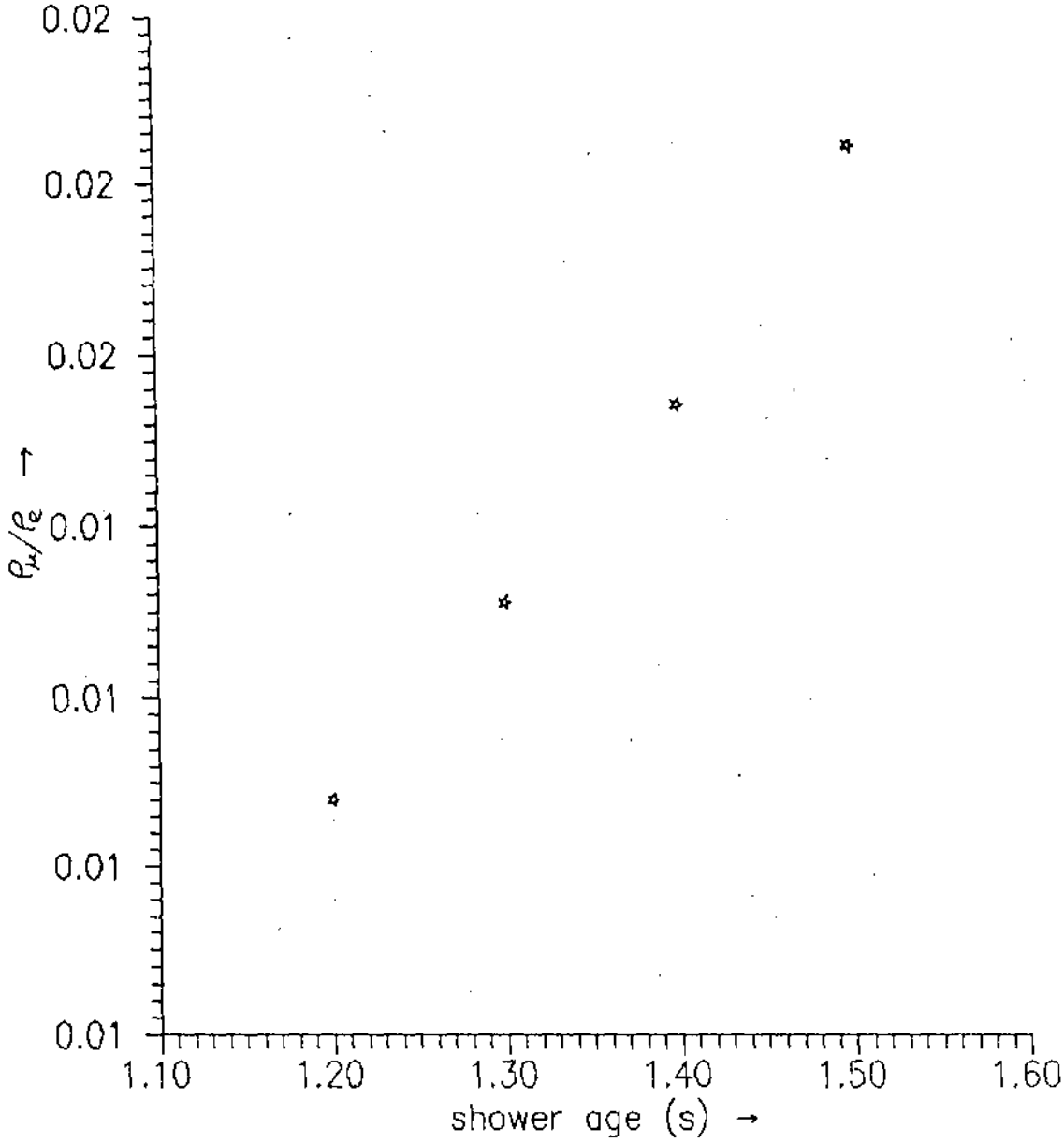

Fig.3.14 Variation of the ratio of muon density to electron density with shower age at core distance 12 m for shower size 2.5×10^5.

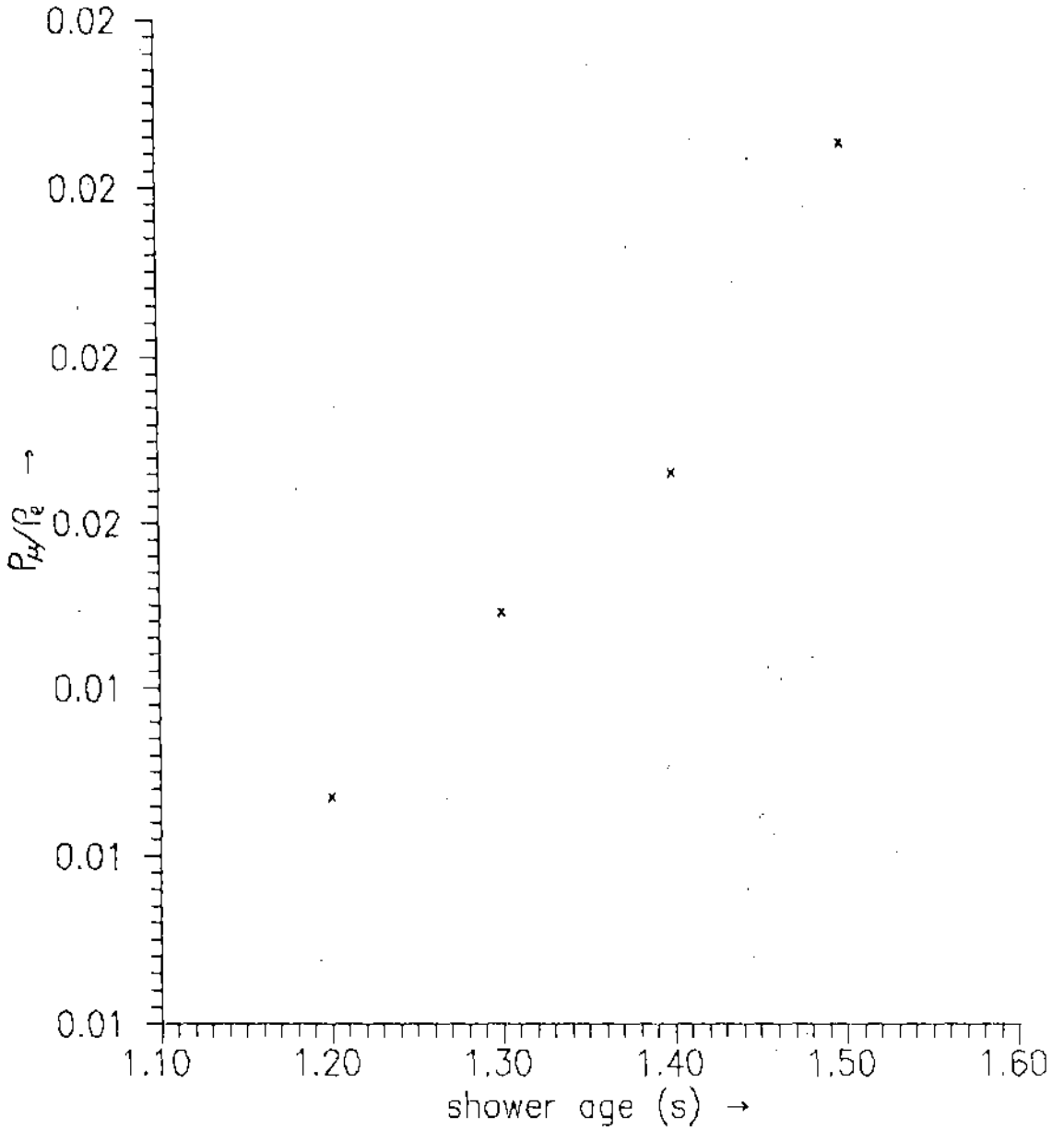

Fig.3.15 Variation of the ratio of muon density to electron density with shower age at core distance 20 m for shower size 2.5×10^5.

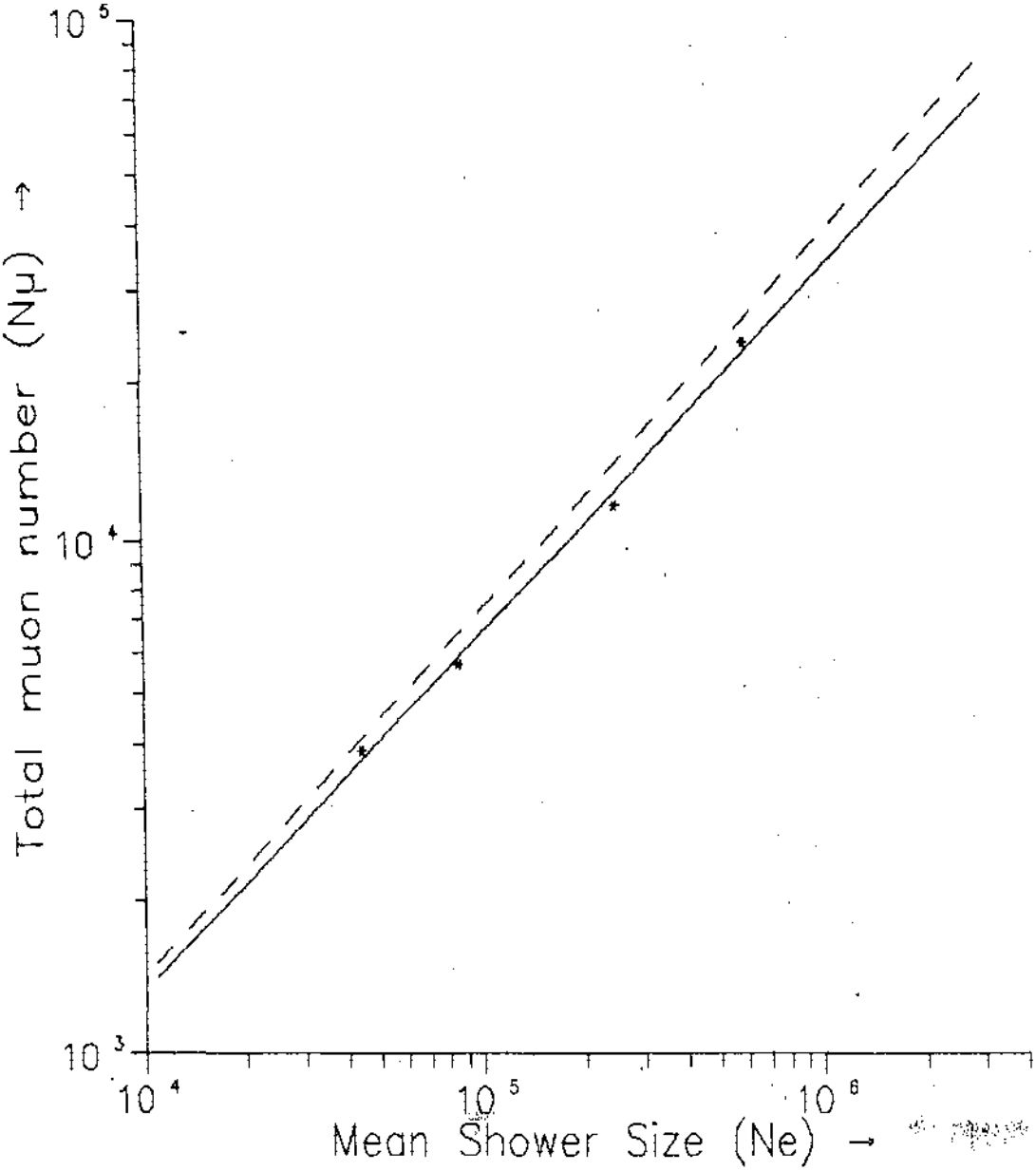

Fig 3.16 Observed muon size dependence on shower size.The dashed line corresponds to simulation results(model F-Y00) of Wrotniak and Yodh(10).

database.

Steady emission of gamma rays from a point source is reflected in an excess of showers from the direction of source compared to the steady flux of charged cosmic ray showers in that direction. In order to examine an excess of showers from a point source, the sky is divided into bins based on equatorial co-ordinates. Signal candidate events are those falling into a square bin of width 5^0 in declination and width 6^0 in right ascension .The angular resolution deduced from the odd-even sub-array comparison method is 1.1° in declination and 1.47° in right ascension.But a wider bin is chosen for the search because all the timing counter did not always give timing information.On the average 5.5 timing information was available in a shower event. Approximately 95% of events from the direction of a source are expected to arrive in the source bin.To find out whether an excess really exists in the number of showers from a given direction it is essential to know the steady flux of charged primary initiated cosmic ray showers (background) in that direction quite accurately.The main problem of estimation of the background correctly is the non-uniform exposure of different right ascension-declination region of sky both in siderial time and in zenith angle.With the time, different right ascension-declination bins drift through different zenith angles and as air showers have a fairly steep zenith angle distribution it is not possible to estimate the background in a straight way. Care has tobtaken to ensure that the source and backgrounds events are collected during the same time in the same zenith angle intervals.The background is normally evaluated from the number of events in equal sized 'off-source' bins located in the same declination strip as that of source bin but at different right ascensions.In the present analysis the background is determined as follows.

Twelve 'off source' right ascension bins, of equal width as the source bin,in the source declination band six on either side of the source bin are selected. Events are collected for each off source bin in such a way that all the 'off source' bins and the 'on source' bin are exposed for equal time and zenith angle. The average rate of events per bin gives the background count. As the background events are collected from an area twelve times larger than that of source events, the background is determined with good statistical accuracy.

Flux is calculated directly from the on-source time.For this purpose effective area of the array is determined using monte carlo simulation method.

Effective area of the array :

To measure the flux of photon induced showers from a point source , one needs to know the effective area of the air shower array as a function of primary energy and zenith angle. The effective area of an air shower array can be obtained through the Monte carlo study of the array response. The effective area is calculated by finding how many of the simulated showers meet the array trigger condition. We follow the procedure prescribed by Crewther and Protheroe (10). Shower size is generated using the parameterization given by Crewther and Protheroe(10) for gamma ray initiated showers. Shower age is sampled according to the proposition of Feriyves et al (11). The number of particles at different radial distances are obtained using NKG function (as the charged particles are expected to follow NKG distribution function). Poisson fluctuation is given to the particle number passing through the detectors. Then each of the simulated showers is checked whether they meet the array trigger requirements or not. A large number of showers is simulated to estimate the effective area of the array. The effective area of the array is plotted against primary gamma ray energy for two different zenith angles and is shown in fig 3.17.

The showers with core falling outside the perimeter of the array are rejected outright. The lowest ~10% of shower sizes are discarded as the angular resolution worsens near the array threshold. The showers with zenith angle less than 45° were only accepted for this analysis. The vertical intensity of the cosmic ray charged particles are calculated first using the effective area obtained from the simulation result. The observed vertical intensity ($I(>8 \times 10^{14}$ eV) = 4.10×10^{-10} $cm^{-2}sr^{-1}s^{-1}$) agrees well with value obtained from the expresion ($I(>E) = (E/2)^{-a} \times 10^{-10}$ $cm^{-2}sr^{-1}s^{-1}$, where E is in PeV and a = 1.55 for E< 2 PeV and a = 2.1 for E>2PeV) of the cosmic ray spectrum given by Hillas (12).

Search Results :

1. Cygnus X-3 :

A search is made for evidence of continuous as well as pulsed UHE emission from this mysterious binary system which has been previously reported as a UHE gamma ray source. The database used in the present analysis was recorded between January 1993 and June 1994 with an effective on source observation time of 212.2 hours. The source is observed at NBU site at zenith angle 14^0 at the upper transit. Figure 3.18 shows the number of showers recorded in a declination

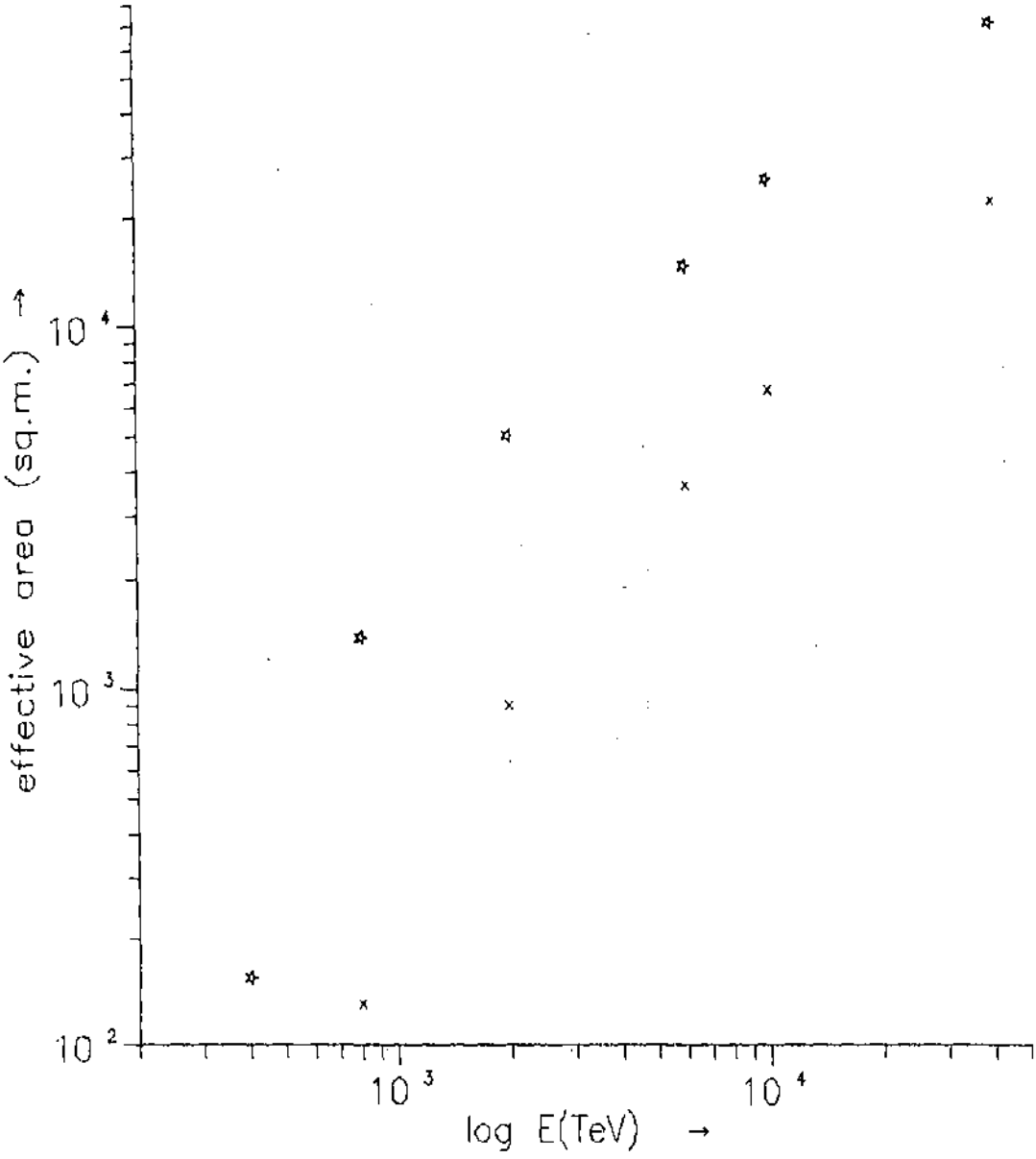

Fig 3.17 Effective area of the array as a function of primary gamma-ray energy. * – zenith angle 0°, x – zenith angle 30°.

band centered on Cygnus X-3 as a function of right ascension. The bins have 5^0 width in declination centered on 40.7^0 , the declination of Cygnus X-3. From the figure it is clear that there is a slight excess (1.79 σ) of showers in the bin centered on the Cygnus X-3 for the full observing period. The total number of air showers observed in the source bin is 26 where the average background is only 18.33.The probability for a random excess of such magnitude is 1.89×10^{-2}. The time averaged integral flux for the excess is $F(>8 \times 10^{14}\ eV) = (4.10 \pm 1.28) \times 10^{-13}$ $cm^{-2}s^{-1}$. The time averaged flux agrees well with the flux obtained in Akeno,MSU,Ooty observations (13,14,15).

The source events are then checked if they are co-related with the well known 4.8 hours periodic variation. For this purpose the arrival times of shower events from the position of Cygnus X-3 have been folded using an ephemeris by Van der klis and Bonnet-Bidaud (16) observed from the X-ray data. Total phase is divided into 10 equal bins.Results are shown in fig 3.19. Concentrations of shower events are seen in the phase bin, .5-.6 in which 6 events are observed . The amount of excess is at 2.11 σ level .The probability that 6 events might occur in any of the 10 phase bins at random out of a background of average value 2.6 per bin is 3.19×10^{-2}. The phase of emission is similar to the the present prefered UHE phase (phase ~ .6).However the statistical significance of these excesses are not high (within the 3σ limit) and a clearer picture will emerge only after analysis of more shower data.

2.Hercules X-1 :

There are several reports of continuous or sporadic UHE emission from Hercules X-1 as discussed in chapter one. NBU UHE database is looked for any evidence of continuous and pulsed emission from the direction of Hercules X-1.The effective on source observation time is 234.5 hours.

Figure 3.20 shows the number of EAS recorded as a function of right ascension in the declination band centered on Hercules X-1. The number of shower observed in the right ascension bin centered on Her X-1 is 28 where the average background is only 23. The poisson probability that this occurrence is due to chance 6.3×10^{-2}. The amount of excess (1.04 σ) is well below the 3σ level. The time average integral flux corresponds to the excess of showers is $F (> 8 \times 10^{14}\ eV) = (2.42 \pm 1.08) \times 10^{-13}\ cm^{-2}s^{-1}$.

Hercules X-1 is known to have an orbital period of 1.7 days.The detected events from the

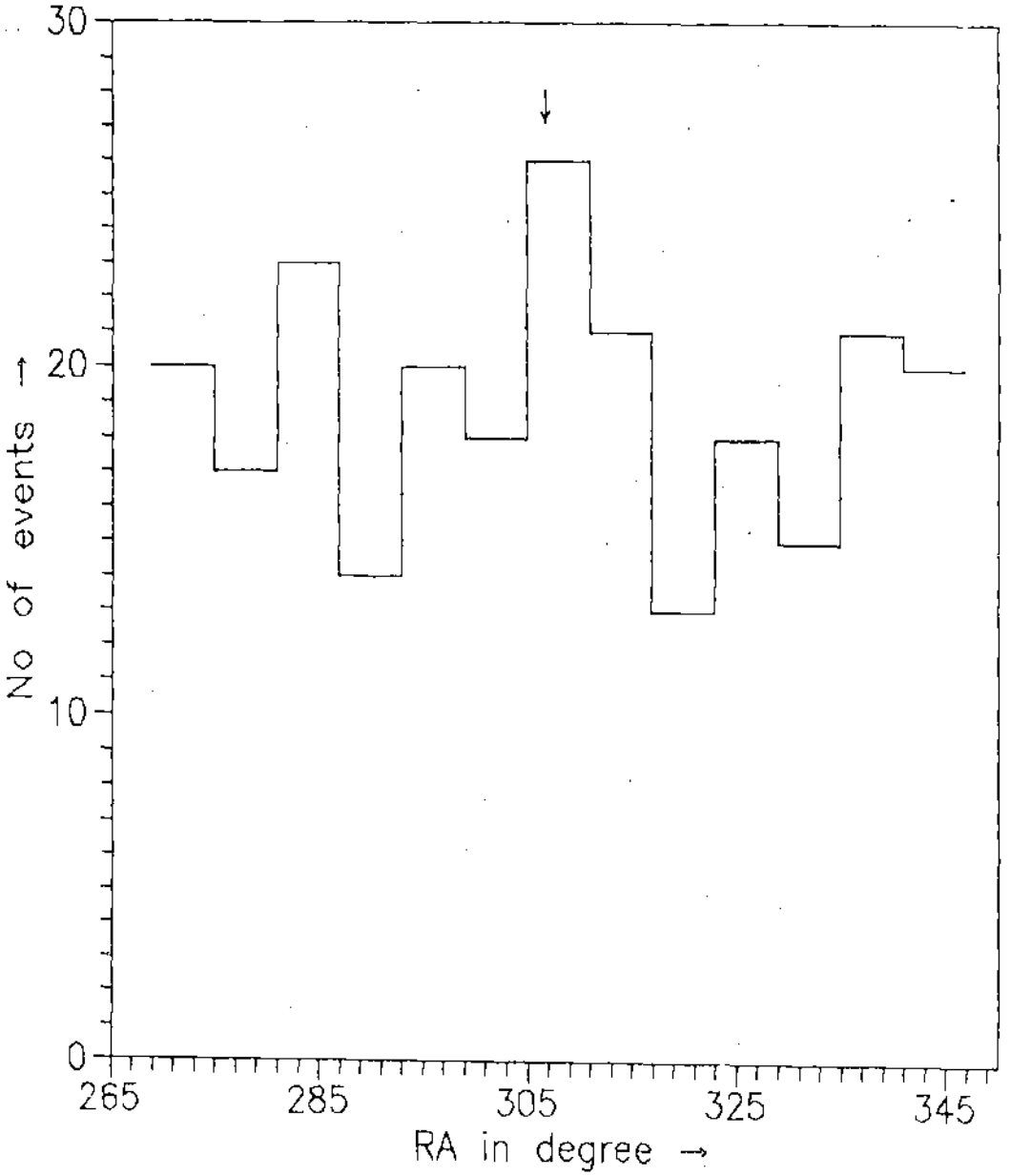

Fig 3.18 Number of observed EAS in the declination band centred on Cygnus X-3 as a function of right ascension.

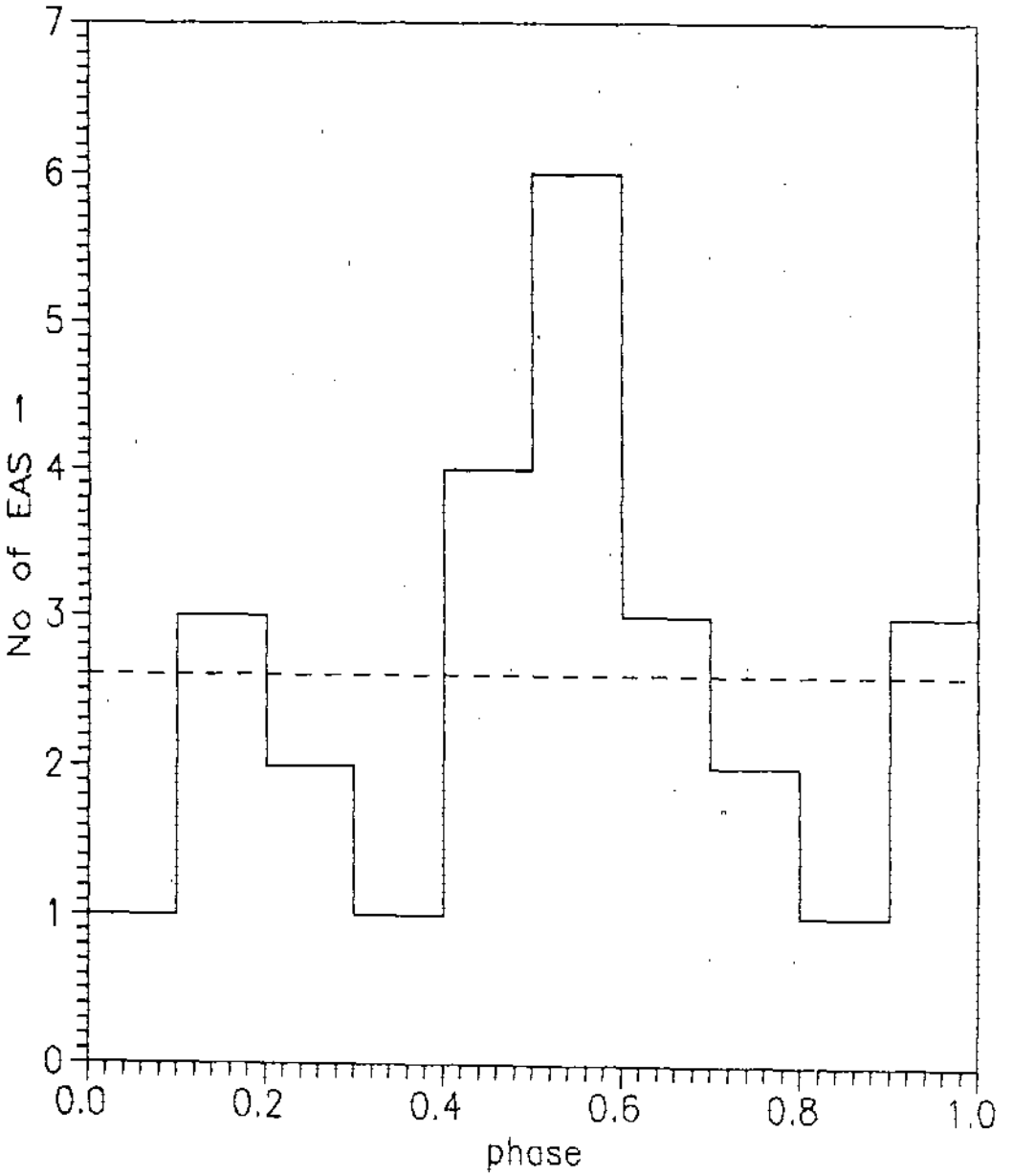

Fig 3.19 Orbital phase distribution of EAS from the direction of Cygnus X-3.

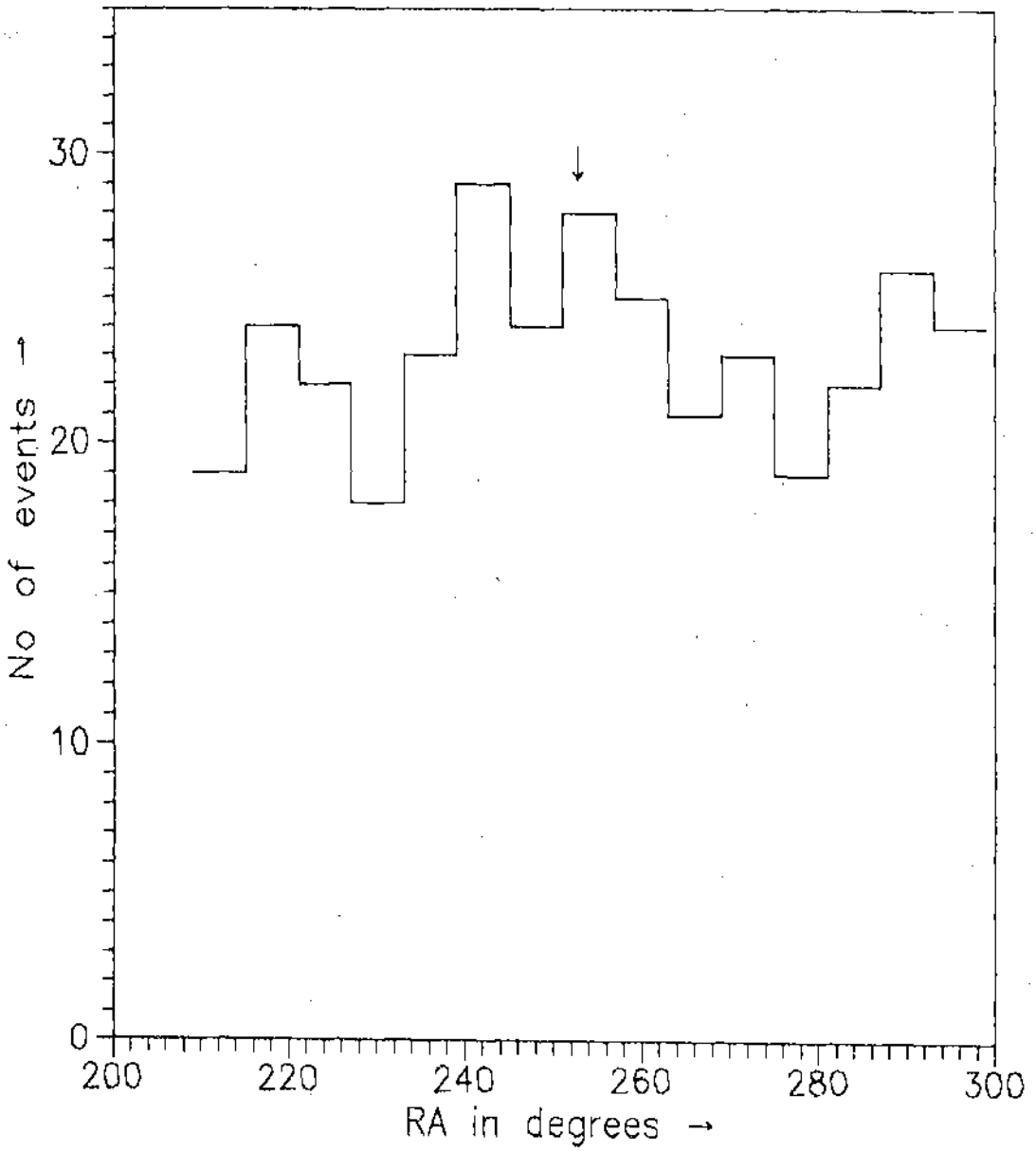

Fig 3.20 Number of observed EAS in the declination band centred on Hercules X-1 as a function of right ascension.

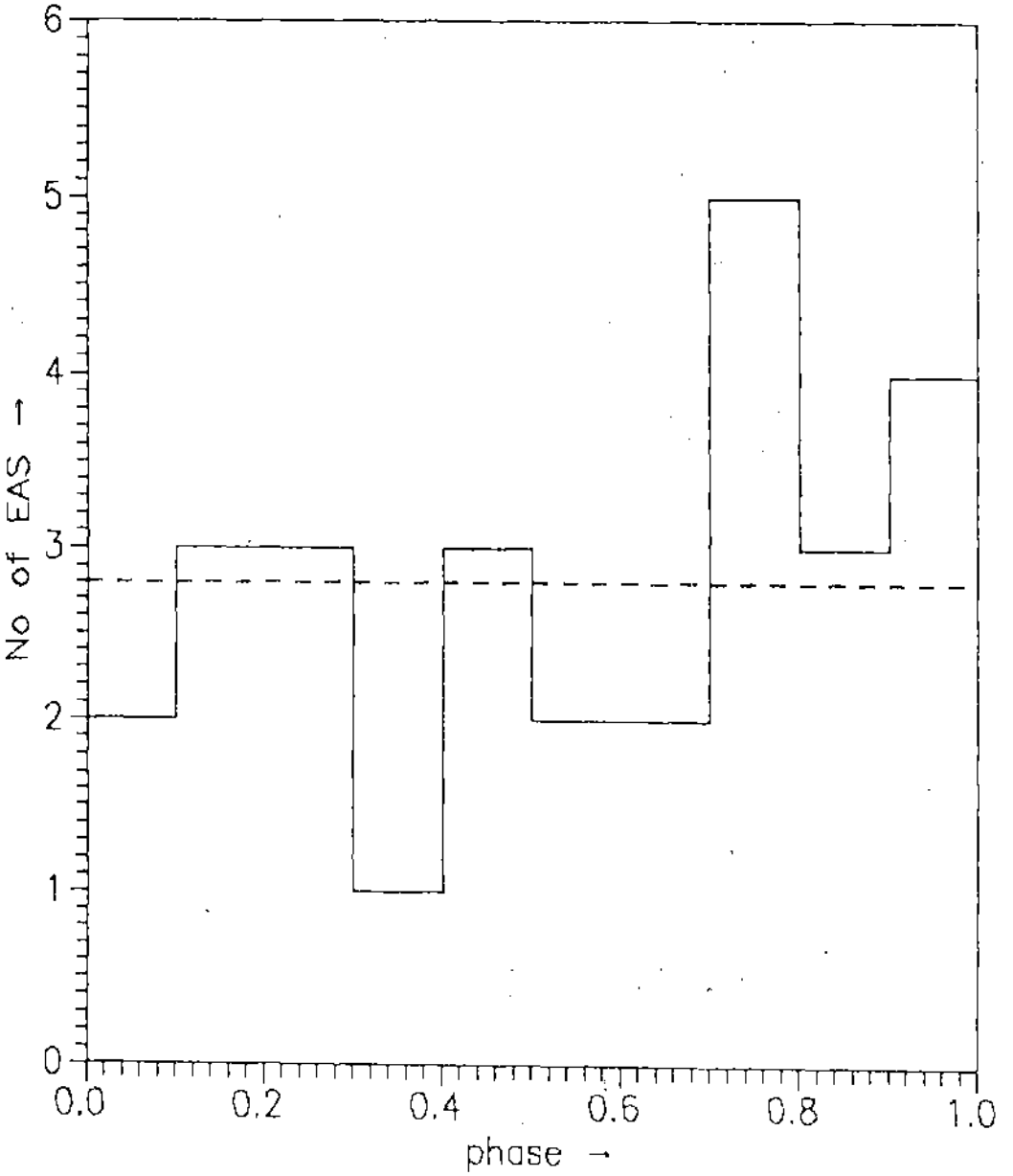

Fig 3.21 Phasogram of the events from the direction of Hercules X−1.

position of Her X-1 i,e, the on source events have been examined for coherence with the orbital period of 1.7 days. The Phasogram is shown in fig 3.21. The orbital period and the epoch are obtained from the ephemeris by Voges et al(19).No significant excess is found at any phase bin.

3.Crab-nebula :

We have searched for steady emission of UHE radiation from the region of Crab-nebula. The total effective observation time is 228.4 hours. Signal events are those falling within a source bin of width 5^0 in declination and 6^0 in right ascension. The number of events in the source bin is compared with the number of background events to search for evidence of emission. The results of this search are that 25 events is observed in the source bin against the average background of 25.05 events.The number of EAS events in the declination band centered on Crab-nebula as a function of right ascension is shown in fig 3.22. We found no evidence for UHE emission from the Crab-nebula.

4.Geminga :

Geminga is yet to be established a UHE potential gamma ray source though recently there are some positive reports for the detection of UHE radiation from the direction of Geminga.In the present analysis a search is made for steady emission of UHE radiation from the direction of Geminga. The right ascension distribution of events in the declination band centered on Geminga is shown in fig 3.23.The number of source events is 18 whereas the average value of the background is 17.92 . No evidence is seen for continuous emission in these data.

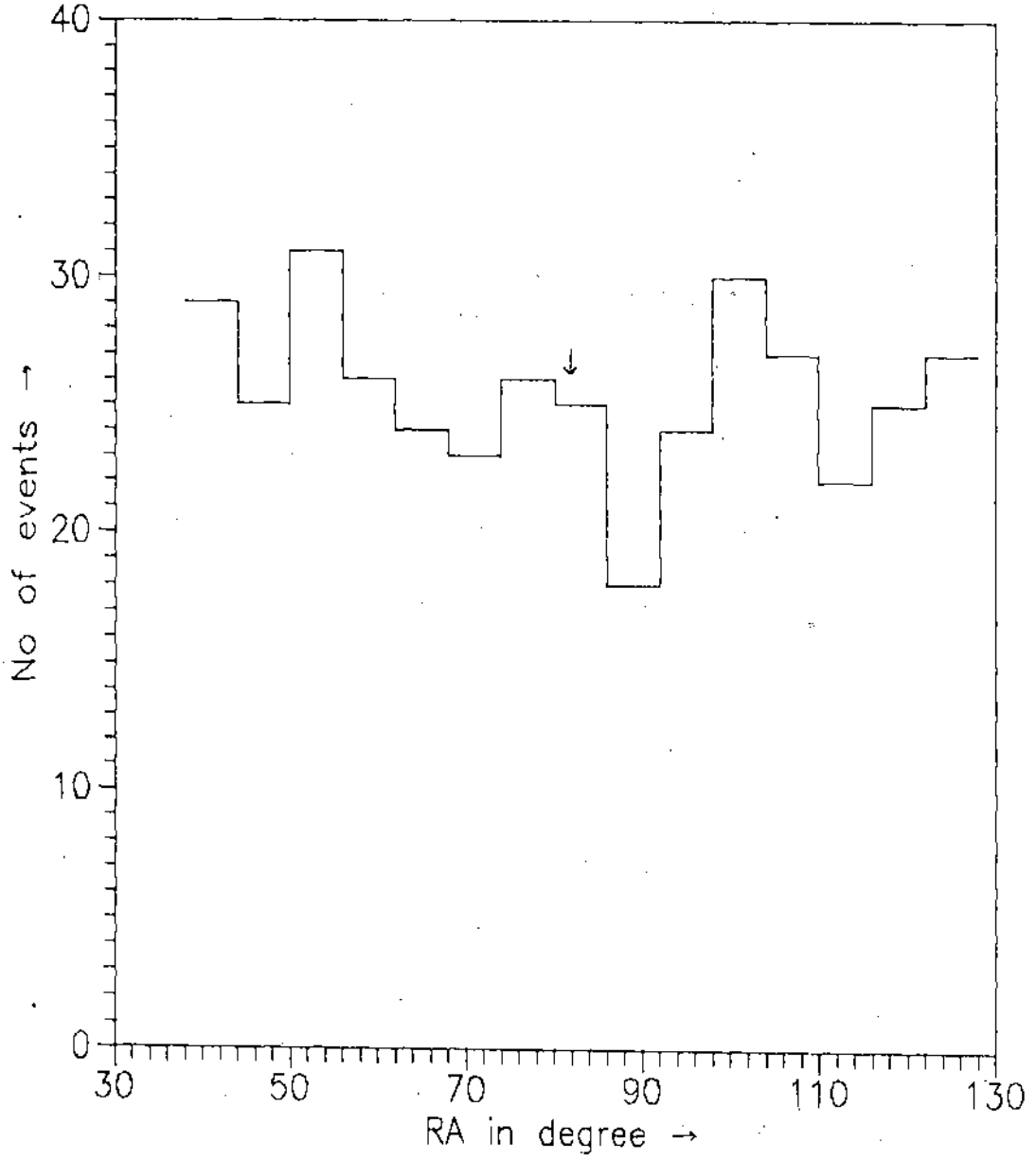

Fig 3.22 Number of observed EAS in the declination band centred on Crab Nabula as a function of right ascension.

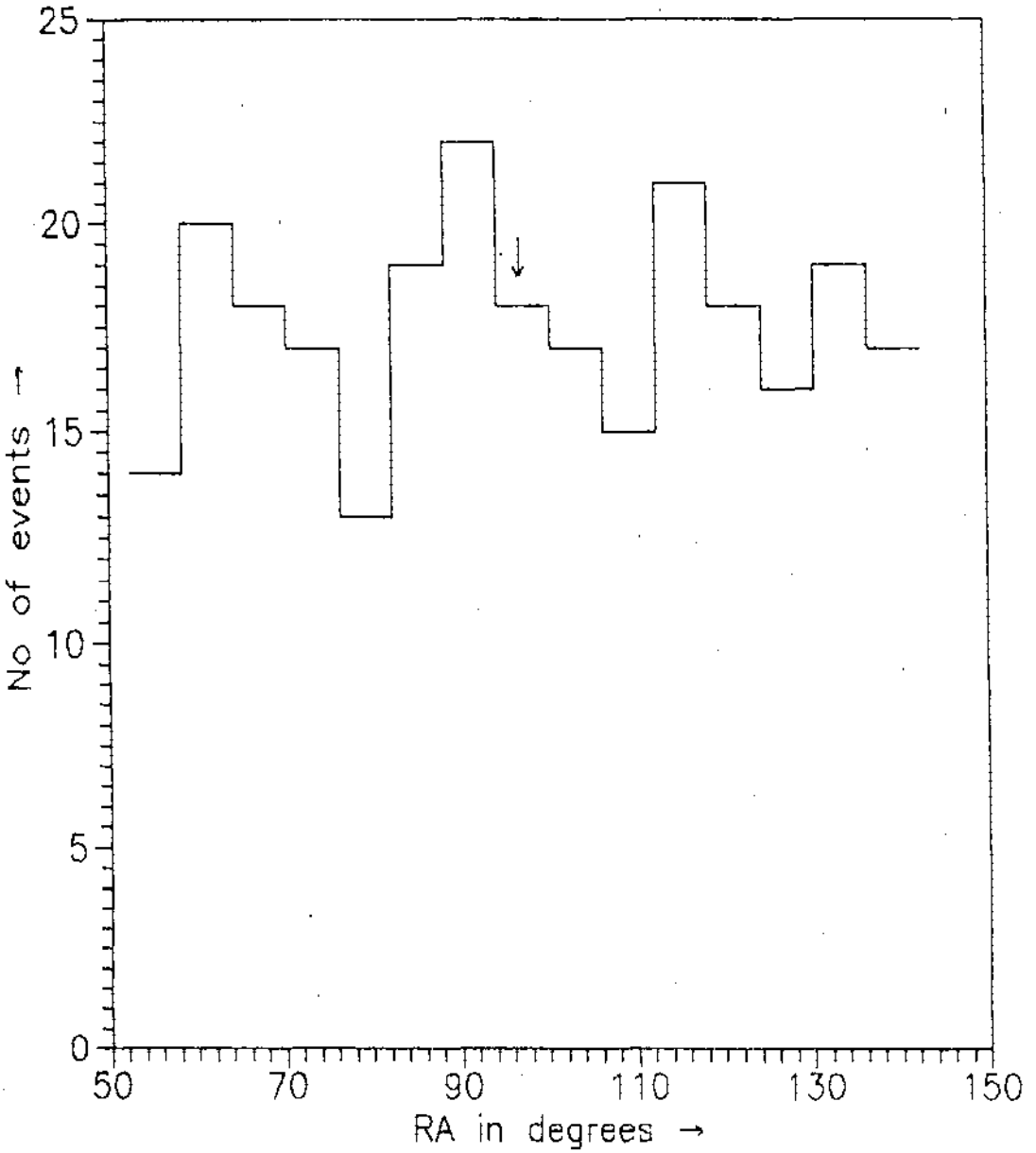

Fig 3.23 Number of observed EAS in the declination band centred on Geminga as a function of right ascension.

*** Chapter 4 ***

Conclusions :

The modern UHE gamma-ray astronomy is now about fifteen years old .But the situation of observation of UHE gamma radiation from discrete sources is still very confusing. Early observations of Cygnus X-3 provided the hope that the UHE radiation from this and similar sources could be studied regularly.However most recent observations have been unable to confirm the existence of such emission.The long standing problem regarding the nature of the primary particles responsible for the positive detections of excess EAS from the direction of the discrete point sources are yet to be solved.

To understand the muon anomaly associated with the subject from its birth in the present investigation the variation of the ratio of muon density to particle density with shower age for a particular shower size at a particular radial distance from the shower core is studied.It is observed that the ratio increases sharply with shower 'age'. It is expected because the muon number does not change much with the atmospheric depth traversed after the maximum development of shower reaches while electron component attenuates rapidly after the maximum development of showers. It is interesting to note that high muon content of the excess showers from the direction of Cygnus X-3 as observed by the Kiel group is also characterised by high 'age' values.Though, in Kiel observation the muon content of the excess showers is compared with the background also having high 'age' values but it may happen that the excess showers from the direction of Cygnus X-3 is characterised by even higher 'age' values. In several other experiments it was also observed that the excess showers from the direction of discrete point sources have high shower 'age' value. It is true that the amount of γ_{muon} excess (67% instead of 10%) could not be explained by high shower age value alone but the present result indicate that the high muon content and high 'age' value may not be independent characteristics of the excess directional showers.

Discrimination of gamma-ray initiated showers from the large background of charged cosmic ray initiated showers based on shower 'age' has been used in several observations on the assumption that ,for same shower size, photon induced showers are older. Fenyves (1), Hillas (2),Cheung and Mackeown(3) from their monte carlo simulation results concluded that in 'age' the gamma-ray induced showers are not older than that of normal showers, though in several observations it is found that the excess showers from the direction of discrete point sources are

characterised by high 'shower age' value.Since in most of the observations the shower from point sources were observed at large angles during most of the observation time (due to high angle of transit of the sources at the arrays) so it may happen that high 'age' values of the excess EAS's are due to high zenith angle.To understand the problem ,variation of shower 'age' with zenith angle is examined.It is found that the variation is slow, and up to zenith angle 30°, shower 'age' is practically independent of zenith angle.In the Kiel observation, showers with zenith angle less than 30° only were accepted for the analysis.So it is difficult to correlate the high 'age' value of the directional excess showers with zenith angle.

In the quest for UHE radiation from potential discrete point sources of the northern hemisphere four sources are studied in the present investigation, Cygnus X-3,Hercules X-1, Crab nebula and Geminga. We found no statistically significant excess of EAS from any of these sources.The Cygnus X-3 data set shows a steady excess of 1.79 σ .The time average integral flux of particles responsible for the excess of showers seen from the direction of the object is obtained as $F(>8 \times 10^{14}\ eV) = (4.10 \pm 1.28) \times 10^{-13} cm^{-2} s^{-1}$ .The phase analysis of the event time of EAS from the direction of the Cygnus X-3 also indicates an excess of 2.11σ in the phase bin .5-.6 . The statistical significance of the excess is not sufficient for any claim of a detection .A clearer picture will emerge only after analysis of more shower data.The Hercules X-1 database shows a marginal steady excess of 1.04σ which corresponds to a time average integral flux of $F(>8 \times 10^{14}\ eV) = (2.42 \pm 1.08) \times 10^{-13} cm^{-2} s^{-1}$.The search for 1.7 day pulsed flux from Hercules X-1 has also been performed.No significant excess can be found at any phase.There is no statistically significant evidence for continuous emission from Crab nebula and Geminga.

There is considerable uncertainty about the present situation of the UHE gamma-radiations from celestial discrete point sources.Early claims of marginal statistical significance have not been substantiated by more recent observations.The performance of the detectors improved with time but the significance of most of the published positive observation remained at a 3σ level.The lack of clear identification of the gamma-ray signature of the positive signal is one of the reason to doubt the reality of the sources.However it is also true that positive evidences of UHE signal from discrete point sources is observed in several independent observations. Moreover the event times of the

excess showers from the direction of Cygnus X-3 are found to be modulated with a period 4.8 hour which is the orbital period of the object and similar to as observed from the x-ray data.Similar characteristics have been observed for few other sources too. So, it appears that the sources are real.But, it has now become clear that long term steady flux from Cygnus X-3 is much less then reported for late seventies and early eighties.These observations suggest that sporadic emission on a wide time ~~of~~ scale may be characteristics of Cygnus X-3 and many other UHE point sources.

Further observations are necessary to provide more information on the nature of the discrete UHE point sources .The present experiment is an ongoing experiment.The data analysis is continuing.It is expected that a clear picture of observation of UHE gamma-ray sources will emerge after analysis of few years data.

*** References ***

References :

Chapter 1

Sec 1

1. Fermi , E. Phys. Rev, 75 (1949) 1169
2. Baade and zwicky Phys Rev. 46(1934) 76
3. Samorski, M. and Stamm,W. Ap J (lett) 268(1983)L17
4. Wdowczyk, J. and Wolfendale, A.W. Nature,305(1983) 609
5. Morrision, P. Nuovo Cimento 7(1958)858
6. Auger,P.,Maze,R. and Grivet-mayer, T.C.R. Acad Sci, Paris, 206(1938)1721

Sec 2

1. Samorski,M. and Stamm, W. Ap J (Lett) 268 (1983) L17
2. Wdowczyk, J. in Proc. of 8th ICRC , London, 2 (1965) 691
3. Maze R. and Zawdzki A. Nuovo Cimento 17 (1960) 625
4. Chadwick P.M. et al , Nature , 318 (1985) 642
5. Giacconi et al , Ap J (Lett) , 148 (1967) L119
6. Vladhimarskii B.M. and Stepanian A.A. , in Proc. 13th ICRC , Denver, 1 (1973) 456
7. Fegan D.J. and Danaher S. in Proc. 17th ICRC, Paris , 1 (1981) 31
8. Hayashida N. et al , in Proc. 17th ICRC ,Paris ,9(1981) 9
9. Parignault et al , Ap J. (Lett) 209 (1976) L73
10. Samorski M. and Stamm W. in Proc. 18th ICRC, Bangalore, 11,(1983) 244
11. Lloyd-Evans J et al , Nature,305 (1983) 784
12. Morello C. et al , in Proc 18th ICRC,Bangalore, 1(1983) 127
13. Tonwar S.C. et al , Ap J. (Lett) 330 (1988) L107
14. Dingus B.L. et al , Phys. Rev. Letts. 61 (1988) 1906
15. Weeks T.C. Space Sci. Rev. 59 (1992) 315
16. Merck M. et al , in Proc 22th ICRC, Dublin, 1 (1991) 261
17. Borione A. et al , in Proc 23th ICRC, Calgary, 1(1993) 385

18. Aglietta M. et al , in Proc 22th ICRC, Dublin, 1(1991) 277
19. Muraki M. et al , in Proc 23th ICRC, calgary, 1(1993) 380
20. Beaman J. et al, in Proc 22th ICRC, Dublin,1 (1991) 297
21. Alexandreas D.E. et al , in Proc 23th ICRC, Calgary, 1(1993) 373
22. Hayashida N. et al , in Proc 22th ICRC, Dublin, 1(1991) 309
23. Cassiday G.L. et al , Phys. Rev. Letts. 62 (1989) 383
24. Teshima M. et al , Phys. rev. Letts. 64 (1990) 1628
25. Hayashida N. et al , in Proc 22th ICRC, Dublin, 1(1991) 309
26. Lawrence M.A. et al , Phys. rev. Letts. 63 (1989) 1121
27. Dowthwaite J.C. et al, Nature , 309 (1984) 691
28. Resvanis L.K. et al. , Ap J (Lett) 328 (1988) L9
29. Vishwanath P.R. et al. , Ap J. 342 (1989) 489
30. Baltrusaits R.M. et al, Ap J. (Letts) 293 (1985) L69
31. Acharya B.S. et al, in Proc 22th ICRC, Dublin, 1(1991) 237
32. Muraki M. et al , in Proc 22th ICRC, Dublin, 1(1991) 245
33. Mckay T.A. et al , in Proc 22th ICRC, Dublin, 1(1991) 245
34. Beaman J. et al. in Proc 22th ICRC, Dublin, 1(1991) 297
35. Gupta S.K. et al , Ap J. (Lett) 354 (1990) L13
36. Merck M. et al , in Proc 22th ICRC, Dublin, 1(1991) 261
37. Alexandreas D.E. et al , in Proc 23th ICRC, Calgary, 1(1993) 373
38. Protheroe R.J. et al , Ap J. (Lett) 280 (1984) L47
39. BASJE collab. in Proc workshop in techniques in UHE gamma-ray astronomy , La Jolla, (1985)
40. Fazio G.C. et al , Ap J. (Lett) 175 (1972) L117
41. Cawlay et al, in Proc 19th ICRC, La Jolla, 1(1985) 131
42. Dzikowski T. et al , in Proc 17th ICRC, Paris, 1(1981) 8
43. Boone J. et al, Ap J. 285 (1984) 264
44. Kirov I.N. et al ,in Proc 19th ICRC, La Jolla , 1(1985) 135
45. Watson A.A. in Proc 19th ICRC, La Jolla, 9 (1985) 111
46. Alexeenko et al, Proc. Int. workshop on VHE gamma-ray astronomy, Crimea, (1989) 187
47. Acharya B.S. et al, Nature, 347 (1990) 364
48. Aglietta M. et al , in Proc. Int. workshop on VHE gamma-ray astronomy, Crimea, (1989) 60

49. Matano T. et al, ICR Report 164-88-10 (1988)
50. Tonwar S.C. et al , Nucl Phys. B. (Proc. Suppl) 14A (1990) 226
51. Smith N.J. et al, in Proc. Int. workshop on VHE gamma-ray astronomy, Crimea, (1989) 55
52. Brazier K.T.S. et al , in Proc 21st ICRC , Adelaide, 1(1990) 292
53. Fruchter A.S. et al, Nature, 333 (1988) 237
54. Sinha S. et al , in Proc 21st ICRC , Adelaide, 2(1990) 370
55. De Jager O.C. et al, Nucl. Phys. B (Proc. Suppl.) 14A (1989) 169
56. Gupta S.K. et al, Astron. Astr. Phys. 241 (1991) L21
57. Kniffen D.A. et al , in Proc 14th ICRC , Munchen, 1(1975) 100
58. Vishnath P.R. et al, Int Astronomical Union Circular (1992) 5612
59. Bowden C.C.G. et al , J.Phys. G 19 (1993) L29
60. Gupta S.K. et al , 23rd ICRC , Calgary , 1(1993) 396
61. Thompson D.L. et al , Ap J. 213 (1977) 252
62. Clay R.W. et al, Aust. J. Phys. 37(1984) 91
63. Alien W.H. et al, in Proc 23rd ICRC , Calgary, 1(1993) 420
64. Stanev T. et al, Phys. Rev. D32 (1985) 1244
65. Halzen F. et al, Phys. Rev. D33 (1986) 2061
66. Edwards P.G. et al, J.Phys. G. Nucl. Phys. 11 (1985) L101
67. Mckomb T.S.L., Protheroe R.J. and Turver K.E. et al, J.Phys.G. 5 (1979) 1613
68. Marshak M. L. et al . Phys. Rev. Lett. 54 (1985) 2079
69. Battistoni G. et al, Phys. Lett. 155B (1985) 465
70. Kifune T. et al, Ap J. 301 (1986) 230
71. Quated from Blake P.R. and Nash W.F. , in Proc 19th ICRC , La Jolla, 7(1985) 215
72. Berezinsky V.S. , Ellis J. and Ioffe B.L., Phys Lett. 172 B (1986) 423
73. Ruddick K et al , Phys.Rev. Lett. 57 (1986) 531
74. Collins J.C. and Olness F. Phys. Lett. 187B (1987) 376
75. Beznikov L.B. and Bugaev E.V. , in Proc 17th ICRC , Paris, 7(1981) 90
76. Drees and Halzen F. Phys Rev. Lett. 61(1988) 275
77. Wdowczyk J. and Wolfandale A.W. in Proc 21st ICRC , Adelaide, 9(1990) 25
78. Halzen F. et al, in Proc 21st ICRC , Adelaide, 9(1990) 142

79. Derrick et al , Phys. Lett. 293B (1992) 465

80. Fomin Yu.A.et al , in Proc 20th ICRC , Moscow, 1(1987) 397

81. Fenyves J. , in Techniques in UHE γ-ray astronomy , ed. Protheroe R.J. and Stephens S.A. University of Adelaide , (1985) 124

82. Hillas A.M. , in Proc 20th ICRC , Moscow, 2(1987) 362

83. Cheung T. and Mackeown P.K. , IL Nuovo Cimento , 11C(1988) 193

Sec 3

1. Fenyves E.J. , in Techniques in UHE γ-ray astronomy , Ed. Protheroe R.J. and Stephens S.A. University of Adelaide , (1985) 124

2. Hillas A.M. , in Proc 20th ICRC , Moscow, 2(1987) 362

3. Cheung T. and Mackeown P.K. , IL Nuovo Cimento , 11C(1988) 193

Chapter 2

Sec 1

1. Sarkar S.K. , Ph.D. Thesis (Unpublished) , University of North Bengal, India, (1987)

2. Goswami G.C. et al, Nucl. Inst. Meth. 192 (1982) 375

3. Goswami G.C. et al , Nucl. Inst. Meth. 199 (1982) 505

Sec 2

1. Moliere C. Cosmic Radiation , Ed. Heisenberg W. , New York, Dover (1946)

2. Nishimura J. and Kamata K. , Prog. Theo. Phys. 7 (1952) 185

3. Greisen K. Progress in Cosmic Ray Phys. , Vol III , Ed. Wilson J.G. , Amstardam, North Holland (1956)

4. Eames P.J.V. et al ,in Proc 20 th ICRC , 2 (1987) 449

5. Hillas A.M. ,in Proc 20 th ICRC, 6 (1987) 432

6. Linsley J. , J.Phys. G. Nucl. Phys. 12(1986) 51

Chapter 3

1. Fenyves E.J. , in Techniques in UHE γ-ray astronomy , Ed. Protheroe R.J. and Stephens S.A. University of Adelaide , (1985) 124
2. Greisen K. Progress in Cosmic Ray Phys. , Vol III , Ed. Wilson J.G. , Amstardam, North Holland (1956)
3. Greisen K. , Ann. Rev.Nucl. Sci. ,10 (1960) 63
4. Hillas A.M. , in Proc 20th ICRC , Moscow, 2(1987) 362
5. Cheung T. and Mackeown P.K. , IL Nuovo Cimento , 11C(1988) 193
6. Clay R.W. et al, IL Nuovo Cimento , 4C (1981) 668
7. Aguirre C. et al. , in Proc. 13th ICRC, Denver, 4 (1973) 2598
8. Hara T. et al , in Proc 16th ICRC , Kyoto , 13 (1979) 148
9. Wrotniak A.K. and Yodh G.B. , in Proc 19 th ICRC , 7 (1985) 1
10. Crewther I.Y. and Protheroe R.J. , J Phys G. Nucl. Phys. 16 (1990) L13
11. Fenyves E.J. Phys. Rev. D37 (1988) 649
12. Hillas A.M. , in Cosmic Ray Workshop, Ed. Gaisser T.K. ,Univ. of Utah, (1983) 16
13. Edwards P.G. et al , in Proc 21st ICRC , 2 (1990) 147
14. Fomin Yu.A.et al , in Proc 20th ICRC , Moscow, 1(1987) 397
15. Tonwar S.C. et al., Ap J. 330 (1988) L107
16. Vandet kirs M. and Bornet-Bideud J.M. , Astr. Ap. 214 (1989) 203
17. Voges W. et al, Space Sc. Rev. 40(1985) 339

Chapter 4

1. Fenyves E.J. , in Techniques in UHE γ-ray astronomy , Ed. Protheroe R.J. and Stephens S.A. University of Adelaide , (1985) 124
2. Hillas A.M. , in Proc 20th ICRC , Moscow, 2(1987) 362
3. Cheung T. and Mackeown P.K. , IL Nuovo Cimento , 11C(1988) 193

Aust. J. Phys., 1993, 46, 589–96

An Analysis of Cosmic Ray Air Showers for the Determination of Shower Age

S. Sanyal, B. Ghosh, S. K. Sarkar, A. Bhadra, A. Mukherjee and N. Chaudhuri

High Energy and Cosmic Ray Centre, North Bengal University,
Darjeeling 734 430, India.

Abstract

A sample of 8651 air showers in the size range $10^{4\cdot3}$–$10^{6\cdot2}$ has been analysed to determine the distribution of the measured age in terms of (i) the number of showers in a specified size range, and (ii) the radial distances in individual showers. It is shown that the radial age distribution in an individual shower leads to an average shower age approximately the same as the prediction of the electron–photon cascade theory. The other results include a study of the variation of (i) shower age, as measured by the χ^2-minimisation technique, with shower size of vertically incident showers, and (ii) the measured electron density at any point with its radial distance from the shower axis, as a function of the age of a large shower group with very small spread in size. A comparison of similar measurements with relevant theory is also included.

1. Introduction

The development in the longitudinal direction of electron–photon cascades in cosmic ray extensive air showers is described by a parameter called the shower age s. The cascade grows to a maximum ($s = 1$) and then rapidly decays. In the lateral direction from the axis of the shower, the electron density distribution in the shower is measured in terms of the radial age $S(r)$ as one of the parameters. In most earlier experiments (Idenden 1990; Hara *et al.* 1981, 1983; Abdullah *et al.* 1981, 1983), the shower age determined by the standard least-squares fitting technique differs from the theoretical value at all atmospheric depths. This was taken to be an indication that a shower must be described by two age parameters, one for its longitudinal development and the other for its lateral development (Hara *et al.* 1983; Sasaki 1971; Capdevielle and Gawin 1982, 1985; Dai *et al.* 1990). This aspect of extensive air showers has been under investigation in recent years at various centres (Idenden 1990; Dai *et al.* 1990; Cheung and MacKeown 1987; Samorski and Stamm 1983). In the present work a critical experimental examination is made of the techniques used to determine the shower age from new measurements on smaller air showers in the size range $10^{4\cdot3}$–$10^{6\cdot2}$. An analysis of shower age has also been made to show its dependence on various shower parameters.

2. Experiment

The air shower array at the North Bengal University campus has been developed in stages since 1980 (Basak *et al.* 1984). At present it consists of 21 electron-

0004-9506/93/040589$05.00

density-sampling plastic scintillation detectors, eight fast timing detectors and two magnet spectrographs. The total area covered by the array is 1176 m^2. The shower size threshold for the array is $N_e = 10^{4\cdot2}$. The radial electron density distribution and muon density distribution are measured simultaneously over a radial distance from the array centre to about 30 m and the muon energy in the range 2·5–220 GeV.

To determine the size of a shower, the electron densities at radial distance intervals of 8 m ($\sim r_0/10$, where r_0 is the Molière radius in air at sea level) were measured by a cluster of 21 scintillation detectors installed at sea level. The dynamic range of the detectors is 1–250 particles/detector and each detector was operated at a threshold of one particle. The shower direction was determined by measuring relative arrival times, while shower size N_e, age parameters s and core location (x_0, y_0) determination was carried out by fitting the radial electron density data of a shower event to an interpolating lateral structure function as given by Hillas and Lapikens (1977):

$$f(r) = c(s)\,(r/r_1)^{a_1+a_2(s-1)}(1 + r/r_1)^{b_1+b_2(s-1)}\,, \qquad (1)$$

where $c(s)$ is the normalisation constant and $a_1 = -0{\cdot}53$, $a_2 = 1{\cdot}54$, $b_1 = -3{\cdot}39$, $b_2 = 0$ and $r_1 = 24\ m$.

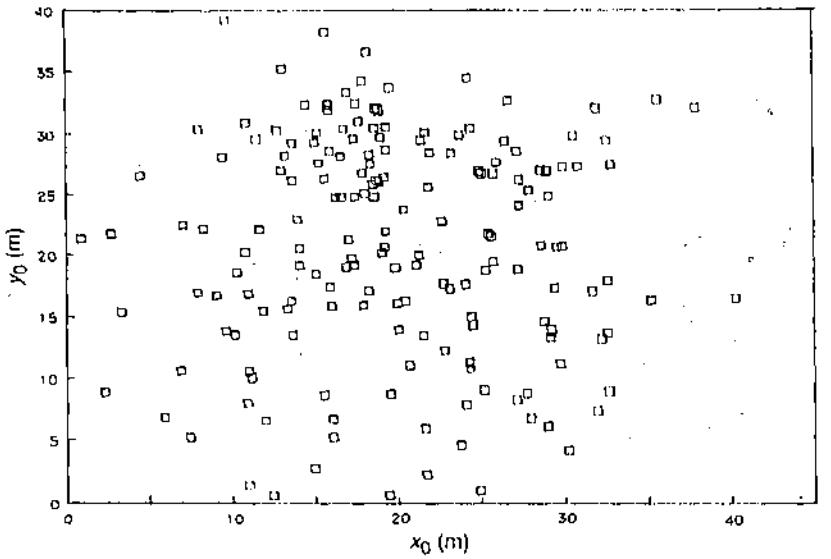

Fig. 1. Distribution of shower core location (x_0, y_0) for a group of 178 showers of $\overline{N}_e = 1{\cdot}2\times10^5$ with $\bar{s} = 1$.

The computed results on the shower core location (x_0, y_0) form a random distribution, as shown in Fig. 1 for a group of 178 showers of size $\overline{N}_e = 1{\cdot}2\times10^5$ with age $\bar{s} = 1$.

(2a) Determination of Radial Age Parameter

Using the Hillas–Lapikens (III$_A$) structure function (1) and assuming that the normalisation constants do not vary much at two neighbouring radial points r_i and r_j measured from the core position (e.g. Fig. 1), we obtain for the radial age parameter, at radial location $r_i - r_j$,

$$S_{ij}(r) = \ln(F_{ij}\, X_{ij}^{2\cdot 07}\, Y_{ij}^{3\cdot 39})/1\cdot 54 \ln X_{ij}\,, \tag{2}$$

where $F_{ij} = f(r_i)/f(r_j)$, $X_{ij} = r_i/r_j$, $Y_{ij} = (1 + x_i)/(1 + x_j)$, with $x = r/r_1$. Substitution of the measured electron densities at the radial points r_i and r_j in the above formula gives $S_{ij}(r)$. With the Nishimura–Kamata-Greisen (NKG) function (Greisen 1960), the expression for $S_{ij}(r)$ under the same conditions as in (2) is

$$S_{ij}(r) = \ln(F_{ij}\, X_{ij}^{2}\, Y_{ij}^{4\cdot 5})/\ln(X_{ij}\, Y_{ij})\,. \tag{3}$$

Some representative results are shown in Table 1.

Table 1. Radial variation of shower age $S_{ij}(r)$ for three shower sizes

		(a) Shower size $N_e = 5\cdot 3\times 10^4$			
Radial distance interval (m)	2·5–5·5	5·5–8·5	8·5–12·5	12·5–17·5	17·5–22·5
HL	$1\cdot 481^{+0\cdot 075}_{-0\cdot 059}$	$1\cdot 535^{+0\cdot 026}_{-0\cdot 024}$	$1\cdot 592^{+0\cdot 034}_{-0\cdot 032}$	$1\cdot 464^{+0\cdot 015}_{-0\cdot 014}$	
NKG		$1\cdot 759^{+0\cdot 038}_{-0\cdot 034}$	$1\cdot 687^{+0\cdot 047}_{-0\cdot 044}$	$1\cdot 384^{+0\cdot 019}_{-0\cdot 018}$	$1\cdot 761^{+0\cdot 050}_{-0\cdot 047}$
		(b) Shower size $N_e = 1\cdot 2\times 10^5$			
Radial distance interval (m)	12·5–17·5	17·5–22·5	22·5–27·5	27·5–32·5	32·5–37·5
HL	$1\cdot 177^{+0\cdot 009}_{-0\cdot 008}$	$1\cdot 779^{+0\cdot 025}_{-0\cdot 023}$	$1\cdot 666^{+0\cdot 007}_{-0\cdot 007}$	$1\cdot 550^{+0\cdot 015}_{-0\cdot 014}$	$1\cdot 738^{+0\cdot 115}_{-0\cdot 123}$
NKG	$1\cdot 002^{+0\cdot 012}_{-0\cdot 011}$	$1\cdot 699^{+0\cdot 032}_{-0\cdot 030}$	$1\cdot 491^{+0\cdot 009}_{-0\cdot 009}$	$1\cdot 312^{+0\cdot 019}_{-0\cdot 017}$	$1\cdot 513^{+0\cdot 133}_{-0\cdot 144}$
		(c) Shower size $N_e = 1\cdot 2\times 10^6$			
Radial distance interval (m)	22·5–27·5	27·5–32·5	32·5–37·5	37·5–45	45–55
HL	$1\cdot 489^{+0\cdot 049}_{-0\cdot 069}$	$1\cdot 971^{+0\cdot 009}_{-0\cdot 163}$	$1\cdot 688^{+0\cdot 121}_{-0\cdot 096}$	$1\cdot 877^{+0\cdot 031}_{-0\cdot 112}$	$1\cdot 775^{+0\cdot 058}_{-0\cdot 052}$
NKG	$1\cdot 271^{+0\cdot 061}_{-0\cdot 085}$	$1\cdot 820^{+0\cdot 085}_{-0\cdot 197}$	$1\cdot 455^{+0\cdot 142}_{-0\cdot 114}$	$1\cdot 654^{+0\cdot 151}_{-0\cdot 128}$	$1\cdot 526^{+0\cdot 065}_{-0\cdot 058}$

The average age parameter of a shower at a particular size is given by

$$\bar{S} = \sum_{ij} \frac{2w_{ij}}{r_j^2 - r_i^2} \int_{r_i}^{r_j} S_{ij}(r) r\, dr\,, \tag{4}$$

where (r_i, r_j) is the radial distance interval within which the radial age parameters are measured experimentally, and w_{ij} is the statistical weight factor of that particular radial distance bin (i, j).

According to electron–photon cascade theory, the shower age is

$$S(\text{theor.}) = 3t/[t + 2\ln(E_0/\epsilon_0) + 2\ln z], \tag{5}$$

where $\epsilon_0 = 0{\cdot}0842$ GeV is the critical energy of an electron in air, t is the air depth in radiation lengths, E_0 is the primary energy and $z = r/r_0$. The average values at different shower sizes are found in the following way:

$$\bar{S}(\text{theor.}) = \frac{6t}{z_2^2 - z_1^2} \int_{z_1}^{z_2} z\,\mathrm{d}z/[t + 2\ln(E_0/\epsilon_0) + 2\ln z]. \tag{6}$$

The average radial ages $\bar{S}$(HL) and $\bar{S}$(NKG), determined from (4) using equations (2) and (3) for the HL and NKG lateral structure functions, are compared with the theoretical average values in Table 2.

Table 2. Comparison of average radial ages with the theoretical average for three shower sizes

N_e	$5{\cdot}3\times10^4$	$1{\cdot}2\times10^5$	$1{\cdot}2\times10^6$
$\bar{S}$(HL)	1·494	1·493	1·733
$\bar{S}$(NKG)	1·703	1·324	1·476
$\bar{S}$(theor.)	1·517	1·434	1·325

(2b) Measurement of Age Parameter from Electron Density Data

The χ^2-minimisation technique using the gradient search method has been used to fit the measured electron densities of individual showers to the chosen interpolation function. The distribution of measured shower age for a sample of 8651 showers in the size range $10^{4{\cdot}3}$–$10^{6{\cdot}2}$ is shown in Fig. 2. Experimentally measured shower ages are compared with those of the Moscow group (quoted in Capdevielle and Gawin 1985) in Table 3.

3. Effect of Age Parameter on Lateral Structure

The radial electron densities ρ, measured at various radial points in a group of 893 showers in the size intervals $(5{\cdot}5$–$6{\cdot}5)\times10^4$, $(1$–$1{\cdot}5)\times10^5$ and $(1$–$1{\cdot}5)\times10^6$, and with the age distribution shown in Fig. 2, are presented in Figs 3, 4 and 5. The fixed size showers of ages s differing by $\sim0{\cdot}1$ are distinguishable only in the data at small core distances, as is made evident in these radial electron density distributions.

The observed showers belonging to the age distribution in Fig. 2 are shown in Fig. 6 as a distribution of shower size $\bar{N}_e$ in shower age $\bar{s}$. The error bars represent the standard errors in the mean s. Standard deviations are shown in the same figure. The plot shows that the age of the electron cascade in a shower observed in a vertical direction at sea level decreases with an increase in shower size. The theoretical calculations on this feature given by Capdevielle and Gawin (1982) and the experimental results of the Akeno group (Hara *et al.* 1981) are shown in the same figure.

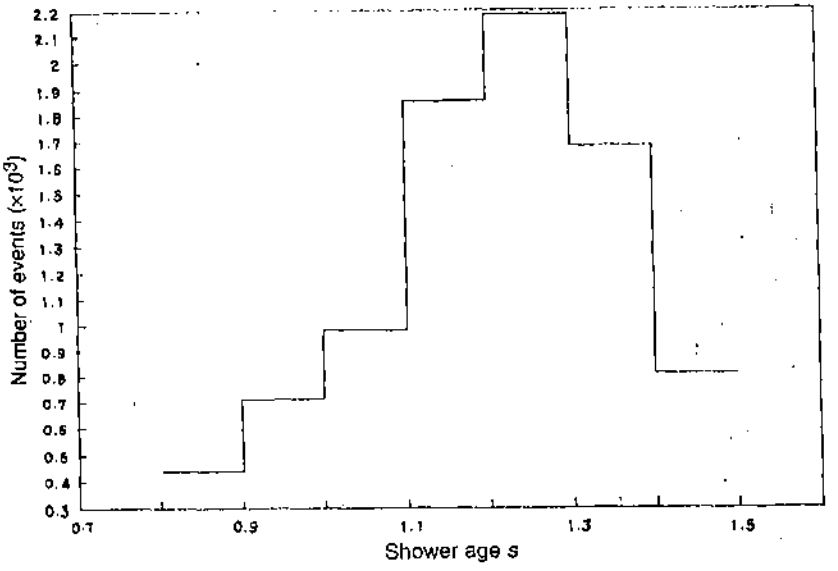

Fig. 2. Distribution of shower age measured by χ^2 minimisation (total 8651 showers).

Table 3. Comparison of present experimental shower ages with those of the Moscow group (quoted in Capdevielle and Gawin 1985)

N_e	$5{\cdot}3\times10^4$	$1{\cdot}2\times10^5$	$1{\cdot}2\times10^6$
Present	1·19	1·10	1·00
Moscow	1·126	1·068	0·924

4. Discussion

The age parameter of cosmic ray extensive air showers has been the subject of further study in recent years. It has been used (Idenden 1990; Cheung and MacKeown 1987; Sumorski and Stamm 1983) to distinguish between ultra-high-energy photon-initiated showers and charged cosmic ray particle-initiated showers. Some workers (Hara *et al.* 1983; Sasaki 1971; Capdevielle and Gawin 1982, 1985; Dai *et al.* 1990) have used the radial age parameter in the shower analysis, in addition to the longitudinal age, to describe the longitudinal development of the shower in the atmosphere. In the present work, it has been shown that the average of the radial shower age at different radial distances over the whole shower disk is almost identical to the theoretical average value of the shower age, as given by electron–photon cascade theory. The age value of a particular shower group determined by the χ^2-minimisation technique is dependent on the shower-detecting area and the detector spacing. A comparison is shown in Table 3 for the present work and the Moscow experiment, which had nearly the same detecting area as in the present experiment.

The shower age measured by the χ^2-minimisation technique has been used as a parameter to show the measured radial electron density distributions in Figs 3, 4 and 5 for three shower size groups, each with different age values.

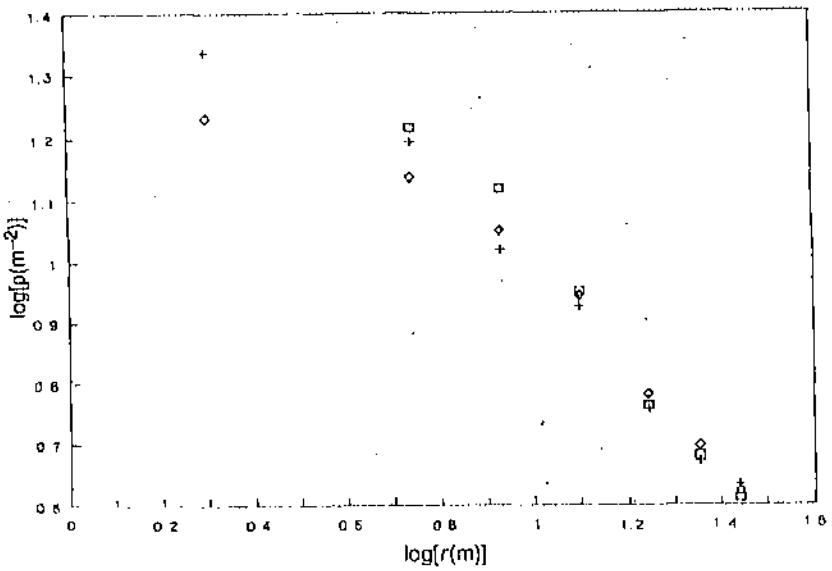

Fig. 3. Radial density distribution of the electron component for N_e in the range $(5–5{\cdot}5)\times10^4$: □ for $s = 0{\cdot}99$; + for $s = 1{\cdot}11$; ◇ for $s = 1{\cdot}19$.

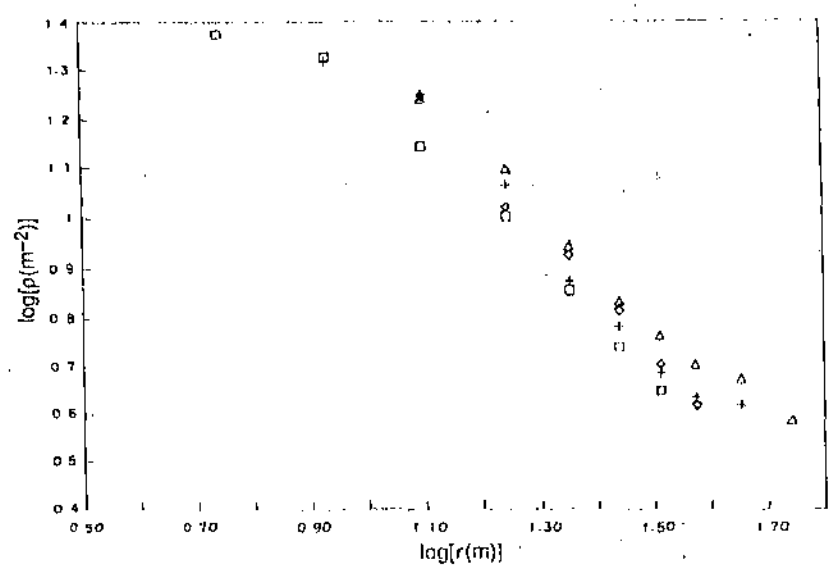

Fig. 4. Radial density distribution of the electron component for N_e in the range $(1–1{\cdot}5)\times10^5$: □ for $s = 0{\cdot}89$; + for $s = 1{\cdot}00$; ◇ for $s = 1{\cdot}10$; and △ for $s = 1{\cdot}20$.

These results are in agreement with expectation (Hillas and Lapikens 1977). A reconfirmation of the earlier results on the variation of the shower age measured by the minimisation technique with shower size published by the Akeno group (Hara *et al.* 1981) and Clay *et al.* (1981) is also given in the present work for

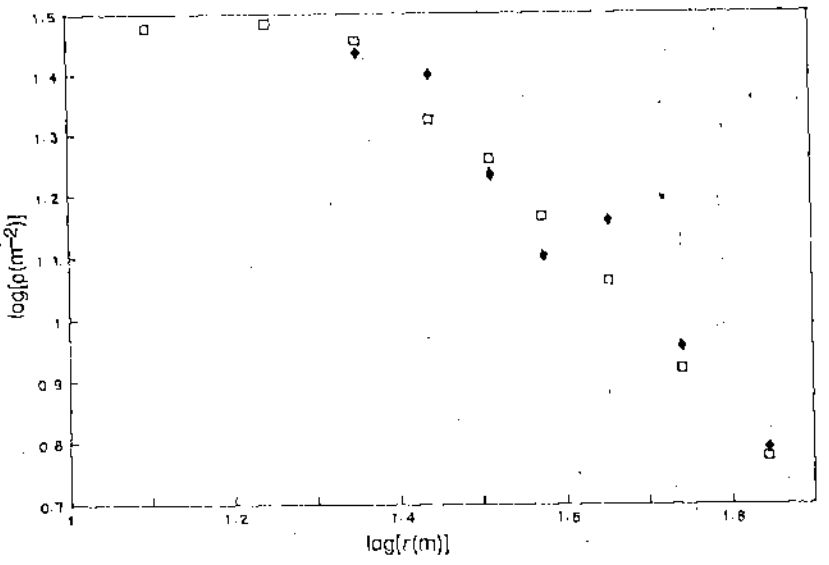

Fig. 5. Radial density distribution of the electron component for N_e in the range $(1\sim 1{\cdot}5)\times10^6$: □ for $s=1{\cdot}00$; ◆ for $s=1{\cdot}07$.

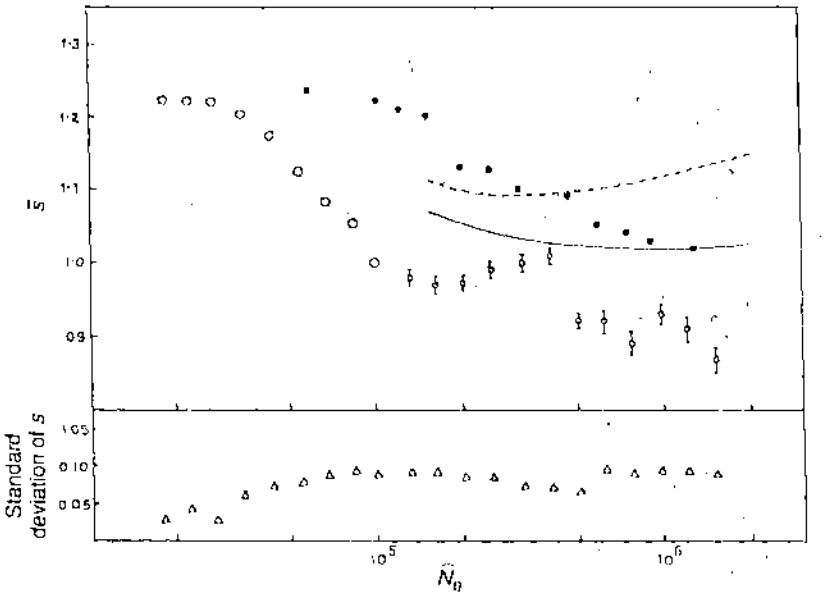

Fig. 6. Distribution of shower size $\bar{N}_e$ with shower age $\bar{s}$: ○, present experiment (sea level); ●, Akeno experiment (900 g cm^{-2}, Hara *et al.* 1981); simulation results (solid curve, scale breaking model; dashed curve, high multiplicity model) of Capdevielle and Gawin (1982). Triangles represent the standard deviation at each point.

vertically incident showers. As can be seen from Fig. 6, a shower of given size developing in the vertical direction over one attenuation length ($\bar{\Lambda} = 112\,\mathrm{g\,cm^{-2}}$ for $N_e \geq 5\times10^5$, Sasaki 1971) increases in age by $\sim$0·07. This result is in good agreement with that measured (0·06/100 $\mathrm{g\,cm^{-2}}$, by Clay *et al.* (1981) and that from the measurements of Hara *et al.* (1981) in the shower size range 10^5–10^6. A similar trend was obtained by Capdevielle and Gawin (1982) for two models, as shown also in Fig. 6. The present results on the variation of shower age with radial distance and with shower size are in accordance with the predictions of the electron–photon cascade theory.

References

Abdullah, M. M., Ashton, F., and Fatemi, J. (1981). Proc. 17th Int. Conf. on Cosmic Rays, Paris, Vol. 6, p. 151.

Abdullah, M. M., Ashton, F., and Fatemi, J. (1983). Proc. 18th Int. Conf. on Cosmic Rays, Bangalore, Vol. 11, p. 181.

Basak, D. K., Chakrabarty, N., Ghosh, B., Goswami, G. C., and Chaudhuri, N. (1984). *Nucl. Instrum. Methods* **227**, 167.

Capdevielle, J. N., and Gawin, J. (1982). *J. Phys.* G **8**, 1317.

Capdevielle, J. N., and Gawin, J. (1985). Proc. 19th Int. Conf. on Cosmic Rays, La Jolla, Vol. 7, p. 139.

Cheung, T., and MacKeown, P. K. (1987). Proc. 20th Int. Conf. on Cosmic Rays, Moscow, Vol. 5, p. 433.

Clay, R. W., Gerhardy, P. R., Liebing, D. F., Thornton, G. J., and Patterson, J. R. (1981). *Nuovo Cimento* **4C**, 668.

Dai, H. Y., He, Y. D., and Huo, A. X. (1990). Proc. 21st Int. Conf. on Cosmic Rays, Adelaide, Vol. 9, p. 5.

Greisen, K. (1960). *Annu. Rev. Nucl. Sci.* **10**, 63.

Hara, T., Hatano, Y., Hayashida, N., Jogo, N., Kamata, K., Kifune, T., Mizumoto, Y., Nagano, M., Tanahashi, G., Tao, Y. H., Kawaguchi, S., Daigo, M., and Hasebe, N. (1981). Proc. 17th Int. Conf. on Cosmic Rays, Paris, Vol. 6, p. 52.

Hara, T., Hatano, Y., Hayashida, N., Kamata, K., Kawaguchi, S., Kifune, T., Nagano, M., and Tanahashi, G. (1983). Proc. 18th Int. Conf. on Cosmic Rays, Bangalore, Vol. 6, p. 94.

Hillas, A. M., and Lapikens, J. (1977). Proc. 15th Int. Conf. on Cosmic Rays, Plovdiv, Vol. 8, p. 460.

Idenden, D. W. (1990). Proc. 21st Int. Conf. on Cosmic Rays, Adelaide, Vol. 9, p. 13.

Samorski, M., and Stamm, W. (1983). Proc. 18th Int. Conf. on Cosmic Rays, Bangalore, Vol. 11, p. 244.

Sasaki, H. (1971). *J. Phys. Soc. Japan* **31**, 1.

Manuscript received 14 January, accepted 26 April 1993

IL NUOVO CIMENTO Vol. 18 C, N. 3 Maggio-Giugno 1995

A New Lateral Distribution Function for Electrons in Extensive Air Showers (EAS) Detected near Sea Level.

B. BHATTACHARYYA, A. BHADRA, A. MUKHERJEE, G. SAHA, S. SANYAL
S. SARKAR, B. GHOSH and N. CHAUDHURI
High Energy and Cosmic Ray Centre, North Bengal University, India

(ricevuto il 5 Luglio 1994; revisionato il 13 Marzo 1995; approvato il 7 Aprile 1995)

Summary. — A detailed analysis of Extensive Air Showers in the size range 10^4–10^6 particles detected near sea level has yielded a new distribution function for the radial distribution of EAS electrons. The goodness-of-fit criteria applied to the present and already existing similar distribution functions confirm that the present function is appropriate in EAS at radial distances beyond 20 m from the shower axis.

PACS 94.40.My – Cascade studies (*e.g.*, extensive air showers).

1. – Introduction.

There has been a number of recent studies on the lateral structure of Cosmic-Ray Extensive Air Showers (EAS) with a view to distinguishing between Primary-Cosmic-Ray (PCR) protons or nuclei-initiated EAS and ultra-high-energy cosmic gamma-ray photon-initiated EAS. In both kinds of EAS a photon-electron cascade develops together with a nucleon cascade longitudinally from the atmospheric depths to which the initiating particles penetrate to make their first nuclear collisions. A photon-electron cascade in EAS with radial symmetry is described laterally at a distance r from the EAS axis by expressing the shower particle density $\Delta(r)$ by

$$\Delta(r) = \frac{N}{r_0^2} f(r/r_0, s), \tag{1}$$

with the shower particle density defined as

$$\Delta(r) = \frac{\Delta N}{(r_0^2)\, 2\pi (r/r_0)\, d(r/r_0)},$$

where N is the total number of particles (size) in EAS; $f(r/r_0, s)$ the lateral structure

function of the EAS; s the age of the electron-photon cascade in the EAS and r_0 the unit of distance chosen for measuring the radial distance of any point in EAS from the EAS axis.

An exact form of the function $f(r/r_0, s)$ is necessary to determine the EAS parameters (shower axis location coordinates (x_0, y_0), shower size N, and shower age s) from a number of measured densities $\Delta(r)$ at various radial distances r from the EAS axis.

A critical analysis of several forms of $f(r/r_0, s)$ used in EAS work in the last four decades was given by Basak *et al.* [1]. The form of $f(r/r_0, s)$ referred to as NKG distribution function was first introduced by Greisen [2] to represent the theoretical results of Nishimura and Kamata [3]. The various forms of $f(r/r_0, s)$ in use [4] are the NKG form and the different modifications [5-13] of the NKG form to take care of the discrepancies with measurement of $\Delta(r)$ *vs.* r observed over a wide range of r.

The purpose of the present paper is to determine, from the experimentally observed lateral particle density distribution, the radial ranges in which three extensively used forms of $f(r/r_0, s)$ are valid on the basis of rigorous «goodness of fit» criterion. A new form for $f(r/r_0, s)$ has also been derived from such analysis of the observed sea level EAS data on $\Delta(r)$ in individual EAS.

2. – EAS data collection and method of analysis.

A closely packed well-defined EAS array operating near sea level at the North Bengal University (26°45′ N) has 35 unshielded scintillation detectors to measure shower particle density $\Delta(r)$ in individual EAS. Eight (8) of these detectors are used to measure relative time delays between their output pulses to determine the arrival directions of the detected EAS. The angular accuracy in direction measurement is within 2° and the error in the EAS axis location is about 1 m.

The shower parameters are determined by fitting a chosen function $f(r/r_0, s)$ to the observed radial distribution of the densities $\Delta(r)$ by minimizing with respect to each of the shower parameters simultaneously the entity defined as

$$\chi^2(x_0, y_0, N, s) = \sum_i^n W_i(\Delta_i^o - \Delta_i^e)^2 . \tag{2}$$

Here Δ_i^o, Δ_i^e are the observed and expected particle densities at the i-th detector in the EAS array and the weight factor W_i of the i-th density data point is the inverse of the variance of the i-th point density Δ_i^e. If the fitting function $f(r/r_0, s)$ is chosen appropriately to predict densities $\Delta_i^e(r)$, a good fit of $f(r/r_0, s)$ to the observed densities $\Delta_i^o(r)$ can be obtained by minimizing χ^2 and hence the constants and parameters in the fitting function can be determined. The number of data points in an EAS is denoted by n.

The method of searching for the minimum value of $\chi^2(x_0, y_0, N, s)$ with respect to each of the EAS parameters simultaneously is the gradient search method in the direction of steepest descent. For fitting the observed density $\Delta^o(r)$ *vs.* r distribution in individual EAS, three forms of the function $f(r/r_0, s)$ have been tried. These are: NKG function $f_{NKG}(r/r_0, s)$ [2], Hillas function $f_H(r/r_0, s)$ [14] and Capdevielle function $f_C(r/r_0, s)$ [15]. The steepest-descent iterative process of minimizing χ^2 was done by the gradient search method and when the minimum of the χ^2-hypersurface

was attained the gradient was reduced to one-half of its former value. This procedure was repeated until the χ^2-value between two successive steps was close enough to a preassigned value.

3. – Results.

Results of a sample of some five thousand recorded EAS events with more than 50% detectors registering particle densities have been analysed shower-size-wise by the standard χ^2 minimization procedure discussed above in sect. 2. The mean of the minimum of the χ^2-values represents the goodness of fit of the observed density distribution of particles in EAS of given size to the fitting function chosen to describe the data.

3·1. *Least-square fitting to the observed density $\Delta^0(r)$ data using* NKG *function $f_{\mathrm{NKG}}(r/r_0, s)$ for $\Delta^e(r)$.* – The shower parameters N and s determined on the basis of $f_{\mathrm{NKG}}(r/r_0, s)$ (eq. (3)) are given in table I.

$$\Delta^e(r) = \frac{N}{r_0^2} f_{\mathrm{NKG}}(r/r_0, s) = \frac{N}{r_0^2}\left[C(s)\left(\frac{r}{r_0}\right)^{s-2}\left(1+\frac{r}{r_0}\right)^{s-4.5}\right], \tag{3}$$

where the photon-electron cascade parameter s is a measure of the development of EAS down to the depth of observation in the atmosphere. Theoretically this shower age parameter s is a function of depth t (measured in radiation unit), the energy of the initiating particle and the radial range r of an EAS. $C(s)$ is the normalization constant to be determined by the fitting procedure, $r_0 = 79$ m (Moliere unit of displacement at sea level).

The observed probability distribution P_χ corresponding to ν degrees of freedom for the reduced chi square $\chi^2_\nu (= \chi^2/\nu)$ for a given shower size over the whole radial range is shown in fig. 1 and for the range 0–20 m in fig. 2.

3·2. *Least-square fitting to the density $\Delta^0(r)$ data using Hillas function $f_{\mathrm{H}}(r/r_0, s)$.* – The observed probability distribution for the reduced χ^2_ν for the same shower size is given in fig. 3 and fig. 4 when $f_{\mathrm{H}}(r/r_0, s)$ (derived from Monte Carlo simulation data) given below (eq. (4)) was used for fitting the EAS density data

$$\Delta^e(r) = \frac{N}{r_0^2} f_{\mathrm{H}}(r/r_0, s) = \frac{N}{r_0^2}\left[C(s)\left(\frac{r}{r_0}\right)^{a_1 + a_2(s-1)}\left(1+\frac{r}{r_0}\right)^{b_1 + b_2(s-1)}\right], \tag{4}$$

where the constants r_0, a_1, a_2, b_1, b_2 are the fitting parameters.

TABLE I.

Range of estimated shower size N (No. of particles)	Radial range of density $\Delta^0(r)$ (measurement in metres)	Range of best-fitting values of s
$(1–5)\cdot10^4$	0–120	0.90–1.35
$(5–9)\cdot10^4$	0–120	0.90–1.35
$(1–5)\cdot10^5$	0–120	0.90–1.35

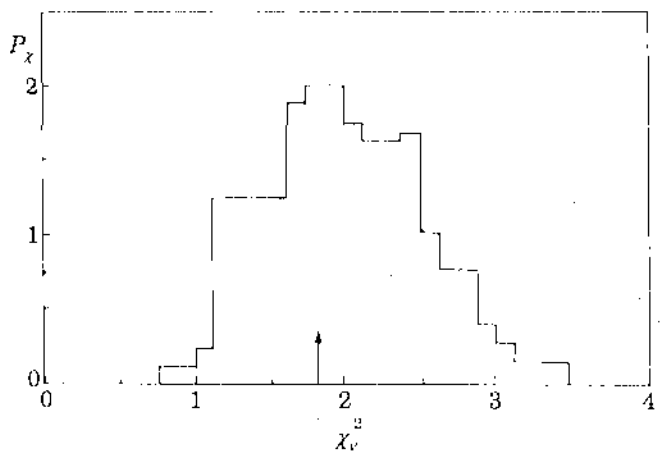

Fig. 1. – The observed probability distribution P_χ for the reduced chi square χ^2_ν using the NKG function in the radial range 0–120 m.

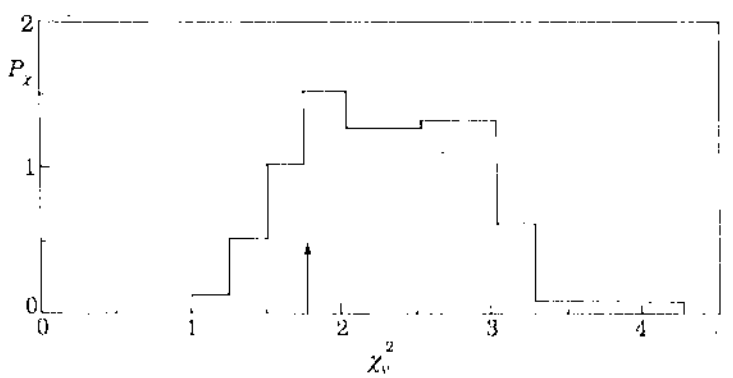

Fig. 2. – Same as in fig. 1, but for the radial range 0–20 m.

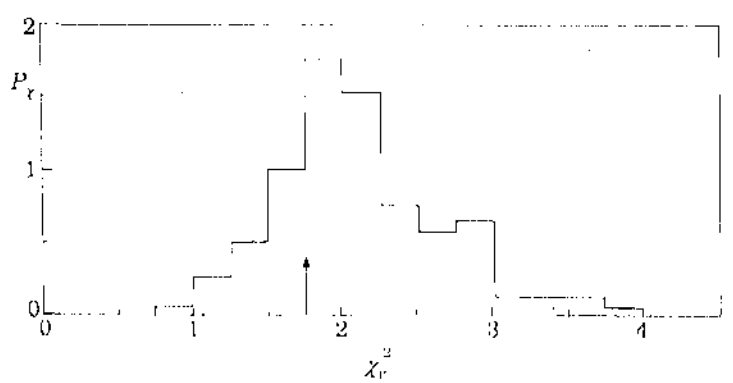

Fig. 3. – Same as in fig. 1, but using Hillas function.

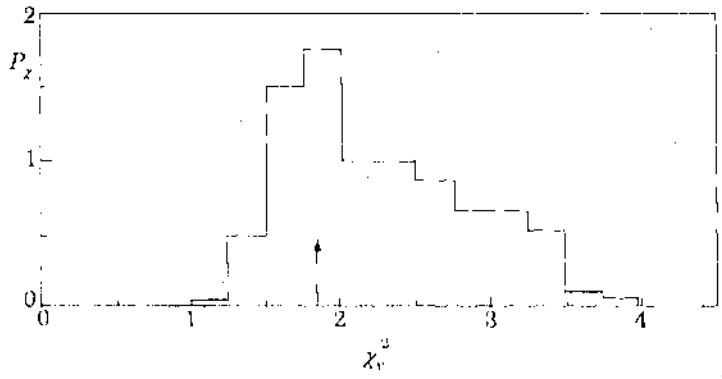

Fig. 4. – Same as in fig. 1, but using Hillas function in the radial range 0–20 m.

3·3. *Least-square fitting to the density* $\Delta^e(r)$ *data using* $f_C(r/r_0, s)$. – Capdevielle *et al.* [15] assumed that the shower age parameter in the fitting function should be the «effective age» for radial development of shower and defined it as

$$s(r) = \alpha \log \beta(r/r_0) + s_l\,, \qquad \text{for} \qquad r \leq 150 \text{ m} \tag{5}$$

where s_l is the longitudinal age parameter at the level of observation and α, β, s_l are constants at sea level for a given shower size.

The observed probability distribution for the reduced χ^2_ν for the same shower size using the $f_C(r/r_0, s)$ (eq. (6)) for fitting the density data is given in fig. 5 and fig. 6.

$$\Delta^e(r) = \frac{N}{r_0^2} f_C(r/r_0, s) = \frac{N}{r_0^2}\left[C(s)\left(\frac{r}{r_0}\right)^{s(r)-2}\left(1+\frac{r}{r_0}\right)^{s(r)-4.5}\right], \tag{6}$$

where $r_0 = 79$ m (Moliere unit of displacement at sea level). The summary of χ^2_ν results from the distribution in fig. 2 to 6 and similar such other distributions (not shown) are given in table II and III.

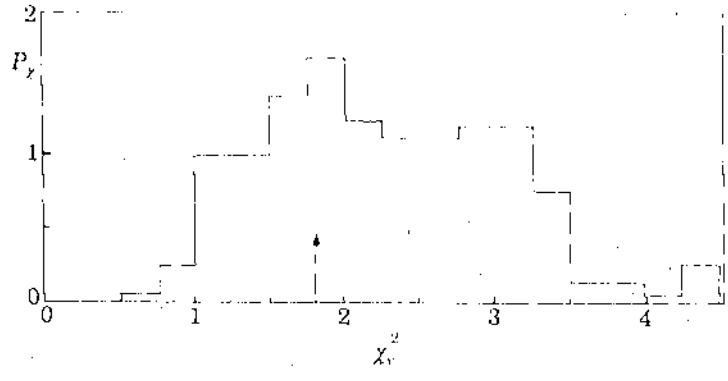

Fig. 5. – Same as in fig. 1, but using Capdevielle function.

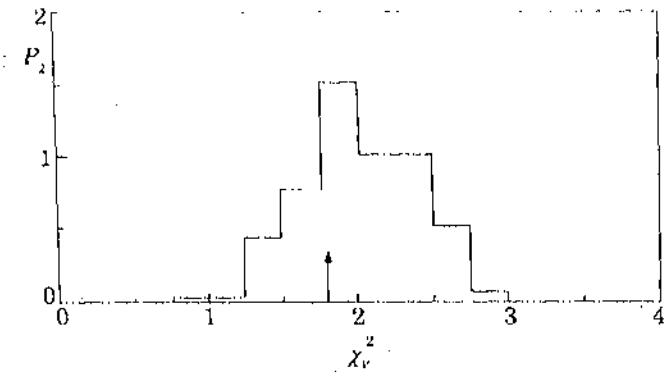

Fig. 6. – Same as in fig. 1, but using Capdevielle function in the radial range 0–20 m.

TABLE II. – *Mean values of the reduced* χ_ν^2 *from fig.* 1, 3 *and* 5 *for the distribution functions (for* EAS *radial range* 0–120 m).

$f_{NKG}(r/r_0, s)$	$f_H(r/r_0, s)$	$f_C(r/r_0, s)$	Proposed $f'(r/r_0, s)$
1.81	1.77	1.80	1.72

TABLE III. – *Mean values of the reduced* χ_ν^2 *in different radial ranges in* EAS *for distribution functions.*

EAS radial ranges in metres	$f_{NKG}(r/r_0, s)$	$f_H(r/r_0, s)$	$f_C(r/r_0, s)$	Proposed function (eq. (7))
0–20	1.77	1.82	1.80	1.83
20–80	1.79	1.77	1.76	1.77
80–120	1.83	1.55	1.82	1.45

4. – Proposed radial distribution function.

The present shower data have also been analysed by using a new distribution function $f'(r/r_0, s)$ (proposed) (eq. (7)) which incorporates two features:

1) the dependence of radial shower age on radial distance and

2) the unit of distance r_0 is taken as the parameter of the fitting function instead of choosing for it a constant value of 79 m (Moliere unit of displacement at sea level).

$$(7)\quad \Delta'(r) = \frac{N}{r_0^2} f'(r/r_0, s) = \frac{N}{r_0^2}\left[C(s)\left(\frac{r}{r_0}\right)^{0.58\,+\,1.54(s(r)\,-\,1)}\left(1+\frac{r}{r_0}\right)^{-3.39\,+\,0.01(s(r)\,-\,1)}\right],$$

where $s(r) = \alpha \ln \beta(r/r_0) + s_1$, for $r \leqslant 150$ m. Here r_0, α, β and s_1 are the fitting parameters.

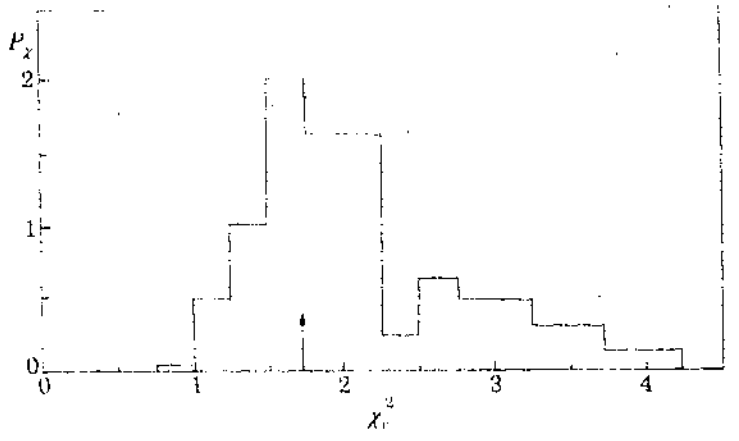

Fig. 7. – Same as in fig. 1, but using the proposed function.

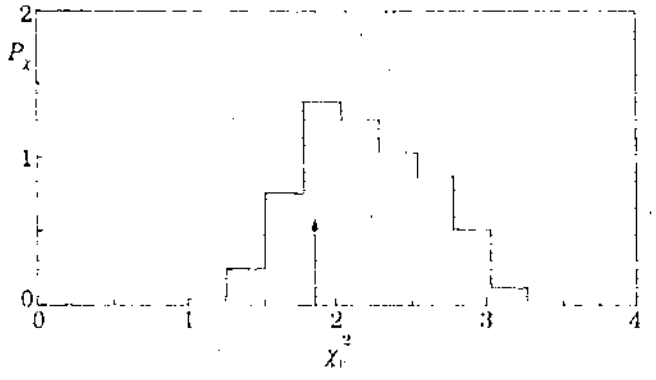

Fig. 8. – Same as in fig. 1, but using the proposed function in the radial range 0–20 m.

Some results for the probability distribution for χ_c^2 using eq. (7) are shown in fig. 7 and fig. 8. The mean values of χ_c^2 for the same shower size in the whole region and in three different radial ranges 0–20 m, 20–80 m, 80–120 m are given in table II and III, respectively.

5. – Discussion and conclusion.

It is necessary to touch upon a few points in connection with the present air shower measurements and analysis. The transition effect arising from multiplication or absorption (absorption is predominant over multiplication) of shower particles in the finite thickness of a plastic scintillator in a density detector of the EAS array was taken into account by correcting the observed density in the manner discussed previously by Basak *et al.* [1, 16] and Asakimori *et al.* [17, 18]. The shape of the average lateral distribution function and the value of the local shower age parameter s measured [1, 16-18] by using thin plastic scintillators is not much dependent on the transition effect near cores of showers in the size range $\sim 10^6$ particles.

The cores of EAS striking the detecting points within the well-defined periphery of the EAS array were located by fitting the measured particle densities registered at the struck detectors to eq. (3) for interpolation of the measured density readings. It has been checked that shower cores thus located are insensitive to the interpolation function chosen. With a close-packed (small detector spacing) well-defined detector array as in the present experiment, the uncertainty in the shower core location from the measured density readings is expected to be minimum compared to what is expected from a detector arrangement with large spacings.

The weighting factor W_i in eq. (2) is the inverse of the variance σ_i^2 (which describes the uncertainty of the i-th data point evaluated by assuming Poisson distribution). Consequently the fits obtained with different lateral distribution function (l.d.fs) will not depend on the detector spacing of an array with well-defined perimeter, the weighting factor W_i and the shower core location procedure.

To obtain a fit of the measured density data of a recorded EAS event to a fitting function (l.d.f) with several parameters, the gradient search method of least squares was used for determining simultaneously the optimum values of the parameters which give a minimum to the function χ^2 (eq. (2)) defined with that l.d.f. This

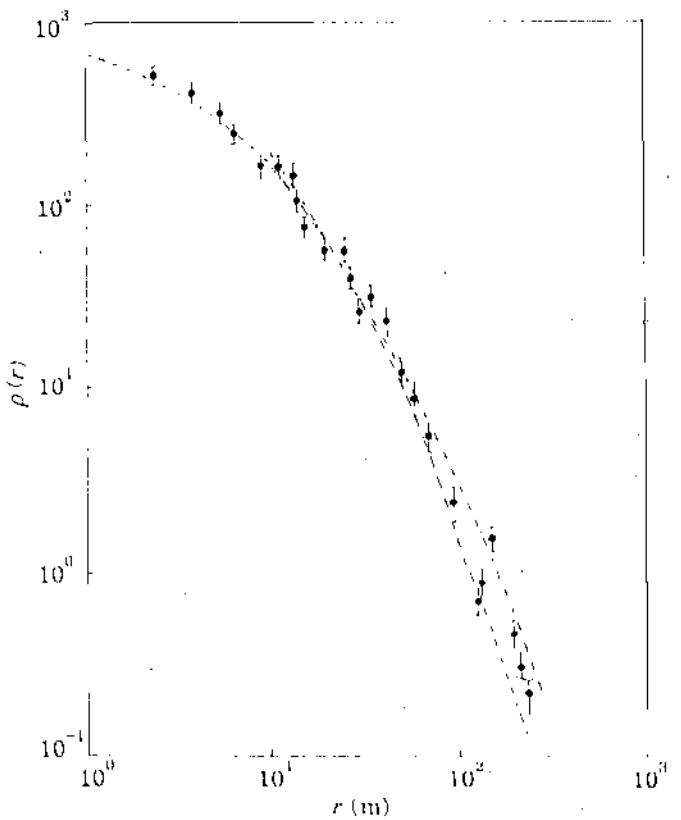

Fig. 9. - Observed lateral electron density distribution along with the theoretical distributions using Hillas (dashed line), Capdevielle (dot-dashed line) and the proposed function (dotted line) in the radial range 0–120 m. $N = 6 \cdot 10^6$, $s = 1.25$.

procedure is expected to obtain a best fit for the multiparameter l.d.f to a large number of density readings in a registered EAS event from a large sample of EAS of fixed size N. The probability distribution for χ^2 as well as the χ^2-values found in the present work by the gradient search method are larger than the expected values due to large intrinsic fluctuations from shower to shower and random sample of density data of an individual EAS with small values of «sample standard deviation σ_i». The error in attaining χ^2-minima by the gradient search with steepest-descent iterative procedure adopted in the present work may contribute to the size of χ^2-near minima.

The results of the fit with different l.d.fs are shown in fig. 9 to indicate the extent to which the present experimental data could discriminate them.

It is seen from table II that $f_{\rm H}(r/r_0, s)$ among the three distributions ($f_{\rm NKG}, f_{\rm H}, f_{\rm C}$) considered above is the best fit to the observed density distribution in the whole 0–120 m radial range of EAS. The results of the reduced χ^2_ν test (table III) for the three successive smaller radial ranges in an EAS of the same size as that used in table II show a varying degree of goodness of fit of the observed data to the same fitting function. Whereas $f_{\rm NKG}(r/r_0, s)$ represents a good fit to 0–20 m radial range, in the 20–80 m radial range $f_{\rm C}(r/r_0, s)$ shows a slight improvement over $f_{\rm H}(r/r_0, s)$ which is best in the 80–120 m range. None of these three functional forms can give a reasonably good fit to the observed data in the whole range 0–120 m.

The choice of $s(r)$ variation with r and the choice of r_0 as an adjustable parameter of the fitting function in place of Moliere unit of displacement at sea level are adjusted in the radial range 20–80 m and 80–120 m. In the 80–120 m range the function under eq. (7) gives the better fit to the observed data ($\chi^2_\nu = 1.45$) than the fits obtained by other functions (eq. (1) to (3)). The result of the χ^2_ν-test (table II) made over the whole shower range 0–120 m shows that the proposed function (eq. (7)) is better than any other fitting functions considered above.

The measured age parameter s (table I) of an EAS of given size is the mean of the s-values obtained at the χ^2 minima using eq. (3) or eq. (4) as the fitting function. The relation between the values of s and s_l values obtained by the analysis using eq. (7) as the fitting function is

$$s_l = s + s_e\,, \qquad \text{for} \qquad r \leqslant 120 \text{ m}\,, \tag{8}$$

with $s_e = 0.15$–0.3.

This experimental relation has been obtained from the analysis over the radial range 0–120 m in muon-rich normal EAS initiated presumably by PCR protons or nuclei. However this form is applicable to recorded EAS events of similar shower size having arrival directions from specific stellar point sources of ultra-high-energy gamma-ray photons. From the measured s-values of such EAS events, one can determine s_l values from relation (8). This determination together with a determination of muon size and hadron size simultaneously in such EAS may unambiguously identify such events as ultra-high-energy gamma-ray photon-initiated events. This relation gives a comparison of the performance of the proposed function (eq. (7)) with the NKG function or Hillas function in terms of the measured longitudinal age parameter s_l and the measured s which represents the shower age parameter of a given shower size that one obtains from a best fit of the data with $f_{\rm NKG}(r/r_0, s)$ or $f_{\rm H}(r/r_0, s)$.

Recently the lateral distributions of particles in simulated EAS have also been studied by using cosmic atomic nuclei and cosmic gamma-ray photons [14, 19, 20]. In the simulation work of Mikocki *et al.*, the lateral distribution of particles in EAS of size range 10^5–10^6 particles at sea level was studied using NKG formula (eq. (3)) as

the fitting function. Their χ^2_ν test for the simulation over the radial range 0–100 m yielded, at the minimum value of $\chi^2_\nu (\simeq 6)$ and the fitting parameters, $r_0 = 41$ m and $\bar{s} = 1.29$–1.35. These results show that $f_{\mathrm{NKG}}(r/r_0, s)$ is not an appropriate fitting function for the observed $J(r)$ distribution over a wide radial range in EAS.

In conclusion it may be stated that the proposed function for radial particle density distribution in EAS can be applied to analyse small- and medium-size EAS of the radial range extending to 120 m at least. It can be also used to derive the longitudinal age parameter s_l from the measured shower age parameters s.

REFERENCES

[1] Basak D. K., Bhattacharyya B. and Chaudhuri N., *Nuovo Cimento C*, 13 (1990) 677.
[2] Greisen K., *Annu. Rev. Nucl. Sci.*, 10 (1960) 63.
[3] Nishimura J. and Kamata K., *Prog. Theor. Phys.*, 5 (1950) 899; 6 (1951) 628; 7 (1952) 185.
[4] Procureur J. and Stamenov J. N., *J. Phys. G.*, 13 (1987) 1579; Nikolsky S. I., Stamenov J. N. and Ushev S. Z., *J. Phys. G.*, 13 (1987) 883; Dedenko L. G., *Proceedings of the XXIII International Conference on Cosmic Rays*, Vol. 4 (Calgary, 1993), p. 231.
[5] Khristiansen G. B., Kulikov G. B. and Solovieva V. I., *Proceedings of the XVII International Conference on Cosmic Rays*, Vol. 6 (Paris, 1981), p. 39.
[6] Kawaguchi S., Suga K., Sakuyama H., *Proceedings of the XIV International Conference on Cosmic Rays*, Vol. 8 (1975), p. 2826.
[7] Dedenko L. G., Nesterova N. M., Nikolsky S. I., Stamenov I. N. and Janminchev V. D., *Proceedings of the XIV International Conference on Cosmic Rays*, Vol. 8 (Munich, 1975), p. 2731.
[8] Kaneko T., Aguirre C., Toyoda Y., Nakatani H., Jadot S., Mackeown P. K., Suga K., Kakimoto F., Mizumoto Y., Murakami K., Nishi K., Nagano M. and Kamata K., *Proceedings of the XIV International Conference on Cosmic Rays*, Vol. 8 (Munich, 1975), p. 2747.
[9] Linsley J., *Proceedings of the XV International Conference on Cosmic Rays*, Vol. 12 (Plovdiv, 1977), p. 56.
[10] Hara T., Hatano Y., Hasebe N., Hayashida N., Jogo N., Kamata K., Kawaguchi S., Kifune T., Nagano M. and Tanahashi G., *Proceedings of the XVI International Conference on Cosmic Rays*, Vol. 13 (Kyoto, 1979), p. 148.
[11] Lagutin A. A., Pljasheshnikov A. V. and Uchaikin V. V., *Proceedings of the XVI International Conference on Cosmic Rays*, Vol. 7 (Kyoto, 1979), p. 18.
[12] Chudakov A. E., Dzhappuev D. D., Lidvansky A. S. and Tizengauzen V. A., *Proceedings of the XVI International Conference on Cosmic Rays*, Vol. 8 (Kyoto, 1979), p. 217.
[13] Nagano M., Hara T., Hatano Y., Nayashida N., Kawaguchi S., Kamata K., Kifune T. and Mizumoto Y., *J. Phys. G.*, 10 (1984) 1295.
[14] Hillas A. M. and Lapikens J., *Proceedings of the XV International Conference on Cosmic Rays*, Vol. 8 (Plovdiv, 1977), p. 460.
[15] Capdevielle J. N., Gawin J. and Procureur J., *Proceedings of the XV International Conference on Cosmic Rays*, Vol. 8 (Plovdiv, 1977), p. 341.
[16] Basak D. K. and Chaudhuri N., *Nuovo Cimento C*, 9 (1986) 846.
[17] Asakimori K., Hara T., Maeda T., Nishijima K., Toyoda Y., Kamamoto K., Yoshida M., Kameda T. and Mizushima K., *Proceedings of the XVII International Conference on Cosmic Rays*, Vol. 11 (Paris, 1981), p. 301.
[18] Asakimori K., Maeda T., Kameda T., Mizushima K. and Misaki Y., *Proceedings of the XIX International Conference on Cosmic Rays*, Vol. 7 (La Jolla, 1985), pp. 107; 179.
[19] Stamenov J. N., *Proceedings of the XX International Conference on Cosmic Rays*, Vol. 8 (Moscow, 1987), p. 258.
[20] Mikocki S., Gress J. and Piorier J., *Proceedings of the XXI International Conference on Cosmic Rays*, Vol. 9 (Adelaide, Australia, 1990), p. 1.

Studies on the Lateral Distribution of the Soft Component in the EAS

B.Bhattacharyya, B.Ghosh, S.K.Sarkar,
S.Sanyal, A.Bhadra, A.Mukherjee & N.Chaudhuri
High Energy & Cosmic Ray Centre
North Bengal University
Darjeeling 734430
INDIA

ABSTRACT

In the NKG formula two defects have been identified. Firstly it is found that the age parameter increases with distance & secondly Moliere radius is somewhat less than what was expected. Different modifications were proposed by various authors by considering one of the above defects. This paper takes into consideration both the defects simultaneously & claims to obtain better results.

1. INTRODUCTION

In the studies of Cosmic Rays, the most used lateral distribution function for the soft component of the EAS, is the NKG formula which is given by

$$\rho(r)=c(s)(N/r_m^2)(r/r_m)^{(s-2)}(1+r/r_m)^{(s-4.5)} \quad (1)$$

Here the Moliere radius r_m =80 m. However by using the Monte Carlo method Allan et al (1975) first noted that the widths of the showers are very much less than that given by NKG formula. The results of Messel & Crawford (1970) were quite wrong. Hillas et al (1977) carried on Monte Carlo calculations by using several new factors which were not used in earlier calculations. They found that the spread of the shower is narrower & the lateral distribution of electrons fit the following formula.

$$\rho(r)=c(s)N/r_h^2(r/r_h)^{a+a(s-1)}(1+r/r_h)^{b+b(s-1)} \quad (2)$$

Here the radius of the disc r_h=24m i.e., nearly 1/4 of Moliere radius. Such effects were also observed by Lagutin et al (1979). Hillas (1981) cited papers to claim that his simulation results agree well with the calculations of the Lagutin.

Some other authors, like Linsley J et al (1962), have taken into consideration the effect of the Zenith angle. Another line of thinking arose by Miyake et al (1968) and Kristiansen (1971). They proposed that a single age parameter is insufficient to describe the lateral distribution of electrons.

Linsley (1973), Aguirre (1973) & Porter (1973) have been noticed that the age parameter increases with distance and it we confirmed by Kristiansen et al (1975) and Kawaguch (1975). Capdevielle et al (1977) have considered this point in detail. By simulation and from the experimental results of the Tien-Shan experiment he concluded that the age parameter varies with the distance according to the formula

$$s(r)=\alpha \ln\beta(r/r_0)+s_t \qquad 150m>r>15m \qquad (3)$$

and the lateral distribution function becomes

$$\rho(r)=c(s)N/r_m^{2}(r/r_m)^{s(r)-2}(1+r/r_m)^{s(r)-4.5} \qquad (4)$$

2. PROPOSED LATERAL DISTRIBUTION FUNCTION

It is found that NKG function still remain as basis of all other distribution functions. Others only modified it. In the present work all the three curves viz. the NKG, the Hillas and the Capdevielle are fitted with the shower data available in the NBI Cosmic Ray Research Centre. It is found that Hillas function fitted better than NKG at a large distance from the core of the axis of the shower where as the Capdevielle distribution fitted better for a smaller distance. So there are some discrepancies in the NKG function. It can be argued that if the discrepancy is due to the effect of the Moliere radius then the Hillas distribution would be appropriate. On the other hand if the variation of the age parameter with distance is responsible for the discrepancy then the Capdevielle function would be appropriate. Moreover the Hillas distribution makes the curve steeper in the regions far away from the axis and the Capdevielle distribution makes it steeper near the axis. Hence there would be no ambiguity in finding out the factors responsible for the departure from the NKG function.

Hence a new formula is proposed which includes both the above features and is given by

$$\rho(r)=c(s)N/r_0^{2}(r/r_0)^{a_1+a_2(s(r)-1)}(1+r/r_0)^{b_1+b_2(s(r)-1)}$$

and $s(r)=\alpha\ln\beta(r/r_0)+s_t$

where $a_1=-0.5$, $a_2=1.54$, $b_1=-3.39$, $b_2=0$ and $r_0=30$ m & N, r, α, β & s_t are the parameter to be fitted

3 RESULTS

The lateral distribution of electrons for

different distribution functions and the variation of age parameter with distance, obtained from the data available in the NBU Cosmic Ray Research Centre are displayed in Fig 1 and Fig 2 respectively.

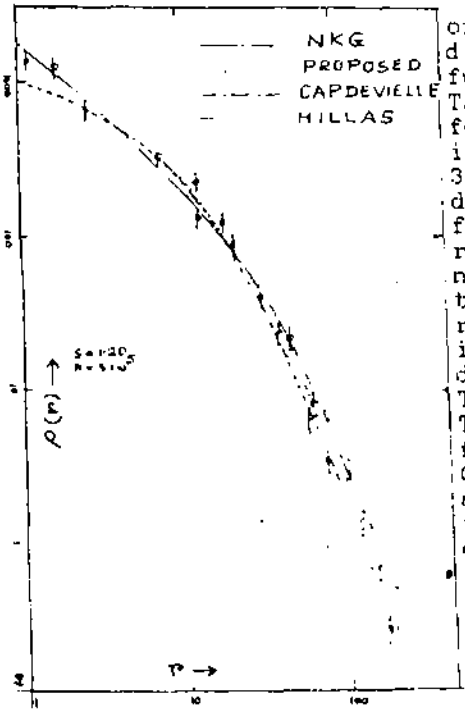

Fig.1: Lateral distribution of electrons.

The average values of χ^2-distribution for different distribution functions are given in Table 1 and the same for the Proposed function is displayed in Fig 3. To find out which distribution function fits better in which region, the whole distance is devided into three segments and the reduced χ^2 distribution is also calculated for different distributions. The results is given in Table 2. Thus it is found that NKG function, Capdevielle function and the Proposed function fits better than other functions in the (0-20)m, (20-80)m and (80-120)m range respectively. In the (20-120)m region the Proposed function fits better than other functions However in the (0-20)m region the Proposed function does not fit well.

TABLE 1

Function	NKG	HILLAS	CAP	PROPOSED
χ^2	1.81	1.77	1.80	1.72

TABLE 2

Values of chi-square

DISTANCE	(0-20)m	(20-80)m	(80-120)m
NKG	1.77	1.79	1.83
HILLAS	1.82	1.77	1.55
CAP	1.80	1.76	1.82
PROPOSED	1.83	1.77	1.45

CONCLUTION

It can be easily seen that the effect of Moliere radius is felt in the (80-120)m region and the reduction is well justfied. In the (20-80)m

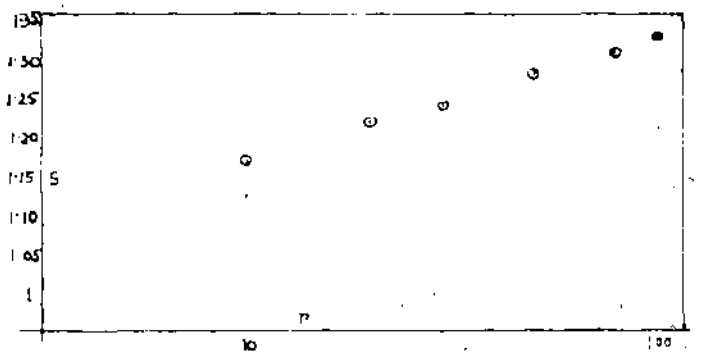

Fig.2 : Variation of Age parameter.

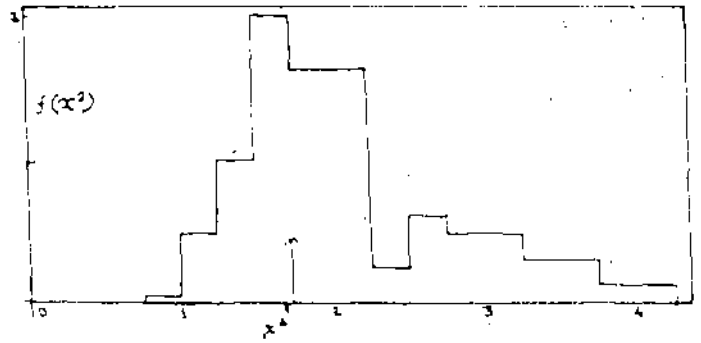

Fig.3 : χ^2 -distribution.

region the shower age parameters variation is most prominent. The proposed form of shower age variation is not applicable in the (0-20)m region and hence the failure of the distribution function in this region takes place.

REFERENCES

Aguirre C. et al., 1973, 13th ICRC, Denver, 4, 2592.
Allan H.R. et al., 1975, 14th ICRC, Munich, 8, 3071.
Capdevielle J. et al., 1977, 15th ICRC, Plovdiv, 8, 341.
Hillas A.M. et al., 1977, 15th ICRC, Plovdiv, 8, 460.
Hillas A.M. et al., 1981, 17th ICRC, Paris, 6, 244.
Kristiansen G.B. et al., 1971, Izv. Ak. Nauk, USSR, 35, 2107
Kristiansen G.B. et al., 1975, 14th ICRC, Munich, 8, 2747
Kawaguchi et al., 1975, 14th ICRC, Munich, 8, 2826.
Lagutin et al., 1979, 16th ICRC, Kyoto, 7, 18.
Linsley J et al., 1962 J. Phys. Soc. Japan, 17, Suppl A, 91
Linsley J et al., 1973, 13th ICRC, Denver, 5, 3212.
Messel, H. & Crawford D., 1970, Electron-photon shower distribution funtion tables. (Pergamon press)
Miyake et al., 1968 Can. J. Phys. 46, 17
Porter N.A. 1973, 13th ICRC, Denver, 5, 2657.

Measurement of the Charge Ratio of High Energy Muons in Cosmic Ray Extensive Air Shower(EAS).

S.K.Sarkar, B.Ghosh, N.Mukherjee, S.Sanyal,
A.Bhadra, A.Mukherjee & N.Chaudhury.
High Energy Cosmic Ray Center
North Bengal University
Darjeeling , INDIA-734430.

ABSTRACT

New results of measurements on the charge ratio of high energy muons in cosmic ray extensive air shower (EAS) are presented.A comparison with some similar results is given for drawing a conclusion.

1. INTRODUCTION

Measurement of muons in cosmic ray EAS studies provide information not only of the primary composition but also on the composition of hadrons in the nuclear active cascade in an EAS.At an average primary cosmic ray energy per nucleon of about ten thousand GeV producing an air shower of size about $\sim 10^4$ particles at sea level,the no of high energy muons,say above 50 GeV,arise from the decay of hadrons(eg, pions,kaons & hyperons) of a number of successive generations forming the nuclear active cascade.Measuring the charge ratio of these muons as a function of their energy one can infer the composition and the relative contribution of pion,kaon and hyperon decay to muons.The first measurement of the charge ratio of air shower muons at energy around 10 GeV is that of Bennett(review article by K.Greisen, Ann.Revs.Nuclear Science 10, 1960).The result for the charge ratio of this measurement is nearly 1.0 indicating that at low energy charge symmetric pion production is predominent.

At higher energies of hadrons,the hadron-nucleus collisions in the nuclear cascade,the kaon and hyperon production is expected to contribute through decay process to muons.

In the present work,measurement on high energy muons in EAS of size between $\sim 10^4$ and $\sim 10^6$ particles, have been carried out by using two solid iron magnets of MDM 500 GeV/c.Low and high energy muons in wide energy range have been recorded simultaneously and the momentum as well as the sign of the charge on each muon determined.

2. EXPERIMENT

Data collection & analysis : An array of 21 closely packed plastic scintillation detectors with spacing of about 8 m at a site near sea level detects incident air shower of size range 10^4 to 10^6 particles over an estimated core distance range of about ~40 m. The shower trajectory and the size of a recorded shower have been determined from the measured time delays and the distribution of radial electron densities. Two shielded magnetic spectrographs installed near the centre of the array determined the trajectories through the spectrographs of the muons in an incident shower. The trajectories of both low and high energy muons in the range 2.5 to 500 GeV have been recorded simultaneously.

3. RESULTS

some two thousand six hundred muons in the recorded air showers in the size range $\sim 10^4$ to $\sim 10^6$ particles have been so far recorded. An analysis has been made to obtain the radial distribution, the energy spectrum at certain radial distances and the charge ratio of muons. Some representative examples of muon radial distribution and energy spectrum are shown in fig.1 & 2. The present results on the charge ratio with momentum are shown graphically in fig.3. It is found that the muon charge ratio has a value close to 1 upto the muon energy of about 20 GeV. Above this energy, the charge ratio increases to about 1.25 around the muon energy of about 450 GeV.

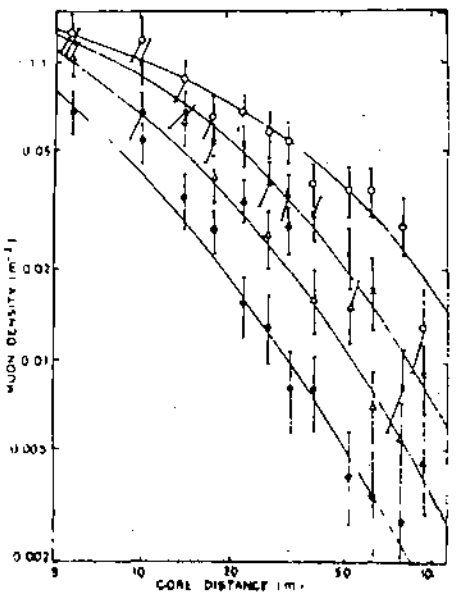

fig.1: Radial distribution of muon at different muon threshold energies : 2.5 GeV. (O), 11.3 GeV. (X), 25.5 GeV. (Δ), 53.7 GeV. (●) for shower of size Ne ~ 1.5 X 10^4

4. DISCUSSION

In fig.4 a comparison is given of the present results with similar results of few earlier measurements on the muon charge ratio. The most of the data points above

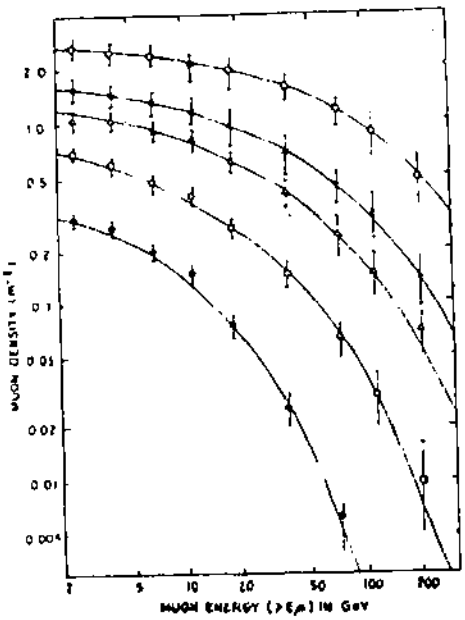

Fig.2 Muon energy spectrum at different radial distances ;05.7 m (O) , 13.6 m (X) , 21.2 m (Δ) , 42.4 m (□) , 89.5 m (●) ,

about muon energy of 25 GeV, except those of Hawkes et al, show a trend for the muon charge ratio rising with increasing energy. It means that at such high energies the hadron-nucleus collisions in the hadronic cascade of EAS produce charge symmetric

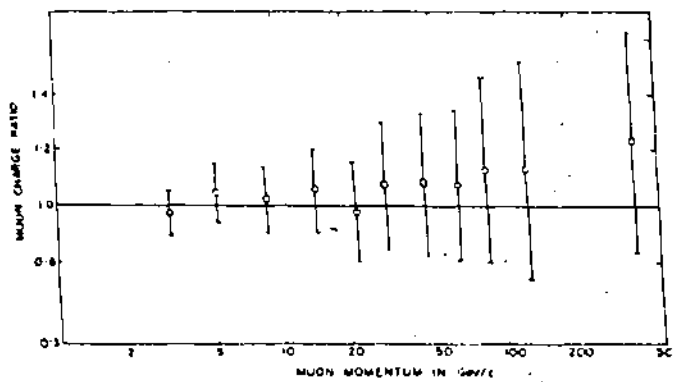

Fig.3: Dependence of charge ratio on muon momentum for the shower size range $\sim 10^4$ to 10^6 particles.

pions as well as heavier mesons and hyperons which generate through decay excess of positive muons. At

such high energies the positive charge excess is similar to that for single muons (unassociated) measured recently by Basini et al (1991).

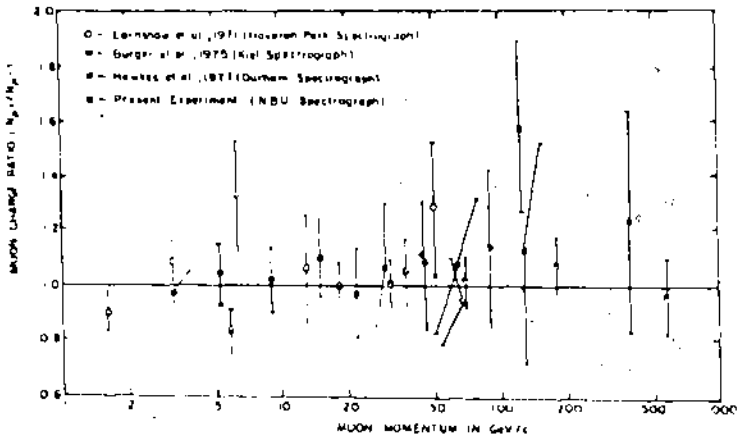

Fig.4: A comparison of the present result, showing the dependence of muon charge ratio on momentum, with the other results.

REFERENCE

Basini et al, 1991, HE 4.1.5, 4 544.
Burger et al, 1975, 14th ICRC EA Session, 8, 2784.
Earnshaw J.C. et al, 1971, Proc. Int. Conf. Cosmic Rays , 3, 1081.
Greisen K., 1960, Ann Revs. Nuclear Sc., **10, 62-107.**
Hawkes R.C. et al, 1977, 15th. ICRC EA Session, 8, 514.

A Study on the Cosmic Ray EAS Age Parameter

S.Sanyal, B.Ghosh, S.K.Sarkar, A.Mukherjee,
A.Bhadra & N.Chaudhuri
High Energy & Cosmic Ray Centre
North Bengal University
Darjeeling 734430 , INDIA

ABSTRACT

An agalysis of 8651 air showers in the size range $10^{4.3}$-$10^{6.2}$ particles shows that (i)for a particular shower the average of the radial shower ages over the whole shower disk is nearly identical with that of the theoretical average value,(ii)the age of a shower of given size developing in the vertical direction increases by~0.07 over 1 attenuation length.

1. INTRODUCTION

In most of the earlier experiments (Abdullah et al.1981,1983; Hara et al.1981,1983;Idenden.1990) the air shower age (s) is determined by standard least square fitting of electron density informations at various radial points of extensive air shower(EAS) front. The age(s) values measured by this method differ from the theoretical values at all atmospheric depths. Some workers(Sasaki.1971; Capdevielle & Gawin.1982,1985; Hara et al.1983; Dai et al.1990) suggested that a shower has to be described by two age parameters, one for its longitudinal development and the other for its lateral development. The present work is concerned with an analysis of shower age in the size range $10^{4.3}$-$10^{6.2}$ particles.

2. EXPERIMENT

The EAS array consists of 21 electron density sampling plastic scintillation detectors at radial distance intervals of about 8m, 8 fast timing detectors and 2 magnet spectrographs covering an area of 1176 m^2. The radial electron density distributions and muon density distributions are measured simultaneously over a radial distance from the array centre upto about 30 m and muon energy in the range 2.5-220 GeV. EAS direction has been determined by measuring relative arrival times and shower size(Ne) , age(s) and core location(x_0,y_0) determination was carried out by the square minimization of the radial electron density data using gradient search method of an EAS event to an interpolating lateral structure function as given by Hillas & Lapikens(1977).

3.DATA ANALYSIS & RESULTS

From Hillas-Lapikens (HL) structure function we obtain for the radial age, $S_{ij}(r)$ at radial location r_i-r_j the following formula,

$$S_{ij}(r)=\ln(F_{ij}X_{ij}^{2.07}Y_{ij}^{3.39})/1.54\ln X_{ij} \quad (1)$$

With NKG function (Greisen,1960) the formula becomes,

$$S_{ij}(r)=\ln(F_{ij}X_{ij}^{2}Y_{ij}^{4.5})/\ln(X_{ij}Y_{ij}), \quad (2)$$

where $F_{ij}(r)=f(r_i)/f(r_j)$, $X_{ij}=r_i/r_j$,

$Y_{ij}=(1+x_i)/(1+x_j)$ with $x=r/r_0$.

The average of the radial ages over the whole shower disk from HLIS(HL)] and from NKGIS(NKG)] lateral structure functions are compared with the theoretical average valuesIS(theo.)] for different shower sizes(Ne) in table 1 below :

TABLE 1.

Ne	$5.3.10^4$	$1.2.10^5$	$1.2.10^6$
S(HL)	1.512	1.412	1.27
S(NKG)	1.765	1.422	1.143
S(theo)	1.517	1.434	1.325

The distribution of shower size(Ne) in the shower age(s) is shown in fig.1. The plot show that the age(s) of the electron cascade in a shower observed in vertical direction at sea level has structure with a decreasing behaviour with increase in size.

4. DISCUSSION

The age parameter of cosmic ray EAS has been a subject of further study because it has been used (Samorski & Stamm,1983; Cheung & Mackeown,1987; Idenden,1990) to distinguish between ultrahigh energy photon initiated EAS and charged cosmic ray particle initiated showers.Some workers(Sasaki,1971; Capdevielle & Gawin,1982,1985; Hara et al.1983) have used in the shower analysis the radial age parameter in addition to longitudinal age to describe longitudinal development of the shower in the atmosphere. In the present work it has been shown that the average value of the radial shower ages over the whole shower disk is nearly identical with the theoretical average value of the shower age as given by the electron-photon cascade theory.

The variation of the measured shower age (s) by chi-square minimization technique with Ne for vertically incident showers is shown in fig.1. The present results are compared with Akeno group (Hara et al.1981) in the same plot. As can be seen from fig.1 a shower of given size developing in the vertical direction over one attenuation length ($\bar{\lambda}$ = 112 gm. cm.$^{-2}$ for Ne$\geq 5.10^5$, Sasaki,1971) increases in age by $\sim$ 0.07. This result is in good agreement with that measured (0.06/100 gm.cm.$^{-2}$) by Clay et al. (1981) and with the measurements of Hara et al. (1981) in the Ne range 10^5-10^6 particles. A trend of such variation is obtained by Capdevielle & Gawin (1982) on two models is also included in the same figure.

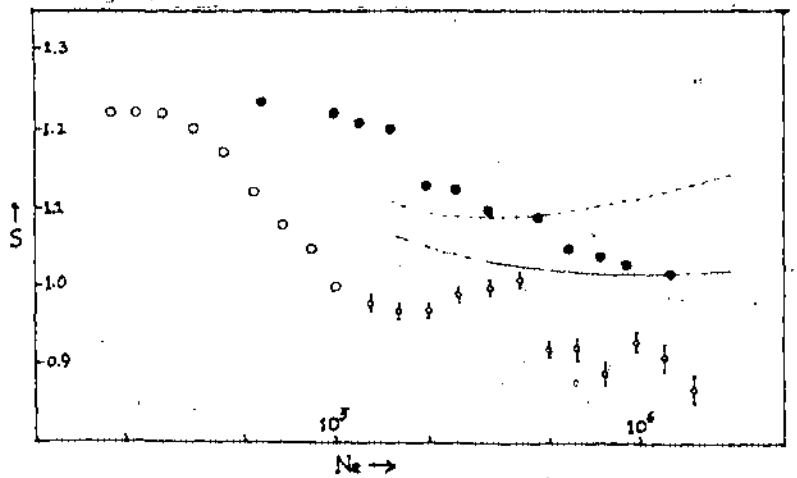

Fig.1:Distribution of Ne in s : O present expt. (sea level); ● Akeno expt.(900 gm.cm.$^{-2}$,Hara et al. (1981); simulation results of Capdevielle & Gawin (1982):——scale breaking model,- - - -high multiplicity model.

REFERENCES

Abdullah,M.M. et al.:1981, Proc. 17th ICRC, 6,151.
Abdullah,M.M. et al.:1983, Proc. 18th ICRC, 11,101.
Capdevielle,J.N.,Gawin,J.:1982, J. Phys. G, 8,1317.
Capdevielle,J.N.,Gawin,J.:1985,Proc.19th ICRC,7,137
Cheung,T.,Mackeown,P.K.:1987,Proc. 20th ICRC,5,453.
Clay,R.W. et al.:1981, Il Nuov. Cim. 4C,6,560.
Dai,H.Y. et al.:1990, Proc. 21st ICRC, 9,5.
Greisen,K.:1960, Ann. Rev. Nucl. Sci., 10,63.
Hara,T. et al.:1981, Proc. 17th ICRC, 6,92.
Hara,T. et al.:1983, Proc. 18th ICRC, 6,94.
Hillas,A.M.,Lapikens,J.:1977,Proc.15th ICRC, 8,460.
Idenden,D.W.:1990, Proc. 21st ICRC, 9,13.
Samorski,M.,Stamm,W.:1983, Proc. 18th ICRC, 11,244.
Sasaki,H.:1971, J. Phys. Soc. Japan, 31,1,1.